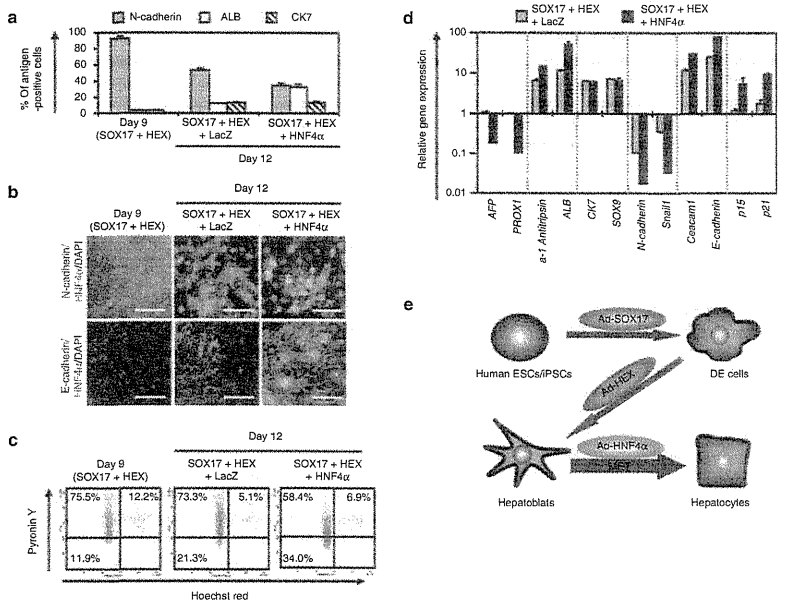

Figure 5 HNF4α promotes hepatic differentiation by activating MET. Human ESCs were differentiated into hepatoblasts according to the protocol described in **Figure 2a**, and then transduced with 3,000 VP/cell of Ad-LacZ or Ad-HNF4α for 1.5 hours, and finally cultured until day 12 of differentiation. (**a**) The hepatoblasts, two factors plus Ad-LacZ-transduced cells (SOX17+HEX+LacZ) (day 12), and the three factors-transduced cells (SOX17+HEX+HNF4α) (day 12) were subjected to immunostaining with anti-N-cadherin, ALB, or CK7 antibodies. The percentage of antigen-positive cells was measured by flow cytometry. (**b**) The cells were subjected to immunostaining with anti-N-cadherin (green), E-cadherin (green), or HNF4α (red) antibodies on day 9 or day 12 of differentiation. Nuclei were counterstained with DAPI (blue). The bar represents 50 μm. Similar results were obtained in two independent experiments. (**c**) The cell cycle was examined on day 9 or day 12 of differentiation. The cells were stained with Pyronin Y (y-axis) and Hoechst 33342 (x-axis) and then analyzed by flow cytometry. The growth fraction of cells is the population of actively dividing cells (G1/S/G2/M). (**d**) The expression levels of *AFP*, *PROX1*, *α-1-antitrypsin*, *ALB*, *CK7*, *SOX9*, *N-cadherin*, *Snail1*, *Ceacam1*, *E-cadherin*, *p15*, and *p21* were examined by real-time RT-PCR on day 9 or day 12 of differentiation. The expression level of hepatoblasts (day 9) was taken as 1.0. All data are represented as means ± SD ($n = 3$). (**e**) The model of efficient hepatic differentiation from human ESCs and iPSCs in this study is summarized. The human ESCs and iPSCs differentiate into hepatocytes via definitive endoderm and hepatoblasts. At each stage, the differentiation is promoted by stage-specific transduction of appropriate functional genes. In the last stage of hepatic differentiation, HNF4α transduction provokes hepatic maturation by activating MET. ESC, embryonic stem cell; HNF4α, hepatocyte nuclear factor 4α; iPSC, induced pluripotent stem cell; MET, mesenchymal-to-epithelial transition; RT-PCR, reverse transcription-PCR; VP, vector particle.

The gene expression levels of hepatocyte markers (*α-1-antitrypsin* and *ALB*)[20] and epithelial markers (*Ceacam1* and *E-cadherin*) were upregulated by HNF4α transduction. On the other hand, the gene expression levels of hepatoblast markers (*AFP* and *PROX1*)[31], mesenchymal markers (*N-cadherin* and *Snail*)[32], and cyclin dependent kinase inhibitor (*p15* and *p21*)[33] were downregulated by HNF4α transduction. HNF4α transduction did not change the expression levels of cholangiocyte markers (*CK7* and *SOX9*). We conclude that HNF4α promotes hepatic maturation by activating MET.

DISCUSSION

This study has two main purposes: the generation of functional hepatocytes from human ESCs and iPSCs for application to drug toxicity screening in the early phase of pharmaceutical development and; elucidation of the HNF4α function in hepatic maturation from human ESCs. We initially confirmed the importance of transcription factor HNF4α in hepatic differentiation from human ESCs by using a published data set of gene array analysis (**Supplementary Figure S1**).[34] We speculated that HNF4α transduction could enhance hepatic differentiation from human ESCs and iPSCs.

To generate functional hepatocytes from human ESCs and iPSCs and to elucidate the function of HNF4α in hepatic differentiation from human ESCs, we examined the stage-specific roles of HNF4α. We found that hepatoblast (day 9) stage-specific HNF4α transduction promoted hepatic differentiation (Figure 1). Because endogenous HNF4α is initially expressed in the hepatoblast,[9,10] our system might adequately reflect early embryogenesis. However, HNF4α transduction at an inappropriate stage (day 6 or day 12) promoted bidirectional differentiation; heterogeneous populations, which contain the hepatocytes and pancreas cells or hepatocytes and cholangiocytes, were obtained, respectively (**Figure 1**), consistent with a previous report that HNF4α plays an important role not only in the liver but also in the pancreas.[12] Therefore, we concluded that HNF4α plays a significant stage-specific role in the differentiation of human ESC- and iPSC-derived hepatoblasts to hepatocytes (**Figure 5e**).

We found that the expression levels of the hepatic functional genes were upregulated by HNF4α transduction (**Figure 3a,b**, and **Supplementary Figures S7** and **S8**). Although the c/EBPα and GATA4 expression levels of the three factors-transduced cells were higher than those of primary human hepatocytes, the FOXA1, FOXA2, FOXA3, and HNF1α, which are known to be important for hepatic direct reprogramming and hepatic differentiation,[35,36] expression levels of three factors-transduced cells were slightly lower than those of primary human hepatocytes (**Supplementary Figure S8**). Therefore, additional transduction of FOXA1, FOXA2, FOXA3, and HNF1α might promote further hepatic maturation. Some previous hepatic differentiation protocols that utilized growth factors without gene transfer led to the appearance only of heterogeneous hepatocyte populations.[4–6] The HNF4α transduction led not only to the upregulation of expression levels of several hepatic markers but also to an almost homogeneous hepatocyte population; the differentiation efficacy based on CYPs, ASGR1, or ALB expression was ~80% (**Figure 3c–e**). The efficient hepatic maturation in this study might be attributable to the activation of many hepatocyte-associated genes by the transduction of HNF4α, which binds to the promoters of nearly half of the genes expressed in the liver.[12] In the later stage of hepatic maturation, hepatocyte-associated genes would be strongly upregulated by endogenous transcription factors but not exogenous HNF4α because transgene expression by Ad vectors was almost disappeared on day 18 (**Supplementary Figure S5**). Another reason for the efficient hepatic maturation would be that sequential transduction of SOX17, HEX, and HNF4α could mimic hepatic differentiation in early embryogenesis.

Next, we examined whether or not the hepatocyte-like cells had hepatic functions. The activity of many kinds of CYPs was upregulated by HNF4α transduction (Figure 4b). Ad-HNF4α-transduced cells exhibit many characteristics of hepatocytes: uptake of LDL, uptake and excretion of ICG, and storage of glycogen (Figure 4a,c,d). Many conventional tests of hepatic characteristics have shown that the hepatocyte-like cells have mature hepatocyte functions. Furthermore, the hepatocyte-like cells can catalyze the toxication of several compounds (Figure 4e). Although the activities to catalyze the toxication of test compounds in primary human hepatocytes are slightly higher than those in the hepatocyte-like cells, the handling of primary human hepatocytes is difficult for a number of reasons: since their source is limited, large-scale primary human hepatocytes are difficult to prepare as a homogeneous population. Therefore, the hepatocyte-like cells derived from human ESCs and iPSCs would be a valuable tool for predicting drug toxicity. To utilize the hepatocyte-like cells in a drug toxicity study, further investigation of the drug metabolism capacity and CYP induction potency will be needed.

We also investigated the mechanisms underlying efficient hepatic maturation by HNF4α transduction. Although the number of cholangiocyte populations did not change by HNF4α transduction, we found that the number of hepatoblast populations decreased and that of hepatocyte populations increased, indicating that HNF4α promotes selective hepatic differentiation from hepatoblasts (**Figure 5a**). As previously reported, HNF4α regulates the expression of a broad range of genes that code for cell adhesion molecules,[13] extracellular matrix components, and cytoskeletal proteins, which determine the main morphological characteristics of epithelial cells.[14,35,37] In this study, we elucidated that MET was promoted by HNF4α transduction (**Figure 5b,d**). Thus, we conclude that HNF4α overexpression in hepatoblasts promotes hepatic differentiation by activating MET (**Figure 5e**).

Using human iPSCs as well as human ESCs, we confirmed that the stage-specific overexpression of HNF4α could promote hepatic maturation (**Supplementary Figure S9**). Interestingly, the differentiation efficacies differed among human iPS cell lines: two of the human iPS cell lines (Dotcom and Tic) were more committed to the hepatic lineage than another human iPS cell line (201B7) (**Supplementary Figure S7**). Therefore, it would be necessary to select a human iPS cell line that is suitable for hepatic maturation in the case of medical applications, such as drug screening and liver transplantation. The difference of hepatic differentiation efficacy among the three iPSC lines might be due to the difference of epigenetic memory of original cells or the difference of the inserted position of the foreign genes for the reprogramming.

To control hepatic differentiation mimicking embryogenesis, we employed Ad vectors, which are one of the most efficient transient gene delivery vehicles and have been widely used in both experimental studies and clinical trials.[38] We used a fiber-modified Ad vector containing the EF-1α promoter and a stretch of lysine residue (KKKKKKK, K7) peptides in the C-terminal region of the fiber knob.[19] The K7 peptide targets heparan sulfates on the cellular surface, and the fiber-modified Ad vector containing the K7 peptides was shown to be efficient for transduction into many kinds of cells including human ESCs and human ESC-derived cells.[7–8,19] Thus, Ad vector-mediated transient gene transfer should be a powerful tool for regulating cellular differentiation.

In summary, the findings described here demonstrate that transcription factor HNF4α plays a crucial role in the hepatic differentiation from human ESC-derived hepatoblasts by activating MET (**Figure 5e**). In the present study, both human ESCs and iPSCs (three lines) were used and all cell lines showed efficient hepatic maturation, indicating that our protocol would be a universal tool for cell line-independent differentiation into functional hepatocytes. Moreover, the hepatocyte-like cells can catalyze the toxication of several compounds as primary human hepatocytes. Therefore, our technology, by sequential transduction of SOX17, HEX, and HNF4α, would be a valuable tool for the efficient generation of functional hepatocytes derived from human ESCs and iPSCs, and the hepatocyte-like cells could be used for the prediction of drug toxicity.

MATERIALS AND METHODS

Human ESC and iPSC culture. A human ES cell line, H9 (WiCell Research Institute, Madison, HI), was maintained on a feeder layer of mitomycin C-treated mouse embryonic fibroblasts (Millipore, Billerica, MA) with Repro Stem (Repro CELL, Tokyo, Japan) supplemented with 5 ng/ml fibroblast

growth factor 2 (FGF2) (Sigma, St Louis, MO). Human ESCs were dissociated with 0.1 mg/ml dispase (Roche Diagnostics, Indianapolis, IN) into small clumps and then were subcultured every 4 or 5 days. H9 was used following the Guidelines for Derivation and Utilization of Human Embryonic Stem Cells of the Ministry of Education, Culture, Sports, Science and Technology of Japan. Two human iPS cell lines generated from the human embryonic lung fibroblast cell line MCR5 were provided from the JCRB Cell Bank (Tic, JCRB Number: JCRB1331; and Dotcom, JCRB Number: JCRB1327).[9,10] These human iPS cell lines were maintained on a feeder layer of mitomycin C-treated mouse embryonic fibroblasts with iPSellon (Cardio, Kobe, Japan) supplemented with 10 ng/ml FGF2. Another human iPS cell line, 201B7, generated from human dermal fibroblasts was kindly provided by Dr S. Yamanaka (Kyoto University).[2] The human iPS cell line 201B7 was maintained on a feeder layer of mitomycin C-treated mouse embryonic fibroblasts with Repro Stem (Repro CELL) supplemented with 5 ng/ml FGF2 (Sigma). Human iPSCs were dissociated with 0.1 mg/ml dispase (Roche Diagnostics) into small clumps and were then subcultured every 5 or 6 days.

In vitro *differentiation*. Before the initiation of cellular differentiation, the medium of human ESCs and iPSCs was exchanged for a defined serum-free medium, hESF9, and cultured as we previously reported.[11] hESF9 consists of hESF-GRO medium (Cell Science & Technology Institute, Sendai, Japan) supplemented with 10 μg/ml human recombinant insulin, 5 μg/ml human apotransferrin, 10 μmol/l 2-mercaptoethanol, 10 μmol/l ethanolamine, 10 μmol/l sodium selenite, 0.5 mg/ml BSA, and 100 ng/ml Activin A (R&D Systems, Minneapolis, MN). To generate mesendoderm cells and DE cells, human ESC-derived cells were transduced with 3,000 vector particles (VP)/cell of Ad-SOX17 for 1.5 hours on day 3 and cultured until day 6 on Matrigel (BD) in hESF-DIF medium (Cell Science & Technology Institute) supplemented with 10 μg/ml human recombinant insulin, 5 μg/ml human apotransferrin, 10 μmol/l 2-mercaptoethanol, 10 μmol/l ethanolamine, 10 μmol/l sodium selenite, 0.5 mg/ml BSA, and 100 ng/ml Activin A (R&D Systems). For induction of hepatoblasts, the DE cells were transduced with 3,000 VP/cell of Ad-HEX for 1.5 hours on day 6 and cultured for 3 days on a Matrigel (BD) in hESF-DIF (Cell Science & Technology Institute) medium supplemented with the 10 μg/ml human recombinant insulin, 5 μg/ml human apotransferrin, 10 μmol/l 2-mercaptoethanol, 10 μmol/l ethanolamine, 10 μmol/l sodium selenite, 0.5 mg/ml BSA, 20 ng/ml bone morphogenetic protein 4 (R&D Systems), and 20 ng/ml FGF4 (R&D Systems). In hepatic differentiation, hepatoblasts were transduced with 3,000 VP/cell of Ad-LacZ or Ad-HNF4α for 1.5 hr on day 9 and were cultured for 11 days on Matrigel (BD) in L15 medium (Invitrogen, Carlsbad, CA) supplemented with 8.3% tryptose phosphate broth (BD), 8.3% fetal bovine serum (Vita, Chiba, Japan), 10 μmol/l hydrocortisone 21-hemisuccinate (Sigma), 1 μmol/l insulin, 25 mmol/l $NaHCO_3$ (Wako, Osaka, Japan), 20 ng/ml hepatocyte growth factor (R&D Systems), 20 ng/ml Oncostatin M (R&D Systems), and 10^{-6} mol/l Dexamethasone (Sigma).

***Ad vectors*.** Ad vectors were constructed by an improved *in vitro* ligation method.[12,13] The human HNF4α gene (accession number NM_000457) was amplified by PCR using primers designed to incorporate the 5′ Not I and 3′ Xba I restriction enzyme sites: Fwd 5′-ggcctctagatggaggcagggagaatg-3′ and Rev 5′-ccccgcggccgcagcggcttgctagataac-3′. The human HNF4α gene was inserted into pBSKII (Invitrogen), resulting in pBSKII-HNF4α, and then the human HNF4α gene was inserted into pHMEF5,[14] which contains the human elongation factor-1α (EF-1α) promoter, resulting in pHMEF-HNF4α. The pHMEF-HNF4α was digested with I-CeuI/PI-SceI and ligated into I-Ceu I/PI-SceI-digested pAdHM41-K7,[15] resulting in pAd-HNF4α. The human EF-1α promoter-driven LacZ-, SOX17-, or HEX-expressing Ad vectors, Ad-LacZ, Ad-SOX17, or Ad-HEX, were constructed previously.[7,8,15] Ad-LacZ, Ad-SOX17, Ad-HEX, and Ad-HNF4α, each of which contains a stretch of lysine residue (K7) peptides in the C-terminal region of the fiber knob for more efficient transduction of human ESCs, iPSCs, and DE cells, were generated and purified as described previously.[7] The VP titer was determined by using a spectrophotometric method.[16]

***LacZ assay*.** Human ESC- and iPSC-derived cells were transduced with Ad-LacZ at 3,000 VP/cell for 1.5 hours. After culturing for the indicated number of days, 5-bromo-4-chloro-3-indolyl β-D-galactopyranoside (X-Gal) staining was performed as described previously.[14]

***Flow cytometry*.** Single-cell suspensions of human ESCs, iPSCs, and their derivatives were fixed with methanol at 4 °C for 20 minutes and then incubated with the primary antibody, followed by the secondary antibody. Flow cytometry analysis was performed using a FACS LSR Fortessa flow cytometer (BD).

***RNA isolation and reverse transcription-PCR*.** Total RNA was isolated from human ESCs, iPSCs, and their derivatives using ISOGENE (Nippon Gene) according to the manufacturer's instructions. Primary human hepatocytes were purchased from CellzDirect, Durham, NC. complementary DNA was synthesized using 500 ng of total RNA with a Superscript VILO cDNA synthesis kit (Invitrogen). Real-time reverse transcription-PCR was performed with Taqman gene expression assays (Applied Biosystems, Foster City, CA) or SYBR Premix Ex Taq (TaKaRa) using an ABI PRISM 7000 Sequence Detector (Applied Biosystems). Relative quantification was performed against a standard curve and the values were normalized against the input determined for the housekeeping gene, glyceraldehyde 3-phosphate dehydrogenase. The primer sequences used in this study are described in **Supplementary Table S1**.

***Immunohistochemistry*.** The cells were fixed with methanol or 4% paraformaldehyde (Wako). After blocking with phosphate-buffered saline containing 2% BSA (Sigma) and 0.2% Triton X-100 (Sigma), the cells were incubated with primary antibody at 4 °C for 16 hours, followed by incubation with a secondary antibody that was labeled with Alexa Fluor 488 (Invitrogen) or Alexa Fluor 594 (Invitrogen) at room temperature for 1 hour. All the antibodies are listed in **Supplementary Table S2**.

***Assay for CYP activity*.** To measure cytochrome P450 3A4, 2C9, and 1A2 activity, we performed Lytic assays by using a P450-GloTM CYP3A4 Assay Kit (Promega, Madison, WI). For the CYP3A4 and 2C9 activity assay, undifferentiated human ESCs, the hepatocyte-like cells, and primary human hepatocytes were treated with rifampicin (Sigma), which is the substrate for CYP3A4 and CYP2C9, at a final concentration of 25 μmol/l or DMSO (0.1%) for 48 hours. For the CYP1A2 activity assay, undifferentiated human ESCs, the hepatocyte-like cells, and primary human hepatocytes were treated with omeprazole (Sigma), which is the substrate for CYP1A2, at a final concentration of 10 μM or DMSO (0.1%) for 48 hours. We measured the fluorescence activity with a luminometer (Lumat LB 9507; Berthold, Oak Ridge, TN) according to the manufacturer's instructions.

***Pyronin Y/Hoechst Staining*.** Human ESC-derived cells were stained with Hoechst33342 (Sigma) and Pyronin Y (PY) (Sigma) in Dulbecco's modified Eagle medium (Wako) supplemented with 0.2 mmol/l HEPES and 5% FCS (Invitrogen). Samples were then placed on ice for 15 minutes, and 7-AAD was added to a final concentration of 0.5 mg/ml for exclusion of dead cells. Fluorescence-activated cell-sorting analysis of these cells was performed on a FACS LSR Fortessa flow cytometer (Becton Dickinson) equipped with a UV-laser.

***Cellular uptake and excretion of ICG*.** ICG (Sigma) was dissolved in DMSO at 100 mg/ml, then added to a culture medium of the hepatocyte-like cells to a final concentration of 1 mg/ml on day 20 of differentiation. After incubation at 37 °C for 60 minutes, the medium with ICG was discarded and the cells were washed with phosphate-buffered saline. The cellular uptake of ICG was then examined by microscopy. Phosphate-buffered saline was then replaced by the culture medium and the cells were incubated at 37 °C for 6 hours. The excretion of ICG was examined by microscopy.

***Periodic Acid-Schiff assay for glycogen*.** The hepatocyte-like cells were fixed with 4% paraformaldehyde and stained using a Periodic Acid-Schiff staining system (Sigma) on day 20 of differentiation according to the manufacturer's instructions.

***Cell viability tests*.** Cell viability was assessed by Alamar Blue assay kit (Invitrogen). After treatment with test compounds[17–20] (troglitazone, acetaminophen, cyclophosphamide, and carbamazepine) (all from Wako) for 2 days, the culture medium was replaced with 0.5 mg/ml solution of Alamar Blue in culturing medium and cells were incubated for 3 hours at 37 °C. The supernatants of the cells were measured at a wavelength of 570 nm with background subtraction at 600 nm in a plate reader. Control refers to incubations in the absence of test compounds and was considered as 100% viability value.

***Uptake of LDL*.** The hepatocyte-like cells were cultured with medium containing Alexa-488-labeled LDL (Invitrogen) for 1 hour, and then the cells that could uptake LDL were assessed by immunohistochemistry and flow cytometry.

***Primary human hepatocytes*.** Cryopreserved human hepatocytes were purchased from CellzDirect (lot Hu8072). The vials of hepatocytes were rapidly thawed in a shaking water bath at 37 °C; the contents of the vial were emptied into prewarmed Cryopreserved Hepatocyte Recovery Medium (CellzDirect) and the suspension was centrifuged at 100*g* for 10 minutes at room temperature. The hepatocytes were seeded at 1.25×10^5 cells/cm^2 in hepatocyte culture medium (Lonza, Walkersville, MD) containing 10% FCS (GIBCO-BRL) onto type I collagen-coated 12-well plates. The medium was replaced with hepatocyte culture medium containing 10% FCS (GIBCO-BRL) 6 hours after seeding. The hepatocytes, which were cultured 48 hours after plating the cells, were used in the experiments.

SUPPLEMENTARY MATERIAL

Figure S1. Genome-wide screening of transcription factors involved in hepatic differentiation emphasizes the importance of the transcription factor HNF4α.
Figure S2. Summary of specific markers for DE cells, hepatoblasts, hepatocytes, cholangiocytes, and pancreas cells.
Figure S3. The formation of DE cells, hepatoblasts, hepatocytes, and cholangiocytes from human ESCs.
Figure S4. Overexpression of HNF4α mRNA in hepatoblasts by Ad-HNF4α transduction.
Figure S5. Time course of LacZ expression in hepatoblasts transduced with Ad-LacZ.
Figure S6. The morphology of the hepatocyte-like cells.
Figure S7. Upregulation of the expression levels of conjugating enzymes and hepatic transporters by HNF4α transduction.
Figure S8. Upregulation of the expression levels of hepatic transcription factors by HNF4α transduction.
Figure S9. Generation of hepatocytes from various human ES or iPS cell lines.
Figure S10. Promotion of MET by HNF4α transduction.
Figure S11. Arrest of cell growth by HNF4α transduction.
Table S1. List of Taqman probes and primers used in this study.
Table S2. List of antibodies used in this study.

ACKNOWLEDGMENTS

We thank Hiroko Matsumura and Misae Nishijima for their excellent technical support. H.M., M.K.F., and T.H. were supported by grants from the Ministry of Health, Labor, and Welfare of Japan. H.M. was also supported by Japan Research foundation For Clinical Phamacology, The Nakatomi Foundation, and The Uehara Memorial Foundation. K.K. (K. Kawabata) was supported by grants from the Ministry of Education, Sports, Science and Technology of Japan (20200076) and the Ministry of Health, Labor, and Welfare of Japan. K.K. (K. Katayama) and F.S. was supported by Program for Promotion of Fundamental Studies in Health Sciences of the National Institute of Biomedical Innovation (NIBIO).

REFERENCES

1. Thomson, JA, Itskovitz-Eldor, J, Shapiro, SS, Waknitz, MA, Swiergiel, JJ, Marshall, VS *et al.* (1998). Embryonic stem cell lines derived from human blastocysts. *Science* **282**: 1145–1147.
2. Takahashi, K, Tanabe, K, Ohnuki, M, Narita, M, Ichisaka, T, Tomoda, K *et al.* (2007). Induction of pluripotent stem cells from adult human fibroblasts by defined factors. *Cell* **131**: 861–872.
3. Murry, CE and Keller, G (2008). Differentiation of embryonic stem cells to clinically relevant populations: lessons from embryonic development. *Cell* **132**: 661–680.
4. Basma, H, Soto-Gutiérrez, A, Yannam, GR, Liu, L, Ito, R, Yamamoto, T *et al.* (2009). Differentiation and transplantation of human embryonic stem cell-derived hepatocytes. *Gastroenterology* **136**: 990–999.
5. Touboul, T, Hannan, NR, Corbineau, S, Martinez, A, Martinet, C, Branchereau, S *et al.* (2010). Generation of functional hepatocytes from human embryonic stem cells under chemically defined conditions that recapitulate liver development. *Hepatology* **51**: 1754–1765.
6. Duan, Y, Ma, X, Ma, X, Zou, W, Wang, C, Bahbahan, IS *et al.* (2010). Differentiation and characterization of metabolically functioning hepatocytes from human embryonic stem cells. *Stem Cells* **28**: 674–686.
7. Inamura, M, Kawabata, K, Takayama, K, Tashiro, K, Sakurai, F, Katayama, K *et al.* (2011). Efficient generation of hepatoblasts from human ES cells and iPS cells by transient overexpression of homeobox gene HEX. *Mol Ther* **19**: 400–407.
8. Takayama, K, Inamura, M, Kawabata, K, Tashiro, K, Katayama, K, Sakurai, F *et al.* (2011). Efficient and directive generation of two distinct endoderm lineages from human ESCs and iPSCs by differentiation stage-specific SOX17 transduction. *PLoS ONE* **6**: e21780.
9. Duncan, SA, Manova, K, Chen, WS, Hoodless, P, Weinstein, DC, Bachvarova, RF *et al.* (1994). Expression of transcription factor HNF-4 in the extraembryonic endoderm, gut, and nephrogenic tissue of the developing mouse embryo: HNF-4 is a marker for primary endoderm in the implanting blastocyst. *Proc Natl Acad Sci USA* **91**: 7598–7602.
10. Taraviras, S, Monaghan, AP, Schütz, G and Kelsey, G (1994). Characterization of the mouse HNF-4 gene and its expression during mouse embryogenesis. *Mech Dev* **48**: 67–79.
11. Parviz, F, Matullo, C, Garrison, WD, Savatski, L, Adamson, JW, Ning, G *et al.* (2003). Hepatocyte nuclear factor 4alpha controls the development of a hepatic epithelium and liver morphogenesis. *Nat Genet* **34**: 292–296.
12. Odom, DT, Zizlsperger, N, Gordon, DB, Bell, GW, Rinaldi, NJ, Murray, HL *et al.* (2004). Control of pancreas and liver gene expression by HNF transcription factors. *Science* **303**: 1378–1381.
13. Battle, MA, Konopka, G, Parviz, F, Gaggl, AL, Yang, C, Sladek, FM *et al.* (2006). Hepatocyte nuclear factor 4alpha orchestrates expression of cell adhesion proteins during the epithelial transformation of the developing liver. *Proc Natl Acad Sci USA* **103**: 8419–8424.
14. Konopka, G, Tekiela, J, Iverson, M, Wells, C and Duncan, SA (2007). Junctional adhesion molecule-A is critical for the formation of pseudocanaliculi and modulates E-cadherin expression in hepatic cells. *J Biol Chem* **282**: 28137–28148.
15. Li, J, Ning, G and Duncan, SA (2000). Mammalian hepatocyte differentiation requires the transcription factor HNF-4alpha. *Genes Dev* **14**: 464–474.
16. Hayhurst, GP, Lee, YH, Lambert, G, Ward, JM and Gonzalez, FJ (2001). Hepatocyte nuclear factor 4alpha (nuclear receptor 2A1) is essential for maintenance of hepatic gene expression and lipid homeostasis. *Mol Cell Biol* **21**: 1393–1403.
17. Khurana, S, Jaiswal, AK and Mukhopadhyay, A (2010). Hepatocyte nuclear factor-4alpha induces transdifferentiation of hematopoietic cells into hepatocytes. *J Biol Chem* **285**: 4725–4731.
18. Suetsugu, A, Nagaki, M, Aoki, H, Motohashi, T, Kunisada, T and Moriwaki, H (2008). Differentiation of mouse hepatic progenitor cells induced by hepatocyte nuclear factor-4 and cell transplantation in mice with liver fibrosis. *Transplantation* **86**: 1178–1186.
19. Koizumi, N, Mizuguchi, H, Utoguchi, N, Watanabe, Y and Hayakawa, T (2003). Generation of fiber-modified adenovirus vectors containing heterologous peptides in both the HI loop and C terminus of the fiber knob. *J Gene Med* **5**: 267–276.
20. Shiojiri, N (1984). The origin of intrahepatic bile duct cells in the mouse. *J Embryol Exp Morphol* **79**: 25–39.
21. Moll, R, Franke, WW, Schiller, DL, Geiger, B and Krepler, R (1982). The catalog of human cytokeratins: patterns of expression in normal epithelia, tumors and cultured cells. *Cell* **31**: 11–24.

22. Antoniou, A, Raynaud, P, Cordi, S, Zong, Y, Tronche, F, Stanger, BZ *et al.* (2009). Intrahepatic bile ducts develop according to a new mode of tubulogenesis regulated by the transcription factor SOX9. *Gastroenterology* **136**: 2325–2333.
23. Offield, MF, Jetton, TL, Labosky, PA, Ray, M, Stein, RW, Magnuson, MA *et al.* (1996). PDX-1 is required for pancreatic outgrowth and differentiation of the rostral duodenum. *Development* **122**: 983–995.
24. Sussel, L, Kalamaras, J, Hartigan-O'Connor, DJ, Meneses, JJ, Pedersen, RA, Rubenstein, JL *et al.* (1998). Mice lacking the homeodomain transcription factor Nkx2.2 have diabetes due to arrested differentiation of pancreatic beta cells. *Development* **125**: 2213–2221.
25. Ingelman-Sundberg, M, Oscarson, M and McLellan, RA (1999). Polymorphic human cytochrome P450 enzymes: an opportunity for individualized drug treatment. *Trends Pharmacol Sci* **20**: 342–349.
26. Henderson, CJ, Otto, DM, Carrie, D, Magnuson, MA, McLaren, AW, Rosewell, I *et al.* (2003). Inactivation of the hepatic cytochrome P450 system by conditional deletion of hepatic cytochrome P450 reductase. *J Biol Chem* **278**: 13480–13486.
27. Yamada, T, Yoshikawa, M, Kanda, S, Kato, Y, Nakajima, Y, Ishizaka, S *et al.* (2002). *In vitro* differentiation of embryonic stem cells into hepatocyte-like cells identified by cellular uptake of indocyanine green. *Stem Cells* **20**: 146–154.
28. Anzenbacher, P and Anzenbacherová, E (2001). Cytochromes P450 and metabolism of xenobiotics. *Cell Mol Life Sci* **58**: 737–747.
29. Zhao, D, Chen, S, Cai, J, Guo, Y, Song, Z, Che, J *et al.* (2009). Derivation and characterization of hepatic progenitor cells from human embryonic stem cells. *PLoS ONE* **4**: e6468.
30. Hatta, K, Takagi, S, Fujisawa, H and Takeichi, M (1987). Spatial and temporal expression pattern of N-cadherin cell adhesion molecules correlated with morphogenetic processes of chicken embryos. *Dev Biol* **120**: 215–227.
31. Shiojiri, N (1981). Enzymo- and immunocytochemical analyses of the differentiation of liver cells in the prenatal mouse. *J Embryol Exp Morphol* **62**: 139–152.
32. Lee, JM, Dedhar, S, Kalluri, R and Thompson, EW (2006). The epithelial-mesenchymal transition: new insights in signaling, development, and disease. *J Cell Biol* **172**: 973–981.
33. Macleod, KF, Sherry, N, Hannon, G, Beach, D, Tokino, T, Kinzler, K *et al.* (1995). p53-dependent and independent expression of p21 during cell growth, differentiation, and DNA damage. *Genes Dev* **9**: 935–944.
34. Si-Tayeb, K, Noto, FK, Nagaoka, M, Li, J, Battle, MA, Duris, C *et al.* (2010). Highly efficient generation of human hepatocyte-like cells from induced pluripotent stem cells. *Hepatology* **51**: 297–305.
35. Sekiya, S and Suzuki, A (2011). Direct conversion of mouse fibroblasts to hepatocyte-like cells by defined factors. *Nature* **475**: 390–393.
36. Huang, P, He, Z, Ji, S, Sun, H, Xiang, D, Liu, C *et al.* (2011). Induction of functional hepatocyte-like cells from mouse fibroblasts by defined factors. *Nature* **475**: 386–389.
37. Satohisa, S, Chiba, H, Osanai, M, Ohno, S, Kojima, T, Saito, T *et al.* (2005). Behavior of tight-junction, adherens-junction and cell polarity proteins during HNF-4alpha-induced epithelial polarization. *Exp Cell Res* **310**: 66–78.
38. Xu, ZL, Mizuguchi, H, Sakurai, F, Koizumi, N, Hosono, T, Kawabata, K *et al.* (2005). Approaches to improving the kinetics of adenovirus-delivered genes and gene products. *Adv Drug Deliv Rev* **57**: 781–802.
39. Nagata, S, Toyoda, M, Yamaguchi, S, Hirano, K, Makino, H, Nishino, K *et al.* (2009). Efficient reprogramming of human and mouse primary extra-embryonic cells to pluripotent stem cells. *Genes Cells* **14**: 1395–1404.
40. Makino, H, Toyoda, M, Matsumoto, K, Saito, H, Nishino, K, Fukawatase, Y *et al.* (2009). Mesenchymal to embryonic incomplete transition of human cells by chimeric OCT4/3 (POU5F1) with physiological co-activator EWS. *Exp Cell Res* **315**: 2727–2740.
41. Furue, MK, Na, J, Jackson, JP, Okamoto, T, Jones, M, Baker, D *et al.* (2008). Heparin promotes the growth of human embryonic stem cells in a defined serum-free medium. *Proc Natl Acad Sci USA* **105**: 13409–13414.
42. Mizuguchi, H and Kay, MA (1998). Efficient construction of a recombinant adenovirus vector by an improved *in vitro* ligation method. *Hum Gene Ther* **9**: 2577–2583.
43. Mizuguchi, H and Kay, MA (1999). A simple method for constructing E1- and E1/E4-deleted recombinant adenoviral vectors. *Hum Gene Ther* **10**: 2013–2017.
44. Kawabata, K, Sakurai, F, Yamaguchi, T, Hayakawa, T and Mizuguchi, H (2005). Efficient gene transfer into mouse embryonic stem cells with adenovirus vectors. *Mol Ther* **12**: 547–554.
45. Tashiro, K, Kawabata, K, Sakurai, H, Kurachi, S, Sakurai, F, Yamanishi, K *et al.* (2008). Efficient adenovirus vector-mediated PPAR gamma gene transfer into mouse embryoid bodies promotes adipocyte differentiation. *J Gene Med* **10**: 498–507.
46. Maizel, JV Jr, White, DO and Scharff, MD (1968). The polypeptides of adenovirus. I. Evidence for multiple protein components in the virion and a comparison of types 2, 7A, and 12. *Virology* **36**: 115–125.
47. Smith, MT (2003). Mechanisms of troglitazone hepatotoxicity. *Chem Res Toxicol* **16**: 679–687.
48. Dai, Y and Cederbaum, AI (1995). Cytotoxicity of acetaminophen in human cytochrome P4502E1-transfected HepG2 cells. *J Pharmacol Exp Ther* **273**: 1497–1505.
49. Chang, TK, Weber, GF, Crespi, CL and Waxman, DJ (1993). Differential activation of cyclophosphamide and ifosphamide by cytochromes P-450 2B and 3A in human liver microsomes. *Cancer Res* **53**: 5629–5637.
50. Miao, XS and Metcalfe, CD (2003). Determination of carbamazepine and its metabolites in aqueous samples using liquid chromatography-electrospray tandem mass spectrometry. *Anal Chem* **75**: 3731–3738.

Biomaterials 33 (2012) 4526–4534

Contents lists available at SciVerse ScienceDirect

Biomaterials

journal homepage: www.elsevier.com/locate/biomaterials

The promotion of hepatic maturation of human pluripotent stem cells in 3D co-culture using type I collagen and Swiss 3T3 cell sheets

Yasuhito Nagamoto [a,b], Katsuhisa Tashiro [b], Kazuo Takayama [a,b], Kazuo Ohashi [d], Kenji Kawabata [b,c], Fuminori Sakurai [a], Masashi Tachibana [a], Takao Hayakawa [e,f], Miho Kusuda Furue [g,h], Hiroyuki Mizuguchi [a,b,i,*]

[a] *Laboratory of Biochemistry and Molecular Biology, Graduate School of Pharmaceutical Sciences, Osaka University, Osaka 565-0871, Japan*
[b] *Laboratory of Stem Cell Regulation, National Institute of Biomedical Innovation, Osaka 567-0085, Japan*
[c] *Laboratory of Biomedical Innovation, Graduate School of Pharmaceutical Sciences, Osaka University, Osaka 565-0871, Japan*
[d] *Institute of Advanced Biomedical Engineering and Science, Tokyo Women's Medical University, Tokyo 162-8666, Japan*
[e] *Pharmaceutics and Medical Devices Agency, Tokyo 100-0013, Japan*
[f] *Pharmaceutical Research and Technology Institute, Kinki University, Osaka 577-8502, Japan*
[g] *Laboratory of Cell Cultures, Department of Disease Bioresources, National Institute of Biomedical Innovation, Osaka 567-0085, Japan*
[h] *Laboratory of Cell Processing, Institute for Frontier Medical Sciences, Kyoto University, Kyoto 606-8507, Japan*
[i] *The Center for Advanced Medical Engineering and Informatics, Osaka University, Osaka 565-0871, Japan*

ARTICLE INFO

Article history:
Received 16 February 2012
Accepted 3 March 2012
Available online 23 March 2012

Keywords:
Hepatocyte
Co-culture
Collagen
Fibroblast
Liver
ECM (extracellular matrix)

ABSTRACT

Hepatocyte-like cells differentiated from human embryonic stem cells (hESCs) or human induced pluripotent stem cells (hiPSCs) are known to be a useful cell source for drug screening. We recently developed an efficient hepatic differentiation method from hESCs and hiPSCs by sequential transduction of FOXA2 and HNF1α. It is known that the combination of three-dimensional (3D) culture and co-culture, namely 3D co-culture, can maintain the functions of primary hepatocytes. However, hepatic maturation of hESC- or hiPSC-derived hepatocyte-like cells (hEHs or hiPHs, respectively) by 3D co-culture systems has not been examined. Therefore, we utilized a cell sheet engineering technology to promote hepatic maturation. The gene expression levels of hepatocyte-related markers (such as cytochrome P450 enzymes and conjugating enzymes) and the amount of albumin secretion in the hEHs or hiPHs, which were 3D co-cultured with the Swiss 3T3 cell sheet, were significantly up-regulated in comparison with those in the hEHs or hiPHs cultured in a monolayer. Furthermore, we found that type I collagen synthesized in Swiss 3T3 cells plays an important role in hepatic maturation. The hEHs or hiPHs that were 3D co-cultured with the Swiss 3T3 cell sheet would be powerful tools for medical applications, such as drug screening.

1. Introduction

Several studies have recently shown the ability of human embryonic stem cells (hESCs) [1] and human induced pluripotent stem cells (hiPSCs) [2] to differentiate into hepatocyte-like cells [3–6]. Although primary human hepatocytes are generally employed for drug toxicity screening in the early phase of pharmaceutical development, these cells have some drawbacks, such as their limited range of sources, difference in variability and functions from batch to batch, and de-differentiation. Because hESC- or hiPSC-derived hepatocyte-like cells (hEHs or hiPHs, respectively) have potential to resolve these problems, they are expected to be applied to drug screening. The hepatic differentiation processes from hESCs and hiPSCs are divided into three-stages, differentiation into definitive endoderm (DE) cells, hepatoblasts, and mature hepatocytes. Hepatic differentiation methods based on the treatment of growth factors have been widely used to generate hepatocyte-like cells from hESCs or hiPSCs [5–9]. However, the hepatic differentiation efficiency is not high enough for medical applications such as drug screening [10]. To promote the efficiency of hepatic differentiation and hepatic maturation, we have developed hepatic differentiation methods that combine the transduction of transcription factor genes involved in liver development

* Corresponding author. Laboratory of Biochemistry and Molecular Biology, Graduate School of Pharmaceutical Sciences, Osaka University, 1-6 Yamadaoka, Suita, Osaka 565-0871, Japan. Tel.: +81 6 6879 8185; fax: +81 6 6879 8186.
E-mail address: mizuguch@phs.osaka-u.ac.jp (H. Mizuguchi).

0142-9612/$ – see front matter © 2012 Elsevier Ltd. All rights reserved.
doi:10.1016/j.biomaterials.2012.03.011

with stimulation by growth factors [11–13]. The hepatocyte-like cells generated by our protocols have levels of expression of hepatocyte-related genes similar to the levels in (cryopreserved) primary human hepatocytes cultured for 48 h after plating [12]. Moreover, we have recently established more efficient and simple methods for hepatic differentiation from hESCs and hiPSCs by sequential transduction of forkhead box A2 (FOXA2) and hepatocyte nuclear factor 1 homeobox A (HNF1α) (in submitted). In that recent study, we showed that the hEHs or hiPHs expressed the genes of hepatocyte-related markers at levels similar to those in primary human hepatocytes and could metabolize various types of drugs.

It is known that cell–cell interactions between hepatocytes and their surrounding cells are essential for liver development and maintenance of liver functions [14–17]. Although primary human hepatocytes rapidly lose their functions under a monolayer culture condition, they could retain their functions, such as albumin secretion and urea synthesis, in three-dimensional (3D) culture and co-culture [18–21]. Moreover, it has been reported that the primary hepatocytes maintain their functions for a long time by the combination of 3D culture and co-culture, namely 3D co-culture [22–24]. In particular, the functions of primary rat hepatocytes cultured in a 3D co-culture, were shown to be more efficiently preserved than the functions of primary rat hepatocytes cultured in monolayer a co-culture [24]. Recently, Kim et al. reported that primary rat hepatocytes are able to maintain their functions in 3D co-culture with an endothelial cell sheet [25]. To perform 3D co-culture with a cell sheet, they employed cell sheet engineering technology using temperature-responsive culture dishes grafted with a temperature-responsive polymer, poly(*N*-isopropylacrylamide). This cell sheet engineering technology make it possible to manipulate a monolayer cell sheet with the extracellular matrices (ECMs) synthesized from the cells [26]. Although 3D culture or co-culture methods have been individually applied to promote hepatic differentiation from ESCs or iPSCs [27–29], few studies have investigated the hepatic differentiation from hESCS or hiPSCs using a 3D co-culture method.

In this study, we examined whether 3D co-culture, which uses the cell sheet engineering technology, could promote hepatic differentiation, and particularly the differentiation into mature hepatocyte-like cells, from hESCs and hiPSCs. Because Swiss 3T3 cells are widely used for co-culture with primary hepatocytes [18–20], we employed Swiss 3T3 cells for 3D co-culture with the hEHs or hiPHs. After hEHs and hiPHs were 3D co-cultured with a Swiss 3T3 cell sheet, we examined the expression levels of hepatocyte-related genes. Moreover, we investigated a Swiss 3T3 cell-derived factor that can promote hepatic maturation from hESCs and hiPSCs.

2. Materials and methods

2.1. hESC and hiPSC culture

A hESC line, H9 (WiCell Research Institute), was maintained on a feeder layer of mitomycin C (MMC)-treated mouse embryonic fibroblasts (MEF, Millipore) with ReproStem (ReproCELL) supplemented with 5 ng/ml fibroblast growth factor 2 (FGF2) (Sigma). hESCs were dissociated with 0.1 mg/ml dispase (Roche Diagnostics) into small clumps and were then subcultured every 4 or 5 days. H9 cells were was used following the Guidelines for Derivation and Utilization of Human Embryonic Stem Cells of the Ministry of Education, Culture, Sports, Science and Technology of Japan. One hiPSC line generated from the human embryonic lung fibroblast cell line MCR5 was provided from the JCRB Cell Bank (Tic, JCRB Number: JCRB1331). Another hiPSC line, 201B7, generated from human dermal fibroblasts was kindly provided by Dr. S. Yamanaka (KyotoUniversity). These hiPSC lines were maintained on a feeder layer of MMC-treated MEF with iPSellon (for Tic, Cardio) or ReproStem (for 201B7, ReproCELL) supplemented with 10 ng/ml (for Tic) or 5 ng/ml (for 201B7) FGF2.hiPSCs were dissociated with 0.1 mg/ml dispase (Roche Diagnostics) into small clumps and were then subcultured every 5 or 6 days.

2.2. Swiss 3T3 cell culture

A mouse fibroblast line, Swiss 3T3, was maintained with RPMI-1640 medium (Sigma) supplemented with fetal bovine serum (10%) (FBS), streptomycin (120 μg/ml), and penicillin (200 μg/ml).

2.3. Ad vectors

The human eukaryotic translation elongation factor 1 alpha 1 (EF-1α) promoter-driven HNF1α- and FOXA2-expressing Ad vectors (Ad-HNF1α and Ad-FOXA2, respectively) were constructed previously (in submitted). All of Ad vectors contain a stretch of lysine residue (K7) peptides in the C-terminal region of the fiber knob for more efficient transduction of hESCs, hiPSCs, and DE cells, in which transduction efficiency was almost 100%, and purified as described previously [11,12,30]. The vector particle (VP) titer was determined by using a spectrophotometric method [31].

2.4. In vitro differentiation

Before the initiation of cellular differentiation, the medium of hESCs and hiPSCs was exchanged for a defined serum-free medium, hESF9, and hESCs and hiPSCs were cultured as previously reported [32]. The differentiation protocol for the induction of DE cells, hepatoblasts, and hepatocytes was based on our previous report with some modifications (in submitted). Briefly, in mesendoderm differentiation, hESCs and hiPSCs were dissociated into single cells by using Accutase (Millipore) and cultured for 2 days on Matrigel (BD Biosciences) in hESF-DIF medium (Cell Science & Technology Institute) supplemented with 10 μg/ml human recombinant insulin, 5 μg/ml human apotransferrin, 10 μM 2-mercaptoethanol, 10 μM ethanolamine, 10 μM sodium selenite, and 0.5 mg/ml bovine serum albumin (BSA) (all from Sigma) (differentiation hESF-DIF medium) containing 100 ng/ml Activin A (R&D Systems) and 10 ng/ml FGF2. To generate DE cells, hESC- or hiPSC-derived mesendoderm cells were transduced with 3000 VP/cell of Ad-FOXA2 for 1.5 h on day 2 and cultured until day 6 on Matrigel in differentiation hESF-DIF medium supplemented with 100 ng/ml Activin A and 10 ng/ml FGF2. For induction of the hepatoblasts, the hESC- or hiPSC-derived DE cells were transduced with each 1500 VP/cell of Ad-FOXA2 and Ad-HNF1α for 1.5 h on day 6 and cultured for 3 days on Matrigel in hepatocyte culture medium (HCM) (Lonza) supplemented with 30 ng/ml bone morphogenetic protein 4 (BMP4) and 20 ng/ml FGF4 (all from R&D Systems). To expand the hepatoblasts, the hepatoblasts were transduced with each 1500 VP/cell of Ad-FOXA2 and Ad-HNF1α for 1.5 h on day 9 and cultured for 3 days on Matrigel in HCM supplemented with 10 ng/ml hepatocyte growth factor (HGF), 10 ng/ml FGF1, 10 ng/ml FGF4, and 10 ng/ml FGF10 (all from R&D Systems).To induce hepatic maturation, the cells were cultured for 2 days on Matrigel in L15 medium (Invitrogen) supplemented with 8.3% tryptose phosphate broth (BD Biosciences), 10% FBS (Vita), 10 μM hydrocortisone 21-hemisuccinate (Sigma), 1 μM insulin, and 25 mM NaHCO3 (Wako) (differentiation *L15 medium*) *containing 20 ng/ml hepatocyte growth factor (HGF),* 20 ng/ml Oncostatin M (OsM) (R&D Systems), and 10^{-6} M Dexamethasone (DEX) (Sigma). As described below, the Swiss 3T3 cell sheet was stratified onto hepatocyte-like cells on day 14 and cultured in differentiation L15 medium supplemented with 20 ng/ml HGF, 20 ng/ml OsM, and 10^{-6} M DEX until day 15. On day 15, Matrigel was stratified onto the cells and cultured in differentiation L15 medium supplemented with 20 ng/ml HGF, 20 ng/ml OsM, and 10^{-6} M DEX until day 25.

2.5. Cell sheet harvesting and stratifying procedure utilizing a gelatin-coated manipulator

The stratifying protocol was performed as previously described with some modifications [25,33]. Briefly, Swiss 3T3 cells were seeded on a 24-well temperature-responsive culture plate (TRCP) (Cell Seed Inc, Tokyo) on day 12. Two days after seeding (day 14), Swiss 3T3 cells were grown to confluence. On the same day (day 14), a gelatin-coated cell sheet manipulator was placed on the Swiss 3T3 cells, and the culture temperature was reduced to 20 °C for 60 min. By removing the manipulator, cultured Swiss 3T3 cells were harvested as a contiguous cell sheet that attached on the gelatin. The Swiss 3T3 cell sheet was then stratified on the hEHs or hiPHs. The culture plate with the manipulator was incubated at room temperature for 60 min to induce adherence between the hEHs or hiPHs and Swiss 3T3 cell sheet. To dissolve the gelatin, the culture plate was incubated at 37 °C for 60 min, and this was followed by several washing steps.

2.6. RNA isolation and reverse transcription-PCR

Total RNA was isolated from the hESC- or hiPSC-derived cells using ISOGENE (Nippon Gene) according to the manufacturer's instructions. cDNA was synthesized using 500 ng of total RNA with a Superscript VILO cDNA synthesis kit (Invitrogen). Real-time RT-PCR was performed with Taqman gene expression assays or Fast SYBR Green Master Mix using an ABI Step One Plus (all from Applied Biosystems). Relative quantification was performed against a standard curve and the values were normalized against the input determined for the housekeeping gene, *glyceraldehyde 3-phosphate dehydrogenase* (*GAPDH*). The primer sequences used in this study are described in Supplementary Tables 1 and 2.

2.7. Preparation of verticalsection

On day 15, the hEHs cultured with or without the Swiss 3T3 cell sheet were frozen in Tissue-Tek O.C.T. Compound (Sakura Finetek), then vertically sectioned and fixed with 4% paraformaldehyde. These sections were monitored by a phase contrast microscope (Olympus).

2.8. ELISA

hESCs or hiPSCs were differentiated into the hepatocyte-like cells as described in Fig. 1A. The culture supernatants, which were incubated for 24 h after fresh medium was added, were collected and analyzed to determine the amount of ALB secretion by ELISA. ELISA kits for ALB were purchased from Bethyl Laboratories. ELISA was performed according to the manufacturer's instructions. The amount of ALB secretion was calculated according to each standard.

2.9. Co-culture and culture in a cell culture insert system (insert-culture)

hESCs were differentiated into the hepatocyte-like cells as described in Fig. 1A until day 14, and then the hESC-derived cells were harvested and seeded onto a 6-well culture plate (Falcon) with Swiss 3T3 (1:1) in a co-culture system. In a insert-culture system, hESC-derived hepatocyte-like cells were harvested and seeded onto a 6-well culture plate alone, and Swiss 3T3 cells were plated in cell culture inserts (membrane pore size 1.0 μm; Falcon), and placed in a well of the culture palate containing hESC-derived hepatocyte-like cells. These cells were cultured in differentiation L15 medium supplemented with 20 ng/ml HGF, 20 ng/ml OsM, and 10^{-6} M DEX until day 25.

2.10. Stratification of type I collagen gel

A type I collagen gel solution was prepared as suggested by Nitta Gelatin: 7 parts of solubilized collagen in HCl (pH 3.0) 2 parts of 5× concentrated RPMI-1640 medium, and 2 parts of reconstitution buffer (0.2 M HEPES, 0.08 M NaOH) to neutralize the collagen gel, were mixed gently but rapidly at 4 °C. Next, the hESC-derived cells were cultured in a type I collagen gel solution for 3h, and then the medium waschanged and the cells were cultured in differentiation L15 medium supplemented with 20 ng/ml HGF, 20 ng/ml OsM, and 10^{-6} M DEX until day 25.

2.11. Inhibition of collagen synthesis

hESCs were differentiated into the hepatocyte-like cells as described in Fig. 1A until stratification of the Swiss 3T3 cell sheet. After stratification of the Swiss 3T3 cell sheet, the cells were cultured in differentiation L15 medium supplemented with 20 ng/ml HGF, 20 ng/ml OsM, 10^{-6} M DEX, and 25 μM 2,2′-Bipyridyl (Wako), an *inhibitor of collagen synthesis,* until day 25.

2.12. Western blotting analysis

Swiss 3T3 cells were cultured with 25 μM 2,2′-Bipyridyl or solvent (0.1% DMSO) for 3 days, and these cells were then homogenized with lysis buffer (1% Nonidet P-40, 1 mM EDTA, 25 mM Tris-HCl, 5 mM NaF, and 150 mM NaCl) containing protease inhibitor mixture (Sigma-Aldrich). After being frozen and thawed, the homogenates were centrifuged at 15,000× g at 4 °C for 10 min, and the supernatants were collected. The lysates were subjected to SDS-PAGE on 7.5% polyacrylamide gel and were then transferred onto polyvinylidene fluoride membranes (Millipore). After the reaction was blocked with 1% skim milk in TBS containing 0.1% Tween 20 at room temperature for 1 h, the membranes were incubated with goat anti-col1a1 Ab (diluted 1/200; Santa Cruz Biotechnology) or mouse anti-β-actin Ab (diluted 1/5000; Sigma) at 4 °C overnight, followed by reaction with horseradish peroxidase-conjugated anti-goat IgG (Chemicon) or anti-mouse IgG (Cell Signaling Technology) at room temperature for 1 h. The band was visualized by ECL Plus Western blotting detection reagents (GE Healthcare) and the signals were read using a LAS-3000 imaging system (FUJI Film).

2.13. Statistical analysis

Statistical analysis was performed using the unpaired two-tailed Student's *t*-test.

3. Results

3.1. Efficient hepatic maturation by stratification of the Swiss 3T3 cell sheet

The hEHs, which were generated by the transduction of *HNF1α* and *FOXA2* genes, were 3D co-cultured with the Swiss 3T3 cell sheet to promote hepatic differentiation and to generate mature hepatocytes from hESCs and hiPSCs. Our differentiation strategy using the stratification of the Swiss 3T3 cell sheet is illustrated in Fig. 1A. The stratifying procedure was performed on day 14 as described in Fig. 1B. The day after stratifying the Swiss 3T3 cell sheet on the hEHs, vertical sections of the monolayer hEHs (hEHs-mono) and the hEHs stratified with the Swiss 3T3 cell sheet (hEHs-Swiss) were prepared (Fig. 1C). We found that Swiss 3T3 cells were successfully harvested and overlaid onto the hEHs as a monolayer cell sheet (Fig. 1C). Moreover, the hEHs seemed to be larger than the Swiss 3T3 cells. The space between the hEHs cells and Swiss 3T3 cells suggests the formation of ECMs (Fig. 1C).

To investigate whether stratification of the Swiss 3T3 cell sheet could promote hepatic maturation of the hEHs, hESCs (H9) were differentiated into the hepatocyte-like cells according to the protocol described in Fig. 1A, and then the gene expression levels of hepatocyte-related markers and the amount of albumin (ALB) secretion in the hEHs-Swiss were measured on day 25 (Fig. 2). By 3D co-culturing of the hepatocyte-like cells with the Swiss 3T3 cell sheet for 10 days (days 15–25), the gene expression levels of hepatocyte-related markers, such as *ALB* (Fig. 2A), *hepatocyte nuclear factor 4 alpha* (*HNF4A*) (Fig. 2B), cytochrome P450 (CYP) enzymes (*CYP2C9*, *CYP7A1*, *CYP1A2*, and *CYP3A5*) (Fig. 2D–G), and conjugating enzymes (*glutathione S-transferase alpha 1* [*GSTA1*], *GSTA2*, and *UDP glucuronosyltransferase* [*UGT1A1*]) (Fig. 2H–J) were significantly increased as compared with those in hEHs-mono. Moreover, the amount of ALB secretion in hEHs-Swiss was also up-regulated as compared with that in hEHs-mono (Fig. 2K). Because it is known that hepatoblasts can differentiate into hepatocytes and cholangiocytes [34,35], we examined the gene expression level of *cytokeratin 7* (*CK7*), a cholangiocyte-related marker, in hEHs-Swiss and hEHs-mono. In 3D co-culture with the Swiss 3T3 cell sheet, the gene expression level of *CK7* was down-regulated in the hEHs-Swiss relative to the hEHs-mono (Fig. 2C). These results clearly showed that stratification of the Swiss 3T3 cell sheet could promote the hepatic maturation of the hEHs and, in turn, suppress the cholangiocyte differentiation.

In order to investigate whether stratification of the Swiss 3T3 cell sheet promotes maturation of hiPHs as well as hEHs, the hiPSCs (Tic and 201B7) were differentiated into the hepatocyte-like cells according to the protocol described in Fig. 1A. The results showed that the gene expression levels of *ALB*, *CYP2C9*, *CYP3A5*, *CYP1A2*, and *GSTA1* in the hiPHs stratified with the Swiss 3T3 cell sheet (hiPHs-Swiss) were up-regulated in comparison with those in the monolayer hiPHs (hiPHs-mono) (Fig. 3A–E). Moreover, the gene expression level of *CK7* was markedly decreased in hiPHs-Swiss (Fig. 3F). The gene expression level of *ALB* in the hiPHs-Swiss differentiated from Tic was higher than that in the hiPHs-Swiss differentiated from 201B7, while the gene expression levels of CYP enzymes in the hiPHs-Swiss differentiated from Tic were lower than those in the hiPHs-Swiss differentiated from 201B7 (Fig. 3A–D). These results showed that stratification of the Swiss 3T3 cell sheet promoted hepatic maturation of both hEHs and hiPHs.

3.2. Identification of maturation factors synthesized from Swiss 3T3 cells

The data described above indicate that hepatic maturation factors were produced in Swiss 3T3 cells. To elucidate the Swiss 3T3 cell-derived hepatic maturation factors, the hEHs were cultured in cell culture-insert systems (insert-cultured), in which the hEHs were co-cultured with Swiss 3T3 cells without physical contacts, or co-cultured with Swiss 3T3 cells. Quantitative PCR analysis revealed that the gene expression levels of *ALB* and *CYP2C9* in the insert-cultured hEHs were increased in comparison with the hEHs-mono, while the expression levels of these genes were lower than

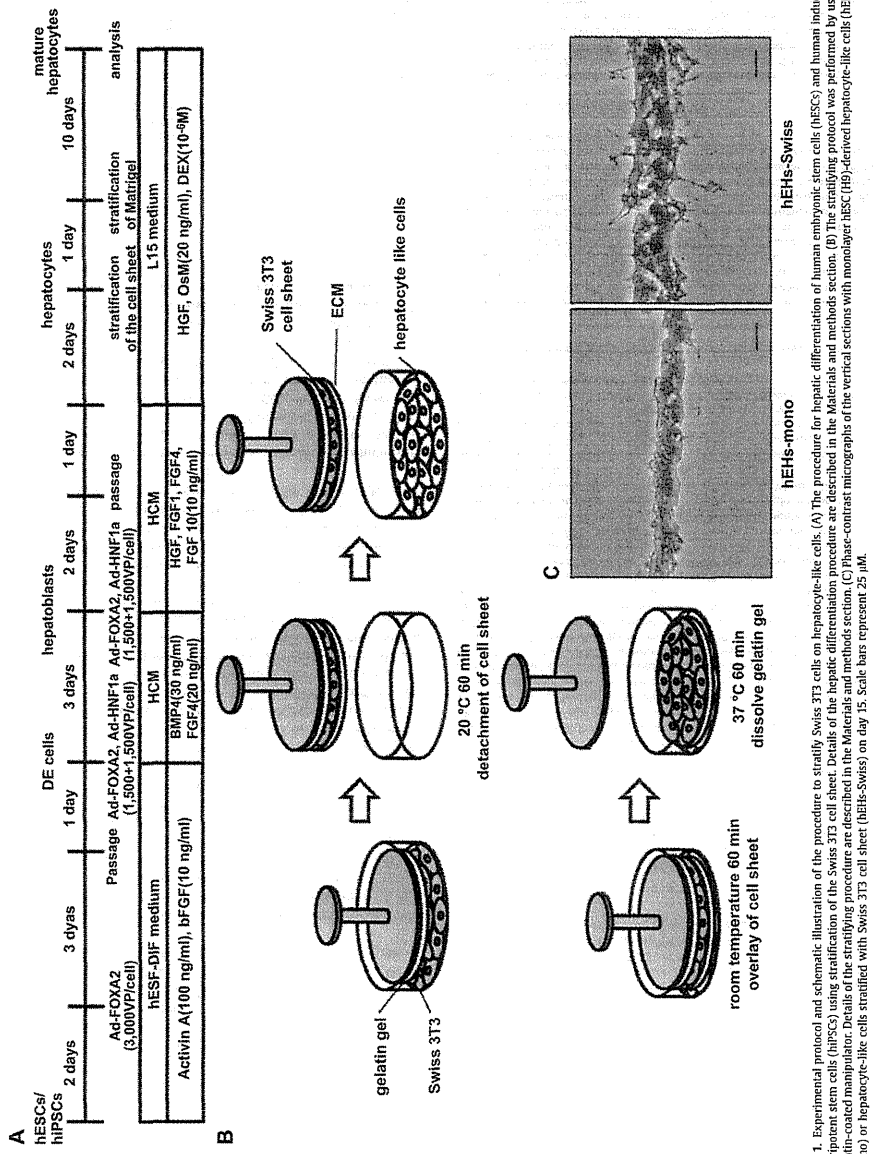

Fig. 1. Experimental protocol and schematic illustration of the procedure to stratify Swiss 3T3 cells on hepatocyte-like cells. (A) The procedure for hepatic differentiation of human embryonic stem cells (hESCs) and human induced pluripotent stem cells (hiPSCs) using stratification of the Swiss 3T3 cell sheet. Details of the hepatic differentiation procedure are described in the Materials and methods section. (B) The stratifying protocol was performed by using gelatin-coated manipulator. Details of the stratifying procedure are described in the Materials and methods section. (C) Phase-contrast micrographs of the vertical sections with monolayer hESC (H9)-derived hepatocyte-like cells (hEHs-mono) or hepatocyte-like cells stratified with Swiss 3T3 cell sheet (hEHs-Swiss) on day 15. Scale bars represent 25 μM.

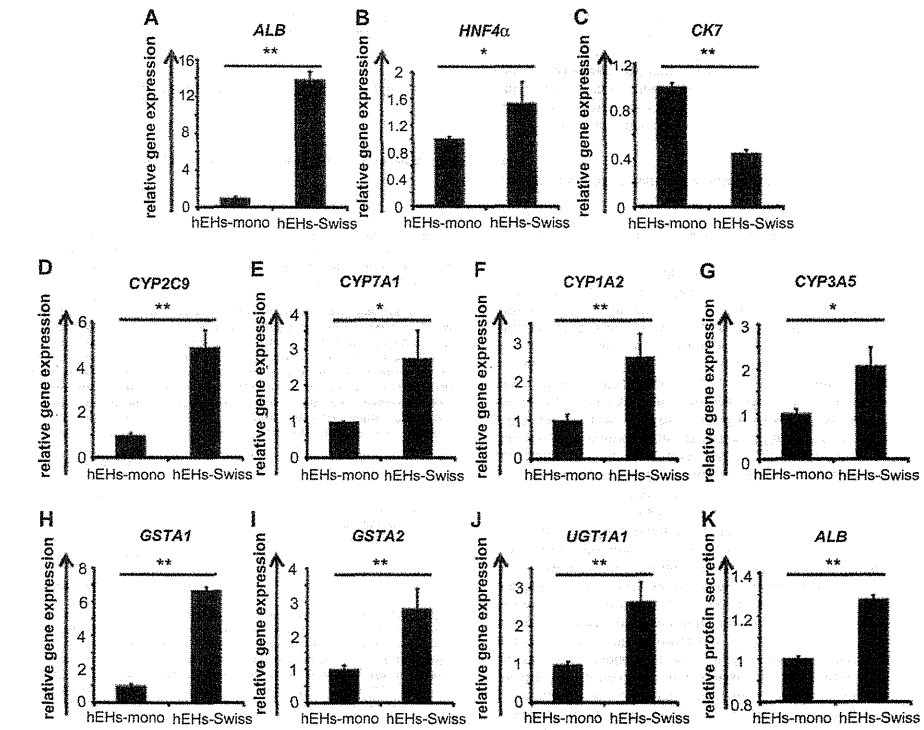

Fig. 2. Stratification of Swiss 3T3 cell sheet on hEHs promotes hepatic maturation. hESCs (H9) were differentiated into hepatocyte-like cells as described in Fig. 1A. (A–K): On day 25, the gene expression levels of *ALB* (A), *HNF4A* (B), *CK7*(C), *CYP2C9* (D), *CYP7A1* (E), *CYP1A2* (F), *CYP3A5* (G), *GSTA1* (H), *GSTA2* (I), and *UGT1A1* (J) were examined in monolayer hESC-derived hepatocyte-like cells (hEHs-mono) and hESC-derived hepatocyte-like cells stratified with Swiss 3T3 cell sheet (hEHs-Swiss) by real-time RT-PCR. The values were graphed as the fold-changes relative to hEHs-mono. (K) On day 25, the amounts of ALB secretion were examined in hEHs-mono or hEHs-Swiss by ELISA. The values were graphed as the fold-changes relative to hEHs-mono. All data are represented as means ± Standard Deviation (SD) ($n = 3$). *$P < 0.05$ **$P < 0.01$.

those in the co-cultured hEHs (Fig. 4A and B). Furthermore, a significant elevation of *CYP1A2* and *CYP3A5* gene expression was observed only in the co-cultured hEHs (Fig. 4C and D). Therefore, these data indicate that physical contacts between hEHs and Swiss 3T3 cells play an important role in hepatic maturation of the hEHs, although Swiss 3T3 cell-derived soluble factors also played a small role in the hepatic maturation.

Because ECMs are important factors in hepatic differentiation [36], we examined the effect of Swiss 3T3 cell-derived ECMs on hepatic maturation of the hEHs. Swiss 3T3 cells abundantly synthesize collagen and almost all of the synthesized collagen is type I collagen [37]. To mimic 3D co-culture with Swiss 3T3 cell sheet, type I collagen gel was stratified onto the hEHs. As a control, Matrigel, which contains abundant type IV collagen but not type I collagen, was stratified onto the hEHs. As with the case of the Swiss 3T3 cell sheet stratification, the hEHs-mono stratified with type I collagen gel showed an elevation of hepatocyte-related marker, but a reduction of cholangiocyte marker (Fig. 5A and B, hEHs-mono). In addition, stratification of type I collagen augmented the hepatic maturation of the Swiss 3T3 cell sheet-stratified hEHs (Fig. 5A and B, hEHs-Swiss). We further examined the role of Swiss 3T3 cell-derived type I collagen on hepatic maturation using 2,2′-Bipyridyl, an inhibitor of collagen synthesize. The collagen synthesis in Swiss 3T3 cells could be efficiently inhibited by treatment with 2,2′-Bipyridyl, as determined by Western blotting analysis (Fig. 5C). Quantitative RT-PCR analysis revealed that the gene expression level of *ALB* was significantly down-regulated, but that of CK7 was up-regulated in the hEHs-Swiss cultured in the presence of 2,2′-Bipyridyl (Fig. 5D and E). Taken together, our findings indicated that type I collagen, which was synthesized from Swiss 3T3 cells, was indispensable for the maturation of the hEHs by Swiss 3T3 cell sheet.

4. Discussion

Our main purpose in the current study was to develop a more efficient method for hepatic maturation of the hEHs and hiPHs, because such a method will be needed to generate more mature hepatocyte-like cells, which have potent activity to metabolize drugs, for wide-spread use of drug screening. Therefore, we

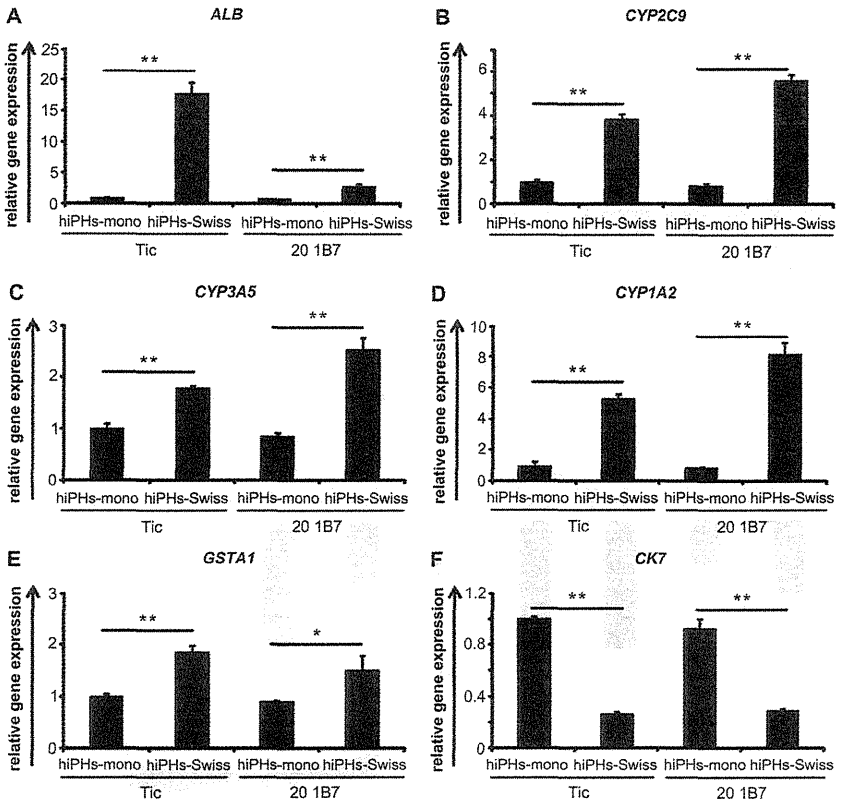

Fig. 3. Stratification of Swiss 3T3 cell sheet on hiPHs promotes hepatic maturation. Human induced pluripotent stem cells (hiPSCs) (Tic and 201B7) were differentiated into hepatocyte-like cells as described in Fig. 1A. (A–F): On day 25, the gene expression levels of *ALB* (A), *CYP2C9* (B), CYP3A5(C), *CYP1A2* (D), *GSTA1* (E), and *CK7* (F) were examined in monolayer hiPSC-derived hepatocyte-like cells (hiPHs-mono) and hiPSC-derived hepatocyte-like cells stratified with Swiss 3T3 cell sheet (hiPHs-Swiss) by real-time RT-PCR. The values were graphed as the fold-changes relative to hiPHs-mono differentiated from Tic. All data are represented as means ± SD ($n = 3$). *$P < 0.05$ **$P < 0.01$.

attempted to employ a cell sheet engineering technology to further induce maturation of the hEHs and hiPHs.

We observed a significant increase in the expression of hepatocyte-related genes in the hEHs- and hiPHs-Swiss as compared with those in the hEHs- and hiPHs-mono, respectively (Figs. 2 and 3), indicating that 3D co-culture with the Swiss 3T3 cell sheet was effective to promote hepatic maturation of the hEHs and hiPHs. On the other hand, Han et al. have recently shown that hESC-derived DE cells cannot be promoted to differentiate into hepatoblasts by co-culture of mouse fibroblast 3T3 cells [38]. Considering that primary rat hepatocytes are also able to grow and retain their functions for a long period of time in the presence of Swiss 3T3 cells [19,20], Swiss 3T3 cells would probably have the capacity to support the functions of freshly isolated mature hepatocytes and hESC- or hiPSC-derived hepatocyte-like cells, but not DE cells. Besides Swiss 3T3 cells, we attempted to maturate the hEHs using 3D co-culture with the bovine carotid artery endothelial cell sheet, because Kim et al. recently succeeded in creating a functional hepatocyte culture system by stacking bovine carotid artery endothelial cell sheets on primary rat hepatocytes [25]. However, our preliminary data showed that Swiss 3T3 cell sheets were superior to the bovine carotid artery endothelial cell sheets in terms of hepatic maturation of hEHs (data not shown). Thus, we conducted the present experiments to facilitate hepatic differentiation of human pluripotent stem cells using Swiss 3T3 cell sheets.

Interestingly, we found a difference in hepatic differentiation efficiency among hiPSC lines (Fig. 3). This might have been due to epigenetic memory of the hiPSC line, because several studies showed that the epigenetic memory of iPSCs affected the differentiation capacity [39,40]. Kleger et al. showed that iPSCs generated from mouse liver progenitor cells, could be more effectively differentiated into hepatocyte-like cells in comparison with iPSCs

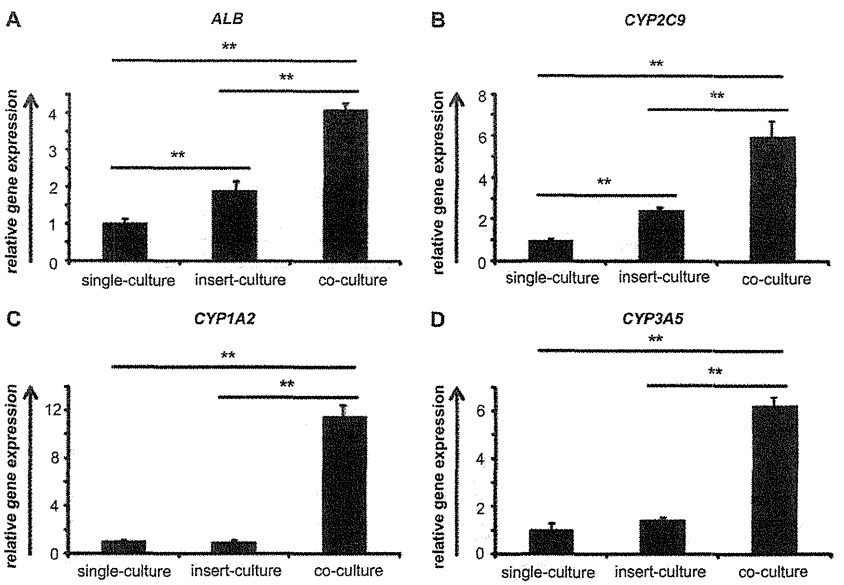

Fig. 4. Physical contacts between hESC-derived hepatocyte-like cells and Swiss 3T3 cells promote hepatic maturation. hESCs (H9) were differentiated into hepatocyte-like cells as described in Fig. 1A until day 14, and then the cells were differentiated into hepatocyte-like cells by single-culture, insert-culture, or co-culture with Swiss 3T3 cells. (A–D): On day 25, the gene expression levels of *ALB* (A), *CYP2C9* (B), *CYP1A2* (C) and *CYP3A5* (D) were examined in hESC-derived hepatocyte-like cells (hEHs) differentiated by single-culture, insert-culture, or co-culture with Swiss 3T3 cells by real-time RT-PCR. The values were graphed as the fold-changes relative to hEHs by single-culture. All data are represented as means ± SD ($n = 3$). **$P < 0.01$.

generated from mouse embryo fibroblasts [41]. Thus, to more efficiently differentiate into hepatocyte-like cells from hiPSCs, it might be valuable to employ hiPSCs generated from freshly isolated human hepatocytes. Moreover, by using our 3D co-culture system, such hiPSCs would be differentiated into more mature hepatocyte-like cells.

We investigated the Swiss 3T3 cell-derived hepatic maturation factors by using cell culture inserts, and found that the physical contacts between Swiss 3T3 cells and the hEHs were the major factors contributing to the hepatic maturation of hEHs (Fig. 4). Because Swiss 3T3 cell-derived soluble factors partially induce maturation of hEHs (Fig. 4A and B), it would also be interesting to search for hepatic maturation factors secreted from Swiss 3T3 cells.

To further investigate the maturation factors, we examined whether type I collagen, which is abundantly synthesized by Swiss 3T3 cells, could promote hepatic maturation. Stratification of type I collagen gel could lead to a promotion of hepatic maturation of hEHs-mono as well as hEHs-Swiss (Fig. 5A). We also found that hepatic maturation by 3D co-culture with the Swiss 3T3 cell sheet was suppressed by inhibition of collagen synthesis (Fig. 5D). Taken together, these results show that type I collagen is one of the key molecules in promotion of hepatic maturation by stratification of Swiss 3T3 cells. It is known that the space of Disse, which faces hepatocytes directly, contains various kinds of ECM proteins, including type I collagen [42]. Because the conditions in 3D co-culture, which contains type I collagen synthesized from Swiss 3T3 cells, can mimic the *in vivo* liver microstructure, including the space of Disse, the hepatic maturation from hEHs and hiPHs might be efficiently promoted. Furthermore, it was also reported that, by the stratification of type I collagen gel in primary rat hepatocyte culture, the cytoskeletal organizations, such as actin localization, in primary rat hepatocytes were changed and stress fibers were obliterated just as in the *in vivo* state [43]. They also showed that the stratification of type I collagen gel in primary rat hepatocyte culture maintained ALB secretion in primary rat hepatocyte. Thus, the alteration of the cytoskeletal organization might also be changed in the hEHs and hiPHs by 3D co-culture with the Swiss 3T3 cell sheet. For these reasons, it could be speculated that stratification of Swiss 3T3 cell sheets positively affects the maturation process of hEHs and hiPHs mediated by cell-to-cell and cell-type I collagen–cell interactions. The expression level of the *CK7* gene in the hEHs was down-regulated by stratification of the Swiss 3T3 cell sheet or type I collagen gel (Figs. 2C and 5B). Although Matrigel, which contains large amount of type IV collagen, is widely used to differentiate hESCs and hiPSCs into hepatocyte-like cells, it is reported that type IV collagen promotes cholangiocyte differentiation [44]. Therefore, it would be important to note that stratification of Swiss 3T3 cell sheet inhibits the cholangiocyte differentiation and thereby allows the cells to drive the way to hepatic differentiation. Although we showed that a Swiss 3T3 cell-derived type I collagen plays an important role in hepatic maturation, it was likely that the other soluble factors would also be involved in the promotion of hepatic maturation.

We employed Swiss 3T3 cells for 3D co-culture with the hEHs and hiPHs. However, it would be an attractive study to employ other kinds of cells such as liver sinusoidal endothelial cells, stellate

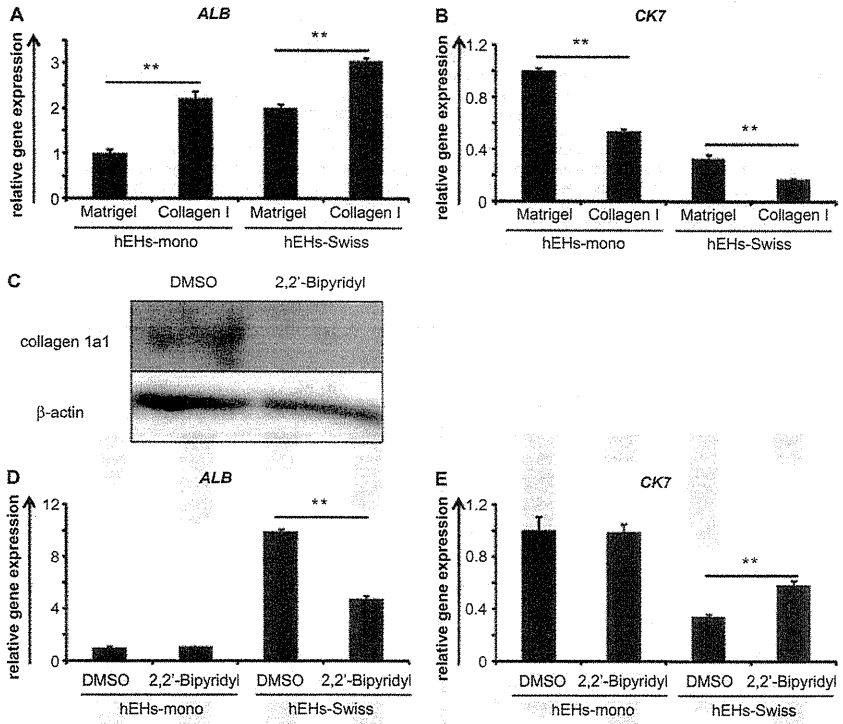

Fig. 5. Stratification of type I collagen gel promotes hepatic maturation. (A and B) hESCs (H9) were differentiated into hepatocyte-like cells as described in Fig. 1A until day 14, and then type I collagen gel (collagen I) or Matrigel are stratified on monolayer hESC-derived hepatocyte-like cells (hEHs-mono) and hESC-derived hepatocyte-like cells stratified with Swiss 3T3 cell sheet (hEHs-Swiss). On day 25, the gene expression levels of *ALB* (A) and *CK7* (B) were examined in hEHs-mono and hEHs-Swiss cultured with Matrigel or type I collagen gel by real-time RT-PCR. (C) Swiss 3T3 cells were cultured with 2,2′-Bipyridyl or solvent (0.1% DMSO) for 3 days, and then the expression of type I collagen precursor, col1a1, in these cells were detected by Western blot analysis. (D and E) hESCs (H9) were differentiated into hepatocyte-like cells as described in Fig. 1A. After stratification of Swiss 3T3 cells on day 14, these cells were treated with 2,2′-Bipyridyl or solvent (0.1% DMSO). On day 25, the gene expression levels of *ALB* (D) and *CK7* (E) were examined in hEHs-mono and hEHs-Swiss treated with 2,2′-Bipyridyl or solvent (0.1% DMSO) by real-time RT-PCR. The values were graphed as the fold-changes relative to hEHs-mono cultured with Matrigel. All data are represented as means ± SD ($n = 3$). $^{**}P < 0.01$.

cells, and Kupffer cells, to mimic the *in vivo* liver microstructure. By mimicking the *in vivo* liver microstructure, basic molecular mechanisms, including cell–cell interactions, in liver development would be clarified. Moreover, because our cell sheet technology allows us to stratify the multiple cell sheets and create layered 3D tissue constructs, combinations with multiple layers consisting of various types of cells might be able to develop an efficient method for hepatic maturation of the hEHs and hiPHs. In addition, by using new biomaterials with cell patterning techniques, more mature hepatocyte-like cells would be probably generated from human pluripotent stem cells, and thereby accelerate the research into tissue generation.

5. Conclusions

We succeeded in promoting the hepatic maturation of both the hEHs and hiPHs by stratification of the Swiss 3T3 cell sheet using a cell sheet engineering technology. We also determined that type I collagen, which is synthesized in Swiss 3T3 cells, plays an important role in hepatic maturation. Since our cell sheet engineering technology enables us to stratify multiple cell sheets, this technology would have the potential to mimic the *in vivo* liver microstructure and to generate hepatocyte-like cells, which have functions similar to primary hepatocytes. Our methods would be powerful tools for *in vitro* applications, such as drug toxicity screening in the early phase of pharmaceutical development.

Acknowledgements

We thank Misae Nishijima, Miki Yoshioka, Nobue Hirata, and Hiroko Matsumura for their excellent technical support. We also thank Tetsutaro Kikuchi (Cell Seed Inc) for providing a cell sheet stamp manipulator system. HM, KK, MKF, and TH were supported by grants from the Ministry of Health, Labor, and Welfare of Japan (MEXT). HM was also supported by Japan Research foundation For Clinical Pharmacology and The Uehara Memorial Foundation. KO was supported by Special Coordination Funds for Promoting Science and Technology from MEXT. FS was supported by Program for Promotion of Fundamental Studies in Health Sciences of the National Institute of Biomedical Innovation (NIBIO).

Appendix A. Supplementary data

Supplementary data associated with this article can be found, in the online version, at doi:10.1016/j.biomaterials.2012.03.011.

References

[1] Thomson JA, Itskovitz-Eldor J, Shapiro SS, Waknitz MA, Swiergiel JJ, Marshall VS, et al. Embryonic stem cell lines derived from human blastocysts. Science 1998;282:1145–7.
[2] Takahashi K, Tanabe K, Ohnuki M, Narita M, Ichisaka T, Tomoda K, et al. Induction of pluripotent stem cells from adult human fibroblasts by defined factors. Cell 2007;131:861–72.
[3] Duan Y, Catana A, Meng Y, Yamamoto N, He S, Gupta S, et al. Differentiation and enrichment of hepatocyte-like cells from human embryonic stem cells in vitro and in vivo. Stem Cells 2007;25:3058–68.
[4] Touboul T, Hannan NR, Corbineau S, Martinez A, Martinet C, Branchereau S, et al. Generation of functional hepatocytes from human embryonic stem cells under chemically defined conditions that recapitulate liver development. Hepatology 2010;51:1754–65.
[5] Brolen G, Sivertsson L, Bjorquist P, Eriksson G, Ek M, Semb H, et al. Hepatocyte-like cells derived from human embryonic stem cells specifically via definitive endoderm and a progenitor stage. J Biotechnol 2010;145:284–94.
[6] Cai J, Zhao Y, Liu Y, Ye F, Song Z, Qin H, et al. Directed differentiation of human embryonic stem cells into functional hepatic cells. Hepatology 2007;45:1229–39.
[7] Snykers S, De Kock J, Rogiers V, Vanhaecke T. In vitro differentiation of embryonic and adult stem cells into hepatocytes: state of the art. Stem Cells 2009;27:577–605.
[8] Kamiya A, Kinoshita T, Miyajima A. Oncostatin M and hepatocyte growth factor induce hepatic maturation via distinct signaling pathways. FEBS Lett 2001;492:90–4.
[9] Si-Tayeb K, Lemaigre FP, Duncan SA. Organogenesis and development of the liver. Dev Cell 2010;18:175–89.
[10] Duan Y, Ma X, Zou W, Wang C, Bahbahan IS, Ahuja TP, et al. Differentiation and characterization of metabolically functioning hepatocytes from human embryonic stem cells. Stem Cells 2010;28:674–86.
[11] Inamura M, Kawabata K, Takayama K, Tashiro K, Sakurai F, Katayama K, et al. Efficient generation of hepatoblasts from human ES cells and iPS cells by transient overexpression of homeobox gene HEX. Mol Ther 2011;19:400–7.
[12] Takayama K, Inamura M, Kawabata K, Katayama K, Higuchi M, Tashiro K, et al. Efficient generation of functional hepatocytes from human embryonic stem cells and induced pluripotent stem cells by HNF4alpha transduction. Mol Ther 2012;20:127–37.
[13] Takayama K, Inamura M, Kawabata K, Tashiro K, Katayama K, Sakurai F, et al. Efficient and directive generation of two distinct endoderm lineages from human ESCs and iPSCs by differentiation stage-specific SOX17 transduction. PLoS One 2011;6:e21780.
[14] Zaret KS. Liver specification and early morphogenesis. Mech Dev 2000;92:83–8.
[15] Matsumoto K, Yoshitomi H, Rossant J, Zaret KS. Liver organogenesis promoted by endothelial cells prior to vascular function. Science 2001;294:559–63.
[16] Kinoshita T, Sekiguchi T, Xu MJ, Ito Y, Kamiya A, Tsuji K, et al. Hepatic differentiation induced by oncostatin M attenuates fetal liver hematopoiesis. Proc Natl Acad Sci USA 1999;96:7265–70.
[17] Ohashi K, Yokoyama T, Yamato M, Kuge H, Kanehiro H, Tsutsumi M, et al. Engineering functional two- and three-dimensional liver systems in vivo using hepatic tissue sheets. Nat Med 2007;13:880–5.
[18] Yamasaki C, Tateno C, Aratani A, Ohnishi C, Katayama S, Kohashi T, et al. Growth and differentiation of colony-forming human hepatocytes in vitro. J Hepatol 2006;44:749–57.
[19] Sato H, Funahashi M, Kristensen DB, Tateno C, Yoshizato K. Pleiotrophin as a Swiss 3T3 cell-derived potent mitogen for adult rat hepatocytes. Exp Cell Res 1999;246:152–64.
[20] Hui EE, Bhatia SN. Micromechanical control of cell-cell interactions. Proc Natl Acad Sci USA 2007;104:5722–6.
[21] Khetani SR, Szulgit G, Del Rio JA, Barlow C, Bhatia SN. Exploring interactions between rat hepatocytes and nonparenchymal cells using gene expression profiling. Hepatology 2004;40:545–54.
[22] Abu-Absi SF, Hansen LK, Hu WS. Three-dimensional co-culture of hepatocytes and stellate cells. Cytotechnology 2004;45:125–40.
[23] Gu J, Shi X, Zhang Y, Chu X, Hang H, Ding Y. Establishment of a three-dimensional co-culture system by porcine hepatocytes and bone marrow mesenchymal stem cells in vitro. Hepatol Res 2009;39:398–407.
[24] Thomas RJ, Bhandari R, Barrett DA, Bennett AJ, Fry JR, Powe D, et al. The effect of three-dimensional co-culture of hepatocytes and hepatic stellate cells on key hepatocyte functions in vitro. Cells Tissues Organs 2005;181:67–79.
[25] Kim K, Ohashi K, Utoh R, Kano K, Okano T. Preserved liver-specific functions of hepatocytes in 3D co-culture with endothelial cell sheets. Biomaterials 2012;33:1406–13.
[26] Harimoto M, Yamato M, Hirose M, Takahashi C, Isoi Y, Kikuchi A, et al. Novel approach for achieving double-layered cell sheets co-culture: overlaying endothelial cell sheets onto monolayer hepatocytes utilizing temperature-responsive culture dishes. J Biomed Mater Res 2002;62:464–70.
[27] Yu YD, Kim KH, Lee SG, Choi SY, Kim YC, Byun KS, et al. Hepatic differentiation from human embryonic stem cells using stromal cells. J Surg Res 2011;170:e253–61.
[28] Tuleuova N, Lee JY, Lee J, Ramanculov E, Zern MA, Revzin A. Using growth factor arrays and micropatterned co-cultures to induce hepatic differentiation of embryonic stem cells. Biomaterials 2010;31:9221–31.
[29] Miki T, Ring A, Gerlach J. Hepatic differentiation of human embryonic stem cells is promoted by three-dimensional dynamic perfusion culture conditions. Tissue Eng Part C Methods 2011;17:557–68.
[30] Kawabata K, Sakurai F, Yamaguchi T, Hayakawa T, Mizuguchi H. Efficient gene transfer into mouse embryonic stem cells with adenovirus vectors. Mol Ther 2005;12:547–54.
[31] Maizel Jr JV, White DO, Scharff MD. The polypeptides of adenovirus. I. Evidence for multiple protein components in the virion and a comparison of types 2, 7A, and 12. Virology 1968;36:115–25.
[32] Furue MK, Na J, Jackson JP, Okamoto T, Jones M, Baker D, et al. Heparin promotes the growth of human embryonic stem cells in a defined serum-free medium. Proc Natl Acad Sci USA 2008;105:13409–14.
[33] Sasagawa T, Shimizu T, Sekiya S, Haraguchi Y, Yamato M, Sawa Y, et al. Design of prevascularized three-dimensional cell-dense tissues using a cell sheet stacking manipulation technology. Biomaterials 2010;31:1646–54.
[34] Lemaigre F, Zaret KS. Liver development update: new embryo models, cell lineage control, and morphogenesis. Curr Opin Genet Dev 2004;14:582–90.
[35] Zhao R, Duncan SA. Embryonic development of the liver. Hepatology 2005;41:956–67.
[36] Suzuki A. Role for growth factors and extracellular matrix in controlling differentiation of prospectively isolated hepatic stem cells. Development 2003;130:2513–24.
[37] Goldberg B. Collagen synthesis as a marker for cell type in mouse 3T3 lines. Cell 1977;11:169–72.
[38] Han S, Dziedzic N, Gadue P, Keller GM, Gouon-Evans V. An endothelial cell niche induces hepatic specification through Dual Repression of Wnt and Notch signaling. Stem Cells 2011;29:217–28.
[39] Kim K, Doi A, Wen B, Ng K, Zhao R, Cahan P, et al. Epigenetic memory in induced pluripotent stem cells. Nature 2010;467:285–90.
[40] Polo JM, Liu S, Figueroa ME, Kulalert W, Eminli S, Tan KY, et al. Cell type of origin influences the molecular and functional properties of mouse induced pluripotent stem cells. Nat Biotechnol 2010;28:848–55.
[41] Kleger A, Mahaddalkar P, Katz SF, Lechel A, Ju JY, Loya K, et al. Increased Reprogramming capacity of mouse liver progenitor cells, compared with differentiated liver cells, Requires BAF Complex. Gastroenterology, in press.
[42] Martinez-Hernandez A. The hepatic extracellular matrix. I. Electron immunohistochemical studies in normal rat liver. Lab Invest 1984;51:57–74.
[43] Dunn JC, Tompkins RG, Yarmush ML. Long-term in vitro function of adult hepatocytes in a collagen sandwich configuration. Biotechnol Prog 1991;7:237–45.
[44] Tanimizu N, Saito H, Mostov K, Miyajima A. Long-term culture of hepatic progenitors derived from mouse Dlk+ hepatoblasts. J Cell Sci 2004;117:6425–34.

EASL EUROPEAN ASSOCIATION FOR THE STUDY OF THE LIVER | JOURNAL OF HEPATOLOGY

Generation of metabolically functioning hepatocytes from human pluripotent stem cells by FOXA2 and HNF1α transduction

Kazuo Takayama[1,2], Mitsuru Inamura[1,2], Kenji Kawabata[2,3], Michiko Sugawara[4], Kiyomi Kikuchi[4], Maiko Higuchi[2], Yasuhito Nagamoto[1,2], Hitoshi Watanabe[1,2], Katsuhisa Tashiro[2], Fuminori Sakurai[1], Takao Hayakawa[5,6], Miho Kusuda Furue[7,8], Hiroyuki Mizuguchi[1,2,9,*]

[1]*Laboratory of Biochemistry and Molecular Biology, Graduate School of Pharmaceutical Sciences, Osaka University, Osaka 565-0871, Japan;* [2]*Laboratory of Stem Cell Regulation, National Institute of Biomedical Innovation, Osaka 567-0085, Japan;* [3]*Laboratory of Biomedical Innovation, Graduate School of Pharmaceutical Sciences, Osaka University, Osaka 565-0871, Japan;* [4]*Tsukuba Laboratories, Eisai Co., Ltd., Ibaraki 300-2635, Japan;* [5]*Pharmaceutics and Medical Devices Agency, Tokyo 100-0013, Japan;* [6]*Pharmaceutical Research and Technology Institute, Kinki University, Osaka 577-8502, Japan;* [7]*Laboratory of Cell Cultures, Department of Disease Bioresources Research, National Institute of Biomedical Innovation, Osaka 567-0085, Japan;* [8]*Laboratory of Cell Processing, Institute for Frontier Medical Sciences, Kyoto University, Kyoto 606-8507, Japan;* [9]*The Center for Advanced Medical Engineering and Informatics, Osaka University, Osaka 565-0871, Japan*

Background & Aims: Hepatocyte-like cells differentiated from human embryonic stem cells (hESCs) and induced pluripotent stem cells (hiPSCs) can be utilized as a tool for screening for hepatotoxicity in the early phase of pharmaceutical development. We have recently reported that hepatic differentiation is promoted by sequential transduction of SOX17, HEX, and HNF4α into hESC- or hiPSC-derived cells, but further maturation of hepatocyte-like cells is required for widespread use of drug screening.
Methods: To screen for hepatic differentiation-promoting factors, we tested the seven candidate genes related to liver development.
Results: The combination of two transcription factors, FOXA2 and HNF1α, promoted efficient hepatic differentiation from hESCs and hiPSCs. The expression profile of hepatocyte-related genes (such as genes encoding cytochrome P450 enzymes, conjugating enzymes, hepatic transporters, and hepatic nuclear receptors) achieved with FOXA2 and HNF1α transduction was comparable to that obtained in primary human hepatocytes. The hepatocyte-like cells generated by FOXA2 and HNF1α transduction exerted various hepatocyte functions including albumin and urea secretion, and the uptake of indocyanine green and low density lipoprotein. Moreover, these cells had the capacity to metabolize all nine tested drugs and were successfully employed to evaluate drug-induced cytotoxicity.
Conclusions: Our method employing the transduction of FOXA2 and HNF1α represents a useful tool for the efficient generation of metabolically functional hepatocytes from hESCs and hiPSCs, and the screening of drug-induced cytotoxicity.

Keywords: FOXA2; HNF1α; Hepatocytes; Adenovirus; Drug screening; Drug metabolism; hESCs; hiPSCs.
Received 14 November 2011; received in revised form 31 March 2012; accepted 4 April 2012; available online 29 May 2012
* Corresponding author. Address: Laboratory of Biochemistry and Molecular Biology, Graduate School of Pharmaceutical Sciences, Osaka University, 1-6 Yamadaoka, Suita, Osaka 565-0871, Japan. Tel.: +81 6 6879 8185; fax: +81 6 6879 8186.
E-mail address: mizuguch@phs.osaka-u.ac.jp (H. Mizuguchi).

Introduction

Hepatocyte-like cells differentiated from human embryonic stem cells (hESCs) [1] or human induced pluripotent stem cells (hiPSCs) [2] have more advantages than primary human hepatocytes (PHs) for drug screening. While application of PHs in drug screening has been hindered by lack of cellular growth, loss of function, and de-differentiation *in vitro* [3], hESC- or hiPSC-derived hepatocyte-like cells (hESC-hepa or hiPSC-hepa, respectively) have potential to solve these problems.

Hepatic differentiation from hESCs and hiPSCs can be divided into four stages: definitive endoderm (DE) differentiation, hepatic commitment, hepatic expansion, and hepatic maturation. Various growth factors are required to mimic liver development [4] and to promote hepatic differentiation. Previously, we showed that transduction of transcription factors in addition to treatment with optimal growth factors was effective to enhance hepatic differentiation [5–7]. An almost homogeneous hepatocyte population was obtained by sequential transduction of SOX17, HEX, and HNF4α into hESC- or hiPSCs-derived cells [7]. However, further maturation of the hESC-hepa and hiPSC-hepa is required for widespread use of drug screening because the drug metabolism capacity of these cells was not sufficient.

In some previous reports, hESC-hepa and hiPSC-hepa have been characterized for their hepatocyte functions in numerous ways, including functional assessment such as glycogen storage and low density lipoprotein (LDL) uptake [7]. To make a more precise judgment as to whether hESC-hepa and hiPSC-hepa can be applied to drug screening, it is more important to assess cytochrome P450 (CYP) induction potency and drug metabolism capacity rather than general hepatocyte function. Although Duan *et al.* have examined the drug metabolism capacity of hESC-hepa, drug metabolites were measured at 24 or 48 h [8]. To precisely estimate the drug metabolism capacity, the amount of metabolites must be measured during the time when production of metabolites is linearly detected (generally before 24 h). To the best of our knowledge, there have been few reports that have examined various drugs metabolism capacity of hESC-hepa and hiPSC-hepa in detail.

In the present study, seven candidate genes (*FOXA2*, *HEX*, *HNF1α*, *HNF1β*, *HNF4α*, *HNF6*, and *SOX17*) were transduced into each stage of hepatic differentiation from hESCs by using an adenovirus (Ad) vector to screen for hepatic differentiation-promoting factors. Then, hepatocyte-related gene expression profiles and hepatocyte functions in hESC-hepa and hiPSC-hepa generated by the optimized protocol, were examined to investigate whether these cells have PHs characteristics. We used nine drugs, which are metabolized by various CYP enzymes and UDP-glucuronosyltransferases (UGTs), to determine whether the hESC-hepa and hiPSC-hepa have drug metabolism capacity. Furthermore, hESC-hepa and hiPSC-hepa were examined to determine whether these cells may be applied to evaluate drug-induced cytotoxicity.

Materials and methods

In vitro differentiation

Before the initiation of cellular differentiation, the medium of hESCs and hiPSCs was exchanged for a defined serum-free medium, hESF9, and cultured as previously reported [9]. The differentiation protocol for the induction of DE cells, hepatoblasts, and hepatocytes was based on our previous report with some modifications [5,6]. Briefly, in mesendoderm differentiation, hESCs and hiPSCs were dissociated into single cells by using Accutase (Millipore) and cultured for 2 days on Matrigel (BD biosciences) in differentiation hESF-DIF medium which contains 100 ng/ml Activin A (R&D Systems) and 10 ng/ml bFGF (hESF-DIF medium, Cell Science & Technology Institute; differentiation hESF-DIF medium was supplemented with 10 μg/ml human recombinant insulin, 5 μg/ml human apotransferrin, 10 μM 2-mercaptoethanol, 10 μM ethanolamine, 10 μM sodium selenite, and 0.5 mg/ml bovine serum albumin, all from Sigma). To generate DE cells, mesendoderm cells were transduced with 3000 VP/cell of Ad-FOXA2 for 1.5 h on day 2 and cultured until day 6 on Matrigel in differentiation hESF-DIF medium supplemented with 100 ng/ml Activin A and 10 ng/ml bFGF. For induction of hepatoblasts, the DE cells were transduced with each 1500 VP/cell of Ad-FOXA2 and Ad-HNF1α for 1.5 h on day 6 and cultured for 3 days on Matrigel in hepatocyte culture medium (HCM, Lonza) supplemented with 30 ng/ml bone morphogenetic protein 4 (BMP4, R&D Systems) and 20 ng/ml FGF4 (R&D Systems). In hepatic expansion, the hepatoblasts were transduced with each 1500 VP/cell of Ad-FOXA2 and Ad-HNF1α for 1.5 h on day 9 and cultured for 3 days on Matrigel in HCM supplemented with 10 ng/ml hepatocyte growth factor (HGF), 10 ng/ml FGF1, 10 ng/ml FGF4, and 10 ng/ml FGF10 (all from R&D Systems). In hepatic maturation, cells were cultured for 8 days on Matrigel in L15 medium (Invitrogen) supplemented with 8.3% tryptose phosphate broth (BD biosciences), 10% FBS (Vita), 10 μM hydrocortisone 21-hemisuccinate (Sigma), 1 μM insulin, 25 mM $NaHCO_3$ (Wako), 20 ng/ml HGF, 20 ng/ml Oncostatin M (OsM, R&D systems), and 10^{-6} M Dexamethasone (DEX, Sigma).

Results

Recently, we showed that the sequential transduction of SOX17, HEX, and HNF4α into hESC-derived mesendoderm, DE, and hepatoblasts, respectively, leads to efficient generation of the hESC-hepa [5–7]. In the present study, to further improve the differentiation efficiency towards hepatocytes, we screened for hepatic differentiation-promoting transcription factors. Seven candidate genes involved in liver development were selected. We then examined the function of the hESC-hepa and hiPSC-hepa generated by the optimized protocol for pharmaceutical use in detail.

Efficient hepatic differentiation by Ad-FOXA2 and Ad-HNF1α transduction

To perform efficient DE differentiation, T-positive hESC-derived mesendoderm cells (day 2) (Supplementary Fig. 1) were transduced with Ad vector expressing various transcription factors (Ad-FOXA2, Ad-HEX, Ad-HNF1α, Ad-HNF1β, Ad-HNF4α, Ad-HNF6, and Ad-SOX17 were used in this study). We ascertained the expression of *FOXA2*, *HEX*, *HNF1α*, *HNF1β*, *HNF4α*, *HNF6*, or *SOX17* in Ad-FOXA2-, Ad-HEX-, Ad-HNF1α-, Ad-HNF1β-, Ad-HNF4α-, Ad-HNF6-, or Ad-SOX17-transduced cells, respectively (Supplementary Fig. 2). We also verified that there was no cytotoxicity of the cells transduced with Ad vector until the total amount of Ad vector reached 12,000 VP/cell (Supplementary Fig. 3). Each transcription factor was expressed in hESC-derived mesendoderm cells on day 2 by using Ad vector, and the efficiency of DE differentiation was examined (Fig. 1A). The DE differentiation efficiency based on CXCR4-positive cells was the highest when Ad-SOX17 or Ad-FOXA2 were transduced (Fig. 1B). To investigate the difference between Ad-FOXA2-transduced cells and Ad-SOX17-transduced cells, gene expression levels of markers of undifferentiated cells, mesendoderm cells, DE cells, and extraembryonic endoderm cells were examined (Fig. 1C). The expression levels of extraembryonic endoderm markers of Ad-SOX17-transduced cells were higher than those of Ad-FOXA2-transduced cells. Therefore, we concluded that FOXA2 transduction is suitable for use in selective DE differentiation.

To promote hepatic commitment, various transcription factors were transduced into DE cells and the resulting phenotypes were examined on day 9 (Fig. 1D). Nearly 100% of the population of Ad-FOXA2-transduced cells and Ad-HNF1α-transduced cells was α-fetoprotein (AFP)-positive (Fig. 1E). We expected that hepatic commitment would be further accelerated by combining FOXA2 and HNF1α transduction. The DE cells were transduced with both Ad-FOXA2 and Ad-HNF1α, and then the gene expression levels of *CYP3A7* [10], which is a marker of fetal hepatocytes, were evaluated (Fig. 1F). When both Ad-FOXA2 and Ad-HNF1α were transduced into DE cells, the promotion of hepatic commitment was greater than in Ad-FOXA2-transduced cells or Ad-HNF1α-transduced cells.

To promote hepatic expansion and maturation, we transduced various transcription factors into hepatoblasts on day 9 and 12 and the resulting phenotypes were examined on day 20 (Fig. 1G). We ascertained that the hepatoblast population was efficiently expanded by addition of HGF, FGF1, FGF4, and FGF10 (Supplementary Fig. 4). The hepatic differentiation efficiency based on asialoglycoprotein receptor 1 (ASGR1)-positive cells was measured on day 20, demonstrating that FOXA2, HNF1α, and HNF4α transduction could promote efficient hepatic maturation (Fig. 1H). To investigate the phenotypic difference between Ad-FOXA2-, Ad-HNF1α-, and Ad-HNF4α-transduced cells, gene expression levels of early hepatic markers, mature hepatic markers, and biliary markers were examined (Fig. 1I). Gene expression levels of mature hepatic markers were up-regulated by FOXA2, HNF1α, or HNF4α transduction. FOXA2 transduction strongly upregulated gene expression levels of both early hepatic markers and mature hepatic markers, while HNF1α or HNF4α transduc-

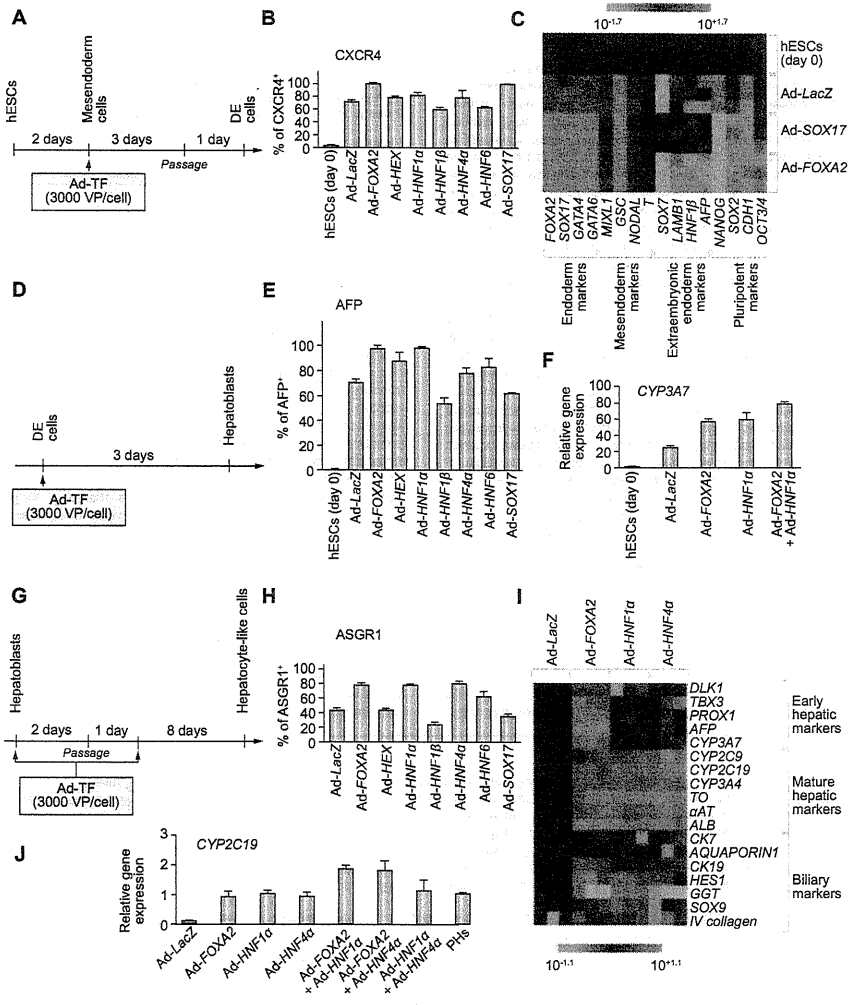

Fig. 1. Efficient hepatic differentiation from hESCs by FOXA2 and HNF1α transduction. (A) The schematic protocol describes the strategy for DE differentiation from hESCs (H9). Mesendoderm cells (day 2) were transduced with 3000 VP/cell of transcription factor (TF)-expressing Ad vector (Ad-TF) for 1.5 h and cultured as described in Fig. 2A. (B) On day 5, the efficiency of DE differentiation was measured by estimating the percentage of CXCR4-positive cells using FACS analysis. (C) The gene expression profiles were examined on day 5. (D) Schematic protocol describing the strategy for hepatoblast differentiation from DE. DE cells (day 6) were transduced with 3000 VP/cell of Ad-TF for 1.5 h and cultured as described in Fig. 2A. (E) On day 9, the efficiency of hepatoblast differentiation was measured by estimating the percentage of AFP-positive cells using FACS analysis. (F) The gene expression level of *CYP3A7* was measured by real-time RT-PCR on day 9. On the *y* axis, the gene expression level of *CYP3A7* in hESCs (day 0) was taken as 1.0. (G) The schematic protocol describes the strategy for hepatic differentiation from hepatoblasts. Hepatoblasts (day 9) were transduced with 3000 VP/cell of Ad-TF for 1.5 h and cultured as described in Fig. 2A. (H) On day 20, the efficiency of hepatic differentiation was measured by estimating the percentage of ASGR1-positive cells using FACS analysis. The detail results of FACS analysis are shown in Supplementary Table 1. (I) Gene expression profiles were examined on day 20. (J) Hepatoblasts (day 9) were transduced with 3000 VP/cell of Ad-TFs (in the case of combination transduction of two types of Ad vector, 1500 VP/cell of each Ad-TF was transduced) for 1.5 h and cultured. Gene expression levels of *CYP2C19* were measured by real-time RT-PCR on day 20. On the *y* axis, the gene expression level of *CYP2C19* in PHs, which were cultured for 48 h after the cells were plated, was taken as 1.0. All data are represented as mean ± SD (n = 3).

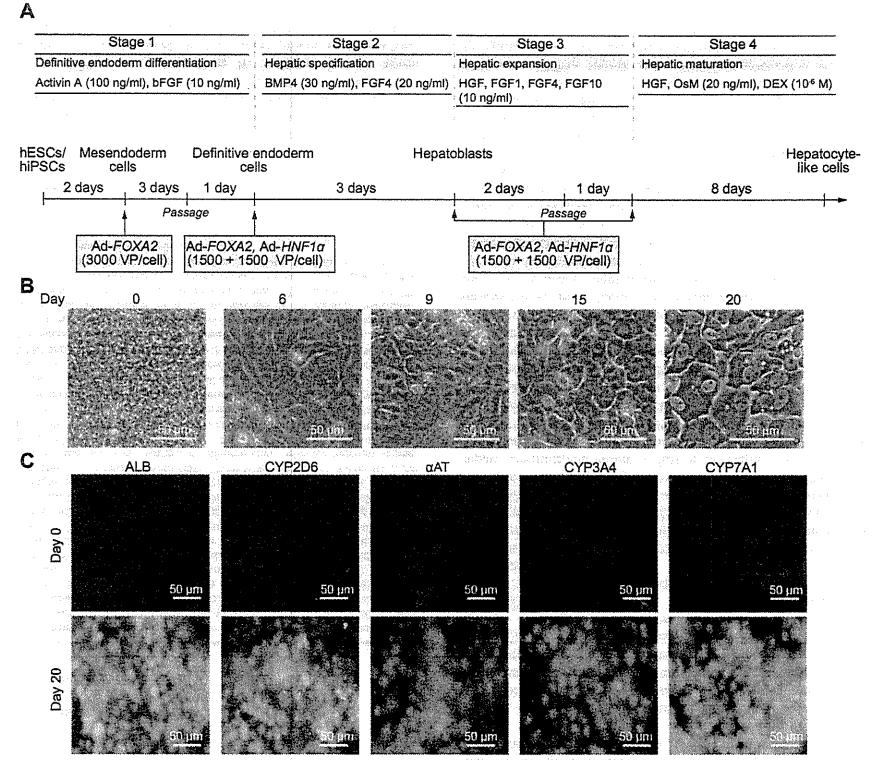

Fig. 2. Hepatic differentiation of hESCs and hiPSCs by FOXA2 and HNF1α transduction. (A) The differentiation procedure of hESCs and hiPSCs into hepatocytes via DE cells and hepatoblasts is schematically shown. Details of the hepatic differentiation procedure are described in Materials and methods. (B) Sequential morphological changes (day 0–20) of hESCs (H9) differentiated into hepatocytes are shown. (C) The expression of the hepatocyte markers (ALB, CYP2D6, αAT, CYP3A4, and CYP7A1, all green) was examined by immunohistochemistry on day 0 and 20. Nuclei were counterstained with DAPI (blue).

tion did not up-regulate the gene expression levels of early hepatic markers. Next, multiple transduction of transcription factors was performed to promote further hepatic maturation. The combination of Ad-FOXA2 and Ad-HNF1α transduction and the combination of Ad-FOXA2 and Ad-HNF4α transduction result in the most efficient hepatic maturation, judged from the gene expression levels of *CYP2C19* (Fig. 1J). This may happen because the mixture of immature hepatocytes and mature hepatocytes coor-

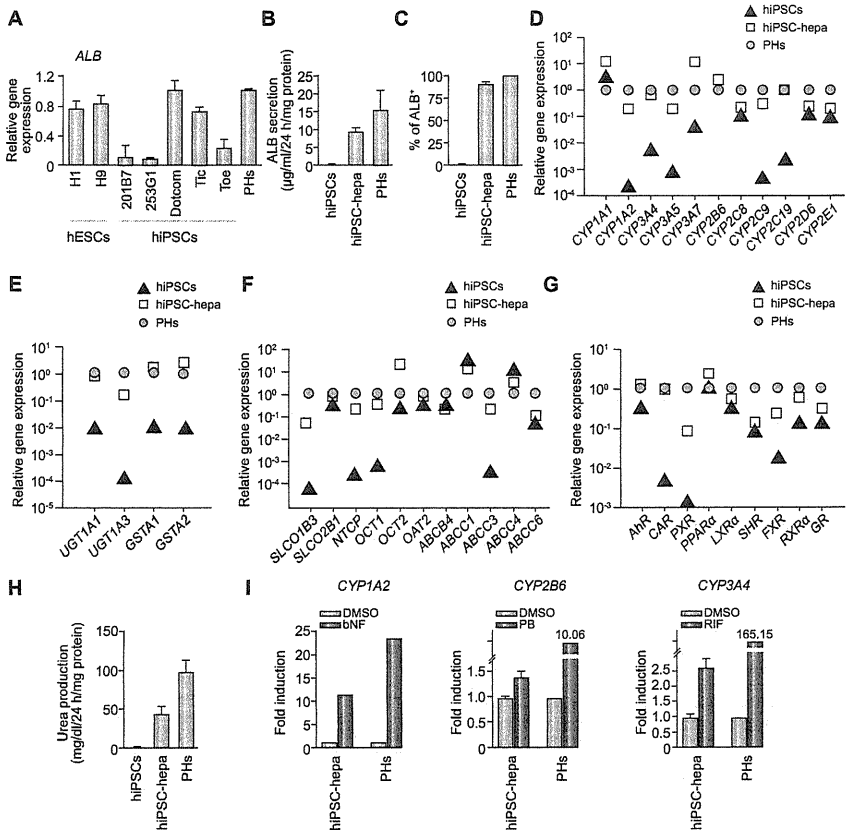

Fig. 3. The hepatic characterization of hiPSC-hepa. hESCs (H1 and H9) and hiPSCs (201B7, 253G1, Dotcom, Tic, and Toe) were differentiated into hepatocyte-like cells as described in Fig. 2A. (A) On day 20, the gene expression level of *ALB* was examined by real-time RT-PCR. On the *y* axis, the gene expression level of *ALB* in PHs, which were cultured for 48 h after cells were plated, was taken as 1.0. (B–I) hiPSCs (Dotcom) were differentiated into hepatocyte-like cells as described in Fig. 2A. (B) The amount of ALB secretion was examined by ELISA in hiPSCs, hiPSC-hepa, and PHs. (C) hiPSCs, hiPSC-hepa, and PHs were subjected to immunostaining with anti-ALB antibodies, and then the percentage of ALB-positive cells was examined by flow cytometry. (D–G) The gene expression levels of CYP enzymes (D), conjugating enzymes (E), hepatic transporters (F), and hepatic nuclear receptors (G) were examined by real-time RT-PCR in hiPSCs, hiPSC-hepa, and PHs. On the *y* axis, the expression level of PHs is indicated. (H) The amount of urea secretion was examined in hiPSCs, hiPSC-hepa, and PHs. (I) Induction of *CYP1A2*, *2B6*, or *3A4* by DMSO or inducer (bNF, PB, or RIF) of hiPSC-hepa and PHs, cultured for 48 h after the cells were plated, was examined. On the *y* axis, the gene expression levels of *CYP1A2*, *2B6*, or *3A4* in DMSO-treated cells, which were cultured for 48 h, were taken as 1.0. All data are represented as mean ± SD (n = 3).

dinately works to induce hepatocyte functions. Taken together, efficient hepatic differentiation could be promoted by using the combination of FOXA2 and HNF1α transduction at the optimal stage of differentiation (Fig. 2A). At the stage of hepatic expansion and maturation, Ad-HNF4α can be substituted for Ad-HNF1α (Fig. 1J). Interestingly, cell growth was delayed by FOXA2 and HNF4α transduction (Supplementary Fig. 5). This delay in cell proliferation might be due to promoted maturation by FOXA2 and HNF1α transduction. As the hepatic differentiation proceeds, the morphology of hESCs gradually changed into a typical hepatocyte morphology, with distinct round nuclei and a polygonal shape (Fig. 2B), and the expression levels of hepatic markers

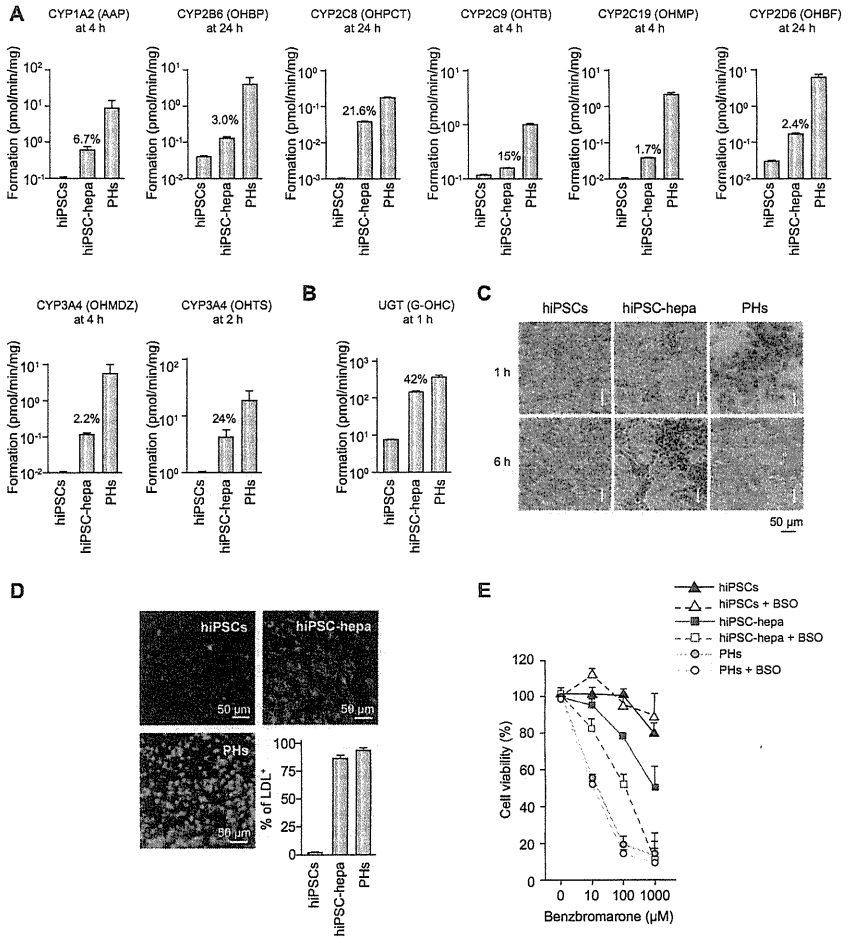

Fig. 4. Evaluation of the drug metabolism capacity and hepatic transporter activity of hiPSC-hepa. hiPSCs (Dotcom) were differentiated into hepatocytes as described in Fig. 2A. (A and B) Quantitation of metabolites in hiPSCs, hiPSC-hepa, and PHs, which were cultured for 48 h after the cells were plated, was examined by treating nine substrates (Phenacetin, Bupropion, Paclitazel, Tolbtamide, *S*-mephenytoin, Bufuralol, Midazolam, Testosterone, and Hydroxyl coumarin; these compounds are substrates for CYP1A2, 2B6, 2C8, 2C9, 2C19, 2D6, 3A4, 3A4 (A) and UGT (B), respectively), and then supernatants were collected at the indicated time. The quantity of metabolites (Acetaminophen [AAP], Hydroxybupropion [OHBP], 6α-hydroxypaclitaxel [OHPCT], Hydroxytolbutamide [OHTB], 4′-hydroxymephenytoin [OHMP], 1′-hydroxybufuralol [OHBF], 1′-hydroxymidazolam [OHMDZ], 6β-hydroxytestosterone [OHTS], 7-Hydroxycoumarin glucuronide [G-OHC], respectively) was measured by LC-MS/MS. The ratios of the activity levels in hiPSC-hepa to the activity levels in PHs rate are indicated in the graph. (C) hiPSCs, hiPSC-hepa, and PHs were examined for their ability to take up ICG (top) and release it 6 h thereafter (bottom). (D) hiPSCs, hiPSC-hepa, and PHs were cultured with medium containing Alexa-Flour 488-labeled LDL (green) for 1 h, and immunohistochemistry was performed. Nuclei were counterstained with DAPI (blue). The percentage of LDL-positive cells was also measured by FACS analysis. (E)

(ALB, CYP2D6, alpha-1-antitrypsin [αAT], CYP3A4, and CYP7A1) increased (Fig. 2C). Hepatic gene expression levels (Supplementary Fig. 6A), amount of ALB secretion (Supplementary Fig. 6B), and CYP2C9 activity level (Supplementary Fig. 6C) of Ad-FOXA2- and Ad-HNF1α-transduced cells were significantly higher than those of Ad-SOX17-, Ad-HEX-, and Ad-HNF4α-transduced cells. These results indicated that FOXA2 and HNF1α transduction promotes more efficiently hepatic differentiation than SOX17, HEX, and HNF4α transduction.

Characterization of the hESC-hepa/hiPSC-hepa

As we have previously reported [6], hepatic differentiation efficiency differs among hESC/hiPSC lines. Therefore, it is necessary to select a hESC/hiPSC line that is suitable for hepatic maturation in the case of medical applications such as drug screening. In the present study, two hESC lines and five hiPSCs lines were differentiated into hepatocyte-like cells, and then their gene expression levels of *ALB* (Fig. 3A) and *CYP3A4* (Supplementary Fig. 7A), and their CYP3A4 activities (Supplementary Fig. 7B) were compared. These data suggest that the iPSC line, Dotcom [11,12], was the most suitable for hepatocyte maturation. To examine whether the iPSC (Dotcom)-hepa has enough hepatic functions as compared with PHs, the amount of albumin (ALB) secretion (Fig. 3B) and the percentage of ALB-positive cells (Fig. 3C) were measured on day 20. The amount of ALB secretion in hiPSC-hepa was similar to that in PHs and the percentage of ALB-positive cells was approximately 90% in iPSC-hepa. We also confirmed that the gene expression levels of CYP enzymes (Fig. 3D), conjugating enzymes (Fig. 3E), hepatic transporters (Fig. 3F), and hepatic nuclear receptors (Fig. 3G) in hiPSC-hepa were similar to those of PHs, although some of them were still lower than those of PHs. Because the gene expression level of the fetal CYP isoform, *CYP3A7*, in hiPSC-hepa was higher than that of PHs, mature hepatocytes and hepatic precursors were still mixed. We have previously confirmed that Ad vector-mediated gene expression in the hepatoblasts (day 9) continued until day 14 and almost disappeared on day 18 [7]. Therefore, the hepatocyte-related genes expressed in hiPSC-hepa are not directly regulated by exogenous FOXA2 or HNF1α. Taken together, endogenous hepatocyte-related genes in hiPSC-hepa should have been upregulated by FOXA2 and HNF1α transduction.

To further confirm that hiPSC-hepa have sufficient levels of hepatocyte functions, we evaluated the ability of urea secretion (Fig. 3H) and glycogen storage (Supplementary Fig. 8). The amount of urea secretion in hiPSC-hepa was about half of that in PHs. HiPSC-hepa exhibited abundant storage of glycogen. Because CYP1A2, 2B6, and 3A4 are involved in the metabolism of a significant proportion of the currently available commercial drugs, we tested the induction of *CYP1A2*, *2B6*, and *3A4* by chemical stimulation (Fig. 3I). *CYP1A2*, *2B6*, and *3A4* are induced by β-naphthoflavone [bNF], phenobarbital [PB], or rifampicin [RIF], respectively. Although undifferentiated hiPSCs did not respond to either bNF, PB, or RIF (data not shown), hiPSC-hepa produced more metabolites in response to chemical stimulation, suggesting that inducible CYP enzymes were detectable in hiPSC-hepa (Fig. 3I). However, the induction potency of *CYP1A2*, *2B6*, and *3A4* in hiPSC-hepa were lower than that in PHs.

Drug metabolism capacity and hepatic transporter activity of hiPSC-hepa

Because metabolism and detoxification in the liver are mainly executed by CYP enzymes, conjugating enzymes, and hepatic transporters, it is important to assess the function of these enzymes and transporters in hiPSC-hepa. Among the various enzymes in liver, CYP1A2, 2B6, 2C8, 2C9, 2C19, 2D6 and 3A4, UGT are the important phase I and II enzymes responsible for metabolism. Nine substrates, Phenacetin, Bupropion, Paclitazel, Tolbtamide, *S*-mephenytoin, Bufuralol, Midazolam, Testosterone, and Hydroxyl coumarin, which are the substrates of CYP1A2, 2B6, 2C8, 2C9, 2C19, 2D6, 3A4, 3A4 (Fig. 4A), and UGT (Fig. 4B), respectively, were used to estimate the drug metabolism capacity of hiPSC-hepa compared with that of PHs. To precisely estimate the drug metabolism capacity, the amounts of metabolites were measured during the phase when production of metabolites was linear (Supplementary Fig. 9). These results indicated that our hiPSC-hepa have the capacity to metabolize these nine substrates, although the activity levels were lower than those of PHs. The hepatic functions of hiPSC-hepa were further evaluated by examining the ability to uptake Indocyanine Green (ICG) and LDL (Fig. 4C and D, respectively). In addition to PHs, hiPSC-hepa had the ability to uptake ICG and to excrete ICG in a culture without ICG for 6 h (Fig. 4C), and to uptake LDL (Fig. 4D). These results suggest that hiPSC-hepa have enough CYP enzyme activity, conjugating enzyme activity, and hepatic transporter activity to metabolize various drugs.

To examine whether our hiPSC-hepa could be used to predict metabolism-mediated toxicity, hiPSC-hepa were incubated with Benzbromarone, which is known to generate toxic metabolites, and then cell viability was measured (Fig. 4E). Cell viability of hiPSC-hepa was decreased depending on the concentration of Benzbromarone. However, cell viability of hiPSC-hepa was much higher than that of PHs. To detect drug–induced cytotoxicity with high sensitivity in hiPSC-hepa, these cells were treated with Buthionine-SR-sulfoximine (BSO), which depletes cellular GST, and result in a decrease of cell viability of hiPSC-hepa as compared with that of non-treated cells (Fig. 4E). These results indicated that hiPSC-hepa would be more useful in drug screening under a condition of knockdown of conjugating enzyme activity.

Discussion

The establishment of an efficient hepatic differentiation technology from hESCs and hiPSCs would be important for the application of hESC-hepa and hiPSC-hepa to drug toxicity screening. Although we have previously reported that sequential transduction of SOX17, HEX, and HNF4α into hESC-derived cells could promote efficient hepatic differentiation [7], further hepatic maturation of the hESC-hepa and hiPSC-hepa was needed for this application. To further improve the differentiation efficiency of every step of hepatic differentiation (hESC to DE cells, DE cells to hepatoblasts, and hepatoblasts to hESC-hepa), we initially performed a screening of transcription factors. In the stage of DE differentiation, FOXA2 transduction could promote the most efficient DE differentiation (Fig. 1C). In the stage of hepatic commitment, expansion, and maturation, the combination of FOXA2 and HNF1α transduction strongly promoted hepatic commitment and maturation (Fig. 1F and J), although in the stage of hepatic expansion and maturation, HNF4α transduction was as efficient as that of HNF1α (Fig. 1J). Since HNF1α is one of the target genes of HNF4α [13], the signaling through HNF4α to HNF1α would be important for efficient hepatic expansion and maturation. Considering these results together, we ascertained a pair of two transcription factors, FOXA2 and HNF1α, that could promote efficient hepatic differentiation from hESCs. In embryogenesis, the expression of FOXA2 and HNF1α is initially detected in DE or hepatoblasts, respectively and the expression levels of both FOXA2 and HNF1α are elevated as the liver develops [14,15]. Therefore, our hepatic differentiation technology, which employs FOXA2 and HNF1α transduction, might mimic the gene expression pattern during embryogenesis.

We found that the gene expression levels of CYP enzymes, conjugating enzymes, hepatic transporters, and hepatic nuclear receptors were upregulated by FOXA2 and HNF1α transduction (Fig. 3D–G). In contrast to the high expression levels of hepatocyte-related genes, CYP induction potency and the drug metabolism capacity of our hiPSC-hepa were lower than those of PHs (Figs. 3I and 4A and B). One of the possible reasons for the difference between gene expression levels of CYP enzymes and CYP induction activity might be that there were insufficient expression levels of hepatic nuclear receptors (such as *PXR*, *SHR*, and *FXR*) in hiPSC-hepa (Fig. 3G). Because many CYPs require high expression levels of hepatic nuclear receptor for efficient drug metabolism [16], transduction of these hepatic nuclear receptor genes in hiPSC-hepa or development of a differentiation method that induces high expression of these nuclear receptors might improve the drug metabolic capacity. Another explanation for the low CYP activities in hiPSC-hepa, maybe that hiPSCs were established from an individual with low CYP activities; infact, it is known that large individual differences in CYP activities are observed among individuals. It might be important to use a hiPSC line established from a person with high CYP activities. It is essential to investigate the reasons behind this significant discordance, an issue that our group is currently planning to study.

In summary, our method, consisting of sequential FOXA2 and HNF1α transduction along with the addition of adequate soluble factors at each step of differentiation, is a valuable tool for the efficient generation of functional hepatocytes derived from hESCs and hiPSCs. The hiPSC-hepa exhibited a number of hepatocyte functions (such as ALB secretion, uptake of LDL or ICG, glycogen storage, and drug metabolism capacity). In addition, the hiPSC-hepa were successfully applied to the evaluation of drug-induced cytotoxicity. Therefore, the hESC-hepa and hiPSC-hepa might be used for drug screening in early phases of pharmaceutical development.

The cell viability of hiPSCs, hiPSC-hepa, PHs, and their BSO-treated cells (0.4 mM BSO was pre-treated for 24 h) was assessed by Alamar Blue assay after 48-hr exposure to differe2nt concentrations of benzbromarone. The cell viability is expressed as a percentage of that in cells treated only with solvent. All data are represented as mean ± SD (n = 3).

Molecular and Cell Biology

Conflict of interest

The authors who have taken part in this study declared that they do not have anything to disclose regarding funding or conflict of interest with respect to this manuscript.

Acknowledgements

We thank Misae Nishijima, Nobue Hirata, Miki Yoshioka, and Hiroko Matsumura for their excellent technical support. We thank Ms. Ong Tyng Tyng for critical reading of the manuscript. HM, MKF, and TH were supported by grants from the Ministry of Health, Labor, and Welfare of Japan. HM was also supported by Japan Research foundation For Clinical Pharmacology, The Nakatomi Foundation, and The Uehara Memorial Foundation. K. Kawabata was supported by Grants from the Ministry of Education, Sports, Science and Technology of Japan (20200076) and the Ministry of Health, Labor, and Welfare of Japan. K. Katayama and FS were supported by Program for Promotion of Fundamental Studies in Health Sciences of the National Institute of Biomedical Innovation (NIBIO).

Supplementary data

Supplementary data associated with this article can be found, in the online version, at http://dx.doi.org/10.1016/j.jhep.2012.04.038.

References

[1] Thomson JA, Itskovitz-Eldor J, Shapiro SS, Waknitz MA, Swiergiel JJ, Marshall VS, et al. Embryonic stem cell lines derived from human blastocysts. Science 1998;282:1145–1147.
[2] Takahashi K, Tanabe K, Ohnuki M, Narita M, Ichisaka T, Tomoda K, et al. Induction of pluripotent stem cells from adult human fibroblasts by defined factors. Cell 2007;131:861–872.
[3] Clayton DF, Darnell Jr JE. Changes in liver-specific compared to common gene transcription during primary culture of mouse hepatocytes. Mol Cell Biol 1983;3:1552–1561.
[4] Snykers S, De Kock J, Rogiers V, Vanhaecke T. In vitro differentiation of embryonic and adult stem cells into hepatocytes: state of the art. Stem cells 2009;27:577–605.
[5] Inamura M, Kawabata K, Takayama K, Tashiro K, Sakurai F, Katayama K, et al. Efficient generation of hepatoblasts from human ES cells and iPS cells by transient overexpression of homeobox gene HEX. Mol Ther 2011;19:400–407.
[6] Takayama K, Inamura M, Kawabata K, Tashiro K, Katayama K, Sakurai F, et al. Efficient and directive generation of two distinct endoderm lineages from human ESCs and iPSCs by differentiation stage-specific SOX17 transduction. PLoS One 2011;6:e21780.
[7] Takayama K, Inamura M, Kawabata K, Katayama K, Higuchi M, Tashiro K, et al. efficient generation of functional hepatocytes from human embryonic stem cells and induced pluripotent stem cells by HNF4alpha transduction. Mol Ther 2012;20:127–137.
[8] Duan Y, Ma X, Zou W, Wang C, Bahbahan IS, Ahuja TP, et al. Differentiation and characterization of metabolically functioning hepatocytes from human embryonic stem cells. Stem cells 2010;28:674–686.
[9] Furue MK, Na J, Jackson JP, Okamoto T, Jones M, Baker D, et al. Heparin promotes the growth of human embryonic stem cells in a defined serum-free medium. Proc Natl Acad Sci U S A 2008;105:13409–13414.
[10] Lacroix D, Sonnier M, Moncion A, Cheron G, Cresteil T. Expression of CYP3A in the human liver–evidence that the shift between CYP3A7 and CYP3A4 occurs immediately after birth. Eur J Biochem 1997;247:625–634.

[11] Nagata S, Toyoda M, Yamaguchi S, Hirano K, Makino H, Nishino K, et al. Efficient reprogramming of human and mouse primary extra-embryonic cells to pluripotent stem cells. Genes Cells 2009;14:1395–1404.
[12] Makino H, Toyoda M, Matsumoto K, Saito H, Nishino K, Fukawatase Y, et al. Mesenchymal to embryonic incomplete transition of human cells by chimeric OCT4/3 (POU5F1) with physiological co-activator EWS. Exp Cell Res 2009;315:2727–2740.
[13] Gragnoli C, Lindner T, Cockburn BN, Kaisaki PJ, Gragnoli F, Marozzi G, et al. Maturity-onset diabetes of the young due to a mutation in the hepatocyte nuclear factor-4 alpha binding site in the promoter of the hepatocyte nuclear factor-1 alpha gene. Diabetes 1997;46:1648–1651.
[14] Ang SL, Wierda A, Wong D, Stevens KA, Cascio S, Rossant J, et al. The formation and maintenance of the definitive endoderm lineage in the mouse: involvement of HNF3/forkhead proteins. Development 1993;119:1301–1315.
[15] Kyrmizi I, Hatzis P, Katrakili N, Tronche F, Gonzalez FJ, Talianidis I. Plasticity and expanding complexity of the hepatic transcription factor network during liver development. Genes Dev 2006;20:2293–2305.
[16] Lehmann JM, McKee DD, Watson MA, Willson TM, Moore JT, Kliewer SA. The human orphan nuclear receptor PXR is activated by compounds that regulate CYP3A4 gene expression and cause drug interactions. J Clin Invest 1998;102:1016–1023.

STEM CELLS AND DEVELOPMENT
Volume 21, Number 18, 2012

DOI: 10.1089/scd.2012.0100

Inhibition of Lnk in Mouse Induced Pluripotent Stem Cells Promotes Hematopoietic Cell Generation

Katsuhisa Tashiro,[1,*] Miyuki Omori,[1,2,*] Kenji Kawabata,[1,3] Nobue Hirata,[1] Tomoko Yamaguchi,[1] Fuminori Sakurai,[2] Satoshi Takaki,[4] and Hiroyuki Mizuguchi[1,2,5]

Embryonic stem (ES) cell- and induced pluripotent stem (iPS) cell-derived hematopoietic stem/progenitor cells (HSPCs) are considered as an unlimited source for HSPC transplantation. However, production of immature hematopoietic cells, especially HSPCs, from ES and iPS cells has been challenging. The adaptor protein Lnk has been shown to negatively regulate HSPC function via the inhibition of thrombopoietin (TPO) and stem cell factor signaling, and Lnk-deficient HSPCs show an enhanced self-renewal and repopulation capacity. In this study, we examined the role of Lnk on the hematopoietic differentiation from mouse ES and iPS cells by the inhibition of Lnk using a dominant-negative mutant of the Lnk (*DN-Lnk*) gene. We generated mouse ES and iPS cells stably expressing a DN-Lnk, and found that enforced expression of a DN-Lnk in ES and iPS cells led to an enhanced generation of Flk-1-positive mesodermal cells, thereby could increase in the expression of hematopoietic transcription factors, including *Scl* and *Runx1*. We also showed that the number of both total hematopoietic cells and immature hematopoietic cells with colony-forming potential in DN-Lnk-expressing cells was significantly increased in comparison with that in control cells. Furthermore, Lnk inhibition by the overexpression of the *DN-Lnk* gene augmented the TPO-induced phosphorylation of Erk1/2 and Akt, indicating the enhanced sensitivity to TPO. Adenovirus vector-mediated transient *DN-Lnk* gene expression in ES and iPS cells could also increase the hematopoietic cell production. Our data clearly showed that the inhibition of Lnk in ES and iPS cells could result in the efficient generation and expansion of hematopoietic cells.

Introduction

Since embryonic stem (ES) cells and induced pluripotent stem (iPS) cells can self-renew indefinitely and differentiate into all types of cells in the 3 germ layers, they are expected to have clinical applications in cell-based therapies [1–4]. For instance, ES cell- and iPS cell-derived hematopoietic cells are considered as an alternative source of adult hematopoietic cells for the treatment of hematological disorders and malignancies. Many groups have reported the differentiation of ES and iPS cells into mature hematopoietic cells, including erythrocytes, myeloid cells, and lymphoid cells [5–10]. However, previous reports have described the generation of only small numbers of mature hematopoietic cells, probably as a result of inefficient generation and expansion of immature hematopoietic cells derived from pluripotent stem cells. Therefore, the use of ES cell- and iPS cell-derived hematopoietic cells as a cell source for therapeutic applications depends on the efficient production of hematopoietic cells, especially immature hematopoietic cells, from pluripotent stem cells.

Recently, inhibitors of differentiation (*ID*) genes, which are negative regulators of E proteins (E2A, HEB, and E2-2) [11], were shown to negatively regulate the hematopoietic differentiation in ES and iPS cells [12]. The same study also showed that the suppression of the ID genes, *ID1* and *ID3* increased the number of ES and iPS cell-derived hematopoietic progenitor cells [12]. These data indicate that negative regulators play an important role in the hematopoietic differentiation process in ES and iPS cells, and that manipulation of the expression of negative regulators would be an effective strategy for the efficient generation of hematopoietic cells from ES and iPS cells.

An adaptor protein Lnk/SH2B3 (hereafter referred to Lnk) is shown to negatively regulate the thrombopoietin (TPO) and stem cell factor (SCF) signaling, both of which are crucial

[1]Laboratory of Stem Cell Regulation, National Institute of Biomedical Innovation, Osaka, Japan.
[2]Laboratory of Biochemistry and Molecular Biology, Graduate School of Pharmaceutical Sciences, Osaka University, Osaka, Japan.
[3]Laboratory of Biomedical Innovation, Graduate School of Pharmaceutical Sciences, Osaka University, Osaka, Japan.
[4]Department of Immune Regulation, National Center for Global Health and Medicine, Research Institute, Tokyo, Japan.
[5]The Center for Advanced Medical Engineering and Informatics, Osaka University, Osaka, Japan.
*These two authors contributed equally to this work.

cytokine-signaling pathways involved in hematopoietic stem cell (HSC) self-renewal, since Lnk-deficient HSCs exhibit an augmented response to TPO and SCF stimulation, and thereby Lnk-deficient mice show the marked HSC expansion in the bone marrow [13–16]. In addition, Lnk is highly expressed in immature hematopoietic cells, particularly in HSCs [17], in contrast to ID genes, which are ubiquitously expressed in many tissues [11,18]. Therefore, we speculated that an inhibition of Lnk function in ES and iPS cells would lead to the efficient generation and expansion of immature hematopoietic cells. In the present study, we investigated the effects of Lnk inhibition on the hematopoietic differentiation of mouse ES and iPS cells, and we found that a suppression of Lnk function by the enforced expression of a dominant-negative mutant of the Lnk (*DN-Lnk*) gene in ES and iPS cells resulted in an increase in the number of both mesodermal cells with hematopoietic differentiation potential and immature hematopoietic cells. These findings indicate that the suppression of the Lnk would be useful for the efficient generation and expansion of ES cell- and iPS cell-derived hematopoietic cells.

Materials and Methods

Plasmid construction and adenovirus vectors

pEF-IRESneo, which contains internal ribosome entry sites (IRES) and a neomycin-resistant gene (*Neo*) downstream of the human elongation factor (EF)-1α promoter, was constructed by replacing the cytomegalovirus (CMV) promoter of pIRESneo (Clontech) with the EF-1α promoter, which is derived from pEF/myc/nuc (Invitrogen). Mouse DN-Lnk cDNA, derived from pMY-DN-Lnk [19], was inserted into pEFIRESneo, resulting in pEF-DNLnk-IRESneo. Adenovirus (Ad) vectors were constructed by an improved in vitro ligation method [20,21]. Mouse DN-Lnk cDNA was inserted into pHMCA5 [22], which contains the CMV enhancer/β-actin promoter with an β-actin intron (CA) promoter (a kind gift from Dr. J. Miyazaki, Osaka University) [23], resulting in pHMCA5-DN-Lnk. pHMCA5-DN-Lnk was digested with I-*Ceu*I/PI-*Sce*I and ligated into I-*Ceu*I/PI-*Sce*I-digested pAdHM4 [20], resulting in pAd-DN-Lnk. Ad-DN-Lnk and Ad-DsRed were generated and purified as described previously [24]. The CA promoter-driven β-galactosidase (LacZ)-expressing Ad vector, Ad-LacZ, and the CA promoter-driven DsRed-expressing Ad vector, Ad-DsRed, were generated previously [24,25]. The vector particle (VP) titer was determined using a spectrophotometric method [26].

Cell culture

The mouse ES cell line, BRC6 (Riken Bioresource Center), and the mouse iPS cell line, 38C2 (a kind gift from Dr. S. Yamanaka, Kyoto University) [27], were used in this study. DN-Lnk- or *Neo*-expressing mouse ES and iPS cell lines were generated as follows. The pEF-IRESneo and pEF-DNLnk-IRESneo were linearized and were then electroporated into mouse ES cells and iPS cells by using Gene Pulser Xcell (250 V, 500 μF; Bio-Rad Laboratory). pEF-IRESneo- or pEF-DNLnk-IRESneo-transfected ES cells and iPS cells were cultured in an ES cell medium containing 100 μg/mL G418 (for ES cells) or 200 μg/mL G418 (for iPS cells) for 10–14 days, and G418-resistant colonies were picked up and expanded. The expression of DN-Lnk was confirmed by conventional reverse transcription–polymerase chain reaction (RT-PCR). Mouse ES cells, iPS cells, and *Neo*- or DN-Lnk-expressing mouse ES and iPS cells were cultured in a leukemia inhibitory factor-containing ES cell medium (Millipore) on mitomycin C-treated mouse embryonic fibroblasts (MEFs) [28]. OP9 stromal cells were cultured in an α-minimum essential medium (α-MEM; Sigma) supplemented with 20% fetal bovine serum (FBS), 2 mM L-glutamine (Invitrogen), and non-essential amino acid (Invitrogen).

In vitro hematopoietic differentiation

For embryoid body (EB) differentiation, mouse ES and iPS cells were trypsinized and collected in an EB medium (EBM) containing the Dulbecco's modified Eagle's medium (Wako) supplemented with 15% FBS, non-essential amino acids (Millipore), penicillin/streptomycin (Invitrogen), 2 mM L-glutamine, and 100 μM β-mercaptoethanol (Nacalai Tesque), and they were plated on a culture dish for 30 min to allow the MEFs to adhere. Nonadherent cells were collected and plated on a round-bottom Lipidure-coated 96-well plate (Nunc) at 3×10^3 cells (ES cells) or 1×10^3 (iPS cells) cells per well. On day 5, half of the medium was exchanged for fresh EBM. EBs were collected on day 7, and a single-cell suspension was prepared by the use of trypsin/ethylenediaminetetraacetic acid. The EB-derived cells (4×10^5 cells) were plated on OP9 stromal cells in the wells of a 6-well plate and were then cultured with an OP9 medium containing recombinant hematopoietic cytokines [100 ng/mL mouse SCF, 100 ng/mL human Flt3-ligand, 20 ng/mL mouse TPO, 5 ng/mL mouse interleukin (IL)-3, and 5 ng/mL human IL-6] to induce and expand the hematopoietic cells. In the case of DN-Lnk transduction using the Ad vector, EB-derived cells were transduced with Ad-LacZ or Ad-DN-Lnk at 3,000 VP/cell for 1.5 h in a 15-mL tube before the transduced EB-derived cells plating on OP9 cells. Hematopoietic cells were collected as described previously [25]. In brief, the floating and loosely attached cells were collected by pipetting and were transferred to 15-mL tubes. The adherent hematopoietic cells were harvested by trypsin treatment, and were then incubated in a tissue culture dish for 30–60 min to eliminate the OP9 stromal cells. Floating cells were collected as hematopoietic cells and transferred to the same 15-mL tubes. These hematopoietic cells were kept on ice for further analysis.

Flow cytometry

The following primary monoclonal antibodies (Abs), conjugated with fluorescein isothiocyanate, phycoerythrin, or allophycocyanin, were used for flow cytometric analysis: anti-CD45 (30-F11; eBioscience), anti-CD11b (M1/70; eBioscience), anti-Sca-1 (D7; eBioscience), anti-Ter119 (Ter-119; eBioscience), anti-CD34 (RAM34; eBioscience), anti-CXCR4 (2B11; BD Bioscience), anti-Gr-1 (RB6-8C5; eBioscience), anti-c-Kit (ACK2 or 2B8; eBioscience), and anti-CD41 (MWReg30; BD Bioscience). Purified rat anti-mouse c-Mpl/TPOR monoclonal Ab was obtained from IBL. Cells (1×10^3–5×10^5) were incubated with monoclonal Abs at 4°C for 30 min and washed twice with a staining buffer (phosphate-buffered saline/2% FBS). For detection of Mpl/TPOR, Dylight649-conjugated goat anti-rat IgG (BioLegend) was used as a secondary Ab. After staining, the hematopoietic cells were analyzed and isolated by flow cytometry on an LSR II and FACSAria flow cytometer, respectively, using FACSDiva software (BD Bioscience).

Colony assay and May-Giemsa staining

The cells (5×10^4 cells) were cultured in a Methocult M3434 medium containing IL-3, IL-6, SCF, and erythropoietin (StemCell Technologies, Inc.) for 10 days. The number of individual colonies was counted by microscopy. The colony number was normalized to the total number of hematopoietic cells. The multipotent hematopoietic progenitor cell-derived colonies (colony-forming unit–granulocyte, erythrocyte, monocyte, megakaryocyte (CFU-GEMM)/CFU-Mix) were picked up, fixed on glass slides using a cytospin centrifuge (Cytospin 4; Thermo Shandon), and stained with May-Grünwald Stain solution (Sigma) and Giemsa solution (Wako).

Western blotting

The adherent hematopoietic cells and OP9 stromal cells were collected, and were then incubated in a new tissue culture dish for 40 min to eliminate adherent OP9 cells. Floating cells were harvested and were subsequently starved in an RPMI1640 medium containing 0.1% FBS and penicillin/streptomycin for 4–6 h. Cells were stimulated with 20 ng/mL TPO for 10 min (for Jak2) or 30 min (for Erk and Akt) before being lyzed in a lysis buffer [20 mM Tris–HCl (pH 8.0), 137 mM NaCl, 1% Triton X-100, 10% glycerol] containing a protease inhibitor cocktail (Sigma) and a phosphatase inhibitor cocktail (Nacalai Tesque). Cell lysates were loaded onto polyacrylamide gels and were transferred to a polyvinylidene fluoride membrane (Millipore). After blocking, the membrane was exposed to mouse anti-phospho-Erk1/2 (Cell Signaling), rabbit anti-Erk1/2 (Sigma), mouse anti-phospho-Akt (Cell Signaling), rabbit anti-total Akt (Cell Signaling), rabbit anti-phospho-Jak2 (Tyr1007/1008; Cell Signaling), or rabbit anti-Jak2 (Cell Signaling), followed by horseradish peroxidase-conjugated secondary antibody. The band was visualized by ECL Plus Western blotting detection reagents (GE Healthcare) or Pierce Western Blotting Substrate Plus (Thermo Scientific), and the signals were read using an LAS-3000 imaging system (Fujifilm).

Reverse transcription–polymerase chain reaction

RT-PCR was carried out as described previously [25]. The sequences of the primers used in this study are listed in Table 1.

Results

Expression of Lnk in mouse ES and iPS cells

We initially investigated Lnk expression in mouse ES cells, iPS cells, ES cell-derived EBs (ES-EBs), and iPS-EBs. As shown in Fig. 1a, Lnk was expressed in undifferentiated ES and iPS cells, and the expression levels of Lnk were significantly increased after EB formation. We further examined whether Lnk was expressed in Flk-1-positive (+) cells, because hematopoietic cells were generated from Flk-1+ cells, a common hemoangiogenic progenitor during ES cell differentiation [29–31]. Quantitative RT-PCR analysis after the purification of Flk-1+ cells from ES-EBs and iPS-EBs revealed that Lnk was highly expressed in Flk-1+ cells (Fig. 1b). These data suggest that Lnk plays some role in the hematopoietic differentiation process in ES and iPS cells.

Enhanced mesodermal differentiation in EB by the inhibition of Lnk

The data described above led to the expectation that hematopoietic cells, including hematopoietic progenitor cells, could be efficiently generated from ES cells and iPS cells by the suppression of Lnk. To inhibit the function of Lnk, we utilized the *DN-Lnk* gene, which was developed by Takizawa et al. [19]. DN-Lnk binds to Lnk, and forms a multimer complex by a homophilic interaction with the N-terminal domain, thereby inhibiting Lnk function [19]. DN-Lnk-expressing ES and iPS cells were generated by introducing a

Table 1. List of Primers Used for Reverse Transcription–Polymerase Chain Reaction

Gene name	*(5′) Sense primers (3′)*	*(5′) Antisense primers (3′)*
Gapdh	ACCACAGTCCATGCCATCAC	TCCACCACCCTGTTGCTGTA
Flk-1	TCTGTGGTTCTGCGTGGAGA	GTATCATTTCCAACCACCC
Lnk	GCCACTTTCTGCAGCTCTTC	GTCCAGGGAGTCAGTGCTTC
Lnk (for real-time)	AGCCACTTTCTGCAGCTCTTC	GTAGAGGTTGTCAGGCATCTCC
DN-Lnk	GGGCTACCAGTGACACCAAT	CACTGTCCACGCTCTGTGAG
Oct-3/4	GTTTGCCAAGCTGCTGAAGC	TCTAGCCCAAGCTGATTGGC
Nanog	ATGGTCTGATTCAGAAGGGC	TTCACCTCCAAATCACTGGC
β-H1	AGTCCCCATGGAGTCAAAGA	CTCAAGGAGACCTTTGCTCA
β-major	CTGACAGATGCTCTCTTGGG	CACAACCCCAGAAACAGACA
Scl/Tal-1	AACAACAACCGGGTGAAGAG	GGGAAAGCACGTCCTGTAGA
Runx1	CTTCCTCTGCTCCGTGCTAC	GACGGCAGAGTAGGGAACTG
Gata1	TTGTGAGGCCAGAGAGTGTG	TTCCTCGTCTGGATTCCATC
Gata2	TAAGCAGAGAAGCAAGGCTCGC	ACAGGCATTGCACAGGTAGTGG
Fli1	CCAACGAACGGAGAGTCATT	ATTCCTTGCCATCCATGTTC
Erg	GGAGCTGTGCAAGATGACAA	GATTAGCAAGGCGGCTACTG
Erg (for real-time)	GGAGTGCAACCCTAGTCAGG	TAGCTGCCGTAGCTCATCC
Sfpi1	CCATAGCGATCACTACTGGGATTT	TGTGAAGTGGTTCTCAGGGAAGT
E47	ATACAGCGAAGGTGCCCACT	CTCAAGGTGCCAACACTGGT

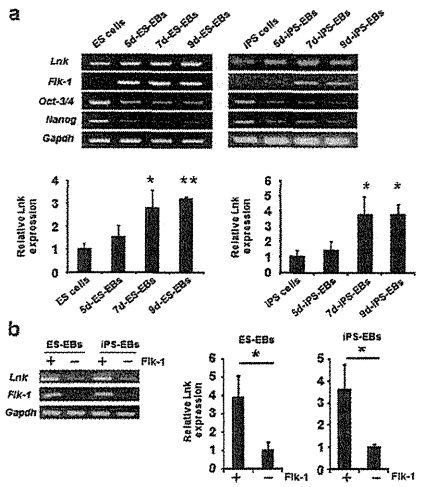

FIG. 1. Lnk is expressed in mouse ES cells, iPS cells, and Flk-1$^+$ hemoangiogenic progenitor cells. **(a)** Total RNA was extracted from undifferentiated ES cells, ES cell-derived EBs cultured for 5, 7, or 9 days (5-day ES-EBs, 7-day ES-EBs, 9-day ES-EBs, respectively), undifferentiated iPS cells, 5-day iPS-EBs, 7-day iPS-EBs, or 9-day iPS-EBs. Then, conventional (*above*) and quantitative (*below*) RT-PCR analysis was carried out. Results shown were the mean of 3 independent experiments with indicated SD. $^*p<0.05$, $^{**}p<0.01$ as compared with undifferentiated ES cells or iPS cells. **(b)** Flk-1$^+$ and Flk-1$^-$ cells were sorted from 7-day ES-EBs or 7-day iPS-EBs using FACSAria. The purity of the Flk-1$^+$ and Flk-1$^-$ cells exceeded 90% and 95%, respectively (data not shown). Total RNA was extracted from both types of cell, and the expression of Lnk was examined by conventional (*left*) and quantitative (*right*) RT-PCR analysis. The data were expressed as mean ± SD ($n=3$); $^*p<0.05$ as compared with Flk-1$^-$ cells. ES, embryonic stem; EBs, embryoid bodies; iPS, induced pluripotent stem; GAPDH, glyceraldehyde-3-phosphate dehydrogenase; RT-PCR, reverse transcription–polymerase chain reaction, SD, standard deviation.

DN-Lnk-expressing plasmid, and *DN-Lnk* mRNA expression was confirmed by RT-PCR (Fig. 2a). In this report, we present data from one DN-Lnk-expressing ES and iPS cell clone, because the same results were obtained from other DN-Lnk-expressing clones. Notably, the expression levels of wild-type Lnk in DN-Lnk-expressing cells were similar to those in *Neo*-expressing cells and their parent cells (Fig. 2a). DN-Lnk-expressing iPS cells maintained the undifferentiated state in culture and possessed pluripotency, as demonstrated by alkaline phosphatase staining, immunostaining, and teratoma formation (Supplementary Fig. S1; Supplementary Data are available online at www.liebertpub.com/scd). Hence, ectopic expression of the *DN-Lnk* gene in ES and iPS cells would not affect their function.

Next, we generated EBs to induce mesodermal cells from DN-Lnk- or *Neo*-expressing ES and iPS cells. EBs were cultured for 7 days, because the proportion of Flk-1$^+$ cells in EBs increased to a peak on day 7, and decreased over the next 2 days in our culture conditions (Supplementary Fig. S2). We found that DN-Lnk-expressing cells on day 7 of the EB culture yielded a modest increase in the number of Flk-1$^+$ hemangiogenic progenitor cells relative to that of *Neo*-expressing cells (Fig. 2b). Interestingly, elevated expression of *Scl/Tal-1*, *Runx1*, and *Gata-1* was observed in DN-Lnk-expressing total EB cells (Fig. 2c). Besides the expression levels of these genes, those of other key transcription factors of blood stem/progenitor cells, including *Gata-2*, *Fli-1*, and *Erg* [32], in DN-Lnk-expressing cells were also upregulated in comparison with those in *Neo*-expressing cells (Fig. 2d). To examine whether increased expression of these transcription factors in DN-Lnk-expressing cells was due to the increased generation of Flk-1$^+$ cells, we performed the gene expression analysis after purification of Flk-1$^+$ cells from DN-Lnk- or *Neo*-expressing total EB cells (Fig. 2e). No difference in the expression of *Runx1*, *Gata-1*, *Gata-2*, *Fli-1*, or *Erg* was observed between DN-Lnk-expressing cells and *Neo*-expressing cells, indicating that elevated expression of these hematopoietic genes in DN-Lnk-expressing EB cells would be largely because of the increased population of Flk-1$^+$ cells. On the other hand, DN-Lnk-expressing Flk-1$^+$ cells showed a 2-fold increase in the expression of *Scl/Tal-1*, an essential transcription factor for the hematopoietic development [33,34], compared with *Neo*-expressing Flk-1$^+$ cells. The increased *Scl/Tal-1* expression thus suggests that an inhibition of Lnk in Flk-1$^+$ cells might contribute to enhance the production of hematopoietic progenitor cells. Taken together, these results raise the possibility that mesodermal cells with a hematopoietic differentiation potential would be efficiently generated in DN-Lnk-expressing cells during EB formation.

Inhibition of Lnk function increases the production of hematopoietic cells

To induce hematopoietic cells, EB-derived cells were cultured on OP9 stromal cells in the presence of hematopoietic cytokines. During culture, cobblestone-forming cells were more frequently observed in DN-Lnk-expressing cells than in *Neo*-expressing cells (Fig. 3a), indicating that DN-Lnk-expressing cells were immature hematopoietic cells with expansion potential. In support of this observation, DN-Lnk-expressing cells showed a significant increase in the number of hematopoietic cells compared to that of *Neo*-expressing cells (Fig. 3b). Importantly, compared to *Neo*-expressing cells, DN-Lnk-expressing cells could more efficiently proliferate on OP9 stromal cells for a period exceeding 14 days (Fig. 3b). Therefore, the proliferation of hematopoietic cells could be augmented by the inhibition of Lnk.

To investigate whether primitive and definitive hematopoiesis could occur in DN-Lnk- or *Neo*-expressing cells, we measured the expression levels of red cell globin by RT-PCR analysis. In both DN-Lnk- and *Neo*-expressing hematopoietic cells, the expression levels of the embryonic globin, *β-H1*, and the adult globin, *β-major*, were decreased and increased, respectively, after culturing on OP9 stromal cells in comparison with those in total EB cells (Fig. 3c). This indicates that DN-Lnk- or *Neo*-expressing cells can show the primitive

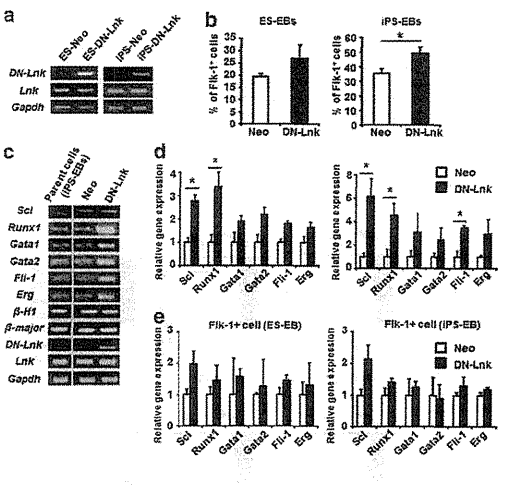

FIG. 2. Increased expression of hematopoietic transcription factors in DN-Lnk-expressing EB cells. **(a)** DN-Lnk-expressing ES cells and iPS cells were generated as described in the Materials and Methods section. DN-Lnk expression was confirmed by RT-PCR. **(b)** EB cells, which were cultured for 7 days, were stained with anti-mouse Flk-1 antibody, and were then subjected to flow cytometric analysis. The data were expressed as the mean ± SD ($n=3$). **(c)** The expression level of hematopoietic marker genes in 7-day iPS-EBs were investigated by semi-quantitative RT-PCR analysis. The *left panel* indicates the parent iPS cell (38C2)-derived 7-day EBs. **(d)** Gene expression analysis of the key transcription factors of hematopoietic stem/progenitor cells in total 7-day ES-EBs (*left*) and 7-day iPS-EBs (*right*). The data were expressed as mean ± SD ($n=3$); $^*p<0.05$ as compared with *Neo*. **(e)** After Flk-1$^+$ cells were sorted from *Neo*- or DN-Lnk-expressing 7-day EB cells, quantitative RT-PCR analysis was performed. *Left*, ES-EB-derived Flk-1$^+$ cells; *right*, iPS-EB-derived Flk-1$^+$ cells.

hematopoiesis followed by definitive hematopoiesis under our culture conditions.

We next examined the colony-forming potential of DN-Lnk-expressing cells. As shown in Fig. 3d, DN-Lnk-expressing cells showed a significant increase in the total colony-forming cell (CFC) number and CFU-granulocyte, macrophage number. Note that the number of CFU-GEMM/CFU-Mix, the most immature multipotent hematopoietic cells, in DN-Lnk-expressing cells was ~5 times as much as that in *Neo*-expressing cells (Fig. 3d). May-Giemsa staining after picking up the colonies revealed that mixed colonies derived from DN-Lnk-expressing cells contained the erythroblasts, granulocytes, macrophages, and megakaryocytes (Fig. 3e), thus confirming the generation of multipotent hematopoietic cells. An elevated CFU-Mix number in DN-Lnk-expressing cells might have been due to the fact that Lnk is highly expressed in immature hematopoietic cells, especially in hematopoietic stem/progenitor cells [13,17]. We also analyzed surface antigen expression in DN-Lnk- or *Neo*-expressing cells by flow cytometry, and found that DN-Lnk-expressing cells showed a higher percentage of CD34$^+$ cells and CD41$^+$ cells (Fig. 3f), suggestive of an increased number of immature hematopoietic cells. In addition, the proportion of CD45$^+$ cells, CD11b$^+$ cells, Gr-1$^+$ cells, or CXCR4$^+$ cells was also increased in DN-Lnk-expressing cells (Fig. 3f). By contrast, a lower percentage of Ter119$^+$ cells were observed in DN-Lnk-expressing cells (Fig. 3f). Consistent with this flow cytometric analysis, we found an increased expression of *Sfpi1* (encoding Pu.1) and *E47*, which are the key factors responsible for hematopoiesis, and a decreased expression of *β-major* globin in DN-Lnk-expressing cells after the cultivation on OP9 stromal cells (Fig. 3c and Supplementary Fig. S3). These results clearly showed that Lnk inhibition promoted the production of hematopoietic cells, including multipotent immature hematopoietic cells and myeloid cells, from mouse ES and iPS cells.

Inhibition of Lnk function in pluripotent stem cell-derived hematopoietic cells augments TPO-mediated signaling

It was previously shown that Lnk negatively regulates various types of hematopoietic cytokine signaling, such as TPO [16]. To investigate whether the increased production of hematopoietic cells from DN-Lnk-expressing cells, described above, is due to the enhanced TPO-mediated signaling, we analyzed protein phosphorylation after TPO stimulation using DN-Lnk-expressing cells. Hematopoietic cells were starved and subsequently stimulated with 20 ng/mL of TPO before the preparation of the cell lysates. The results showed the elevated phosphorylation of Jak2, Erk1/2, and Akt, all of which are downstream of TPO signaling, in DN-Lnk-expressing cells (Fig. 4a). We also found almost no difference in the percentage of Mpl/TPOR-positive cells between DN-Lnk-expressing cells and *Neo*-expressing cells (Fig. 4b), indicating that enhanced TPO signaling in DN-Lnk-expressing cells does not result from the increased percentage of Mpl/TPO-expressing cells. Thus, our data suggest that Lnk inhibition by *DN-Lnk* gene transduction would augment the activation of signaling molecules upon stimulation with cytokines, and thus Lnk inhibition would promote the production of hematopoietic cells in DN-Lnk-expressing cells.

Increased generation of hematopoietic progenitor cells from mouse pluripotent stem cells by transient transduction of a DN-Lnk gene

Our groups have shown that Ad vector-mediated transient, but not constitutive, transduction of differentiation-related genes in pluripotent stem cells could result in the efficient generation of functional cells, such as adipocytes, osteoblasts, hepatocytes, and hematopoietic cells [25,28,35–37]. We expected that the transient inhibition of Lnk in iPS cells could also

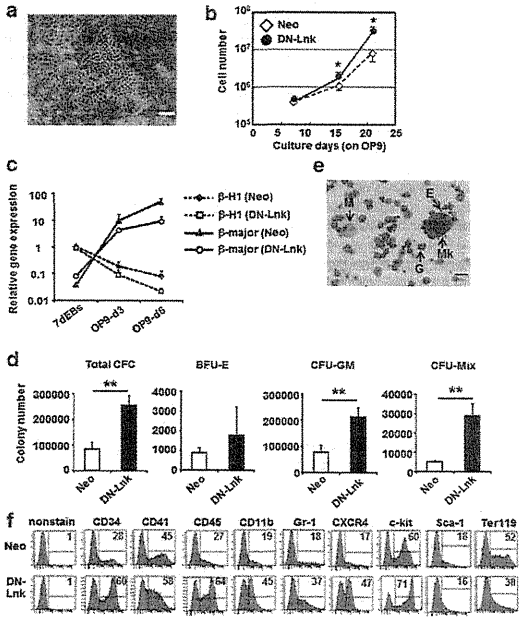

FIG. 3. Efficient generation of hematopoietic cells from iPS cells by overexpression of the *DN-Lnk* gene. EBs derived from *Neo*- or DN-Lnk-expressing iPS cells were cultured for 7 days, and were then plated and cultured on OP9 cells with hematopoietic cytokines to induce and expand the hematopoietic cells. **(a)** Morphology of cobblestone-forming cells derived from DN-Lnk-expressing cells on OP9 stromal cells. Scale bar indicates 100 μm. **(b)** The number of hematopoietic cells was counted on days 7 and 14, after the EB cells were plated on OP9 cells. The data were expressed as mean±SD ($n=3$); $^{*}p<0.05$ as compared with *Neo*. **(c)** Seven-day-cultured EB cells (7-day EBs) were cultured on OP9 cells for 3 or 6 days (OP9-d3 or OP9-d6, respectively). Total RNA was extracted from each cell, and the expression levels of the embryonic *β-H1* globin and the adult *β-major* globin in the cells were measured by real-time PCR. **(d)** After the EB cells had been cultured on OP9 stromal cells for 7 days, the hematopoietic cells were cultured in a methylcellulose-containing medium with hematopoietic cytokines. Ten days later, the number of hematopoietic colonies was then determined using light microscopy. The number of total colonies or subdivided colonies (by morphological subtypes BFU-E, CFU-GM, and CFU-Mix) is shown. The colony number was normalized to the total number of cells. The data were expressed as mean±SD ($n=3$); $^{**}p<0.01$ as compared with *Neo*. **(e)** Cytospin preparation from a DN-Lnk-expressing cell-derived CFU-Mix obtained from the cultures described in **(d)**. E, erythrocyte; G, granulocyte; M, macrophage; Mk, megakaryocyte. Scale bar indicates 30 μm. **(f)** After the EB cells were cocultured with OP9 stromal cells for 14 days, the hematopoietic cells were collected as described in the Materials and Methods section. Hematopoietic cells derived from *Neo*- or DN-Lnk-expressing iPS cells were stained with each antibody, and were then subjected to flow cytometric analysis. The proportion of antigen-positive cells is indicated in the histograms. Representative results from 1 of 3 independent experiments performed are shown. CFC, colony-forming cell; BFU-E, burst-forming unit; CFU-GM, colony-forming unit–granulocyte and monocyte; CFU-Mix/CFU-GEMM, CFU–granulocyte, erythrocyte, monocyte, and megakaryocyte.

accelerate the hematopoietic differentiation. To test this expectation, we generated a DN-Lnk-expressing Ad vector, Ad-DN-Lnk, and examined the effects of transient Lnk inhibition on hematopoietic cell differentiation. The transduction efficiency in EBs, which was transduced with a DsRed-expressing Ad vector, was approximately 40%, as determined by flow cytometry (data not shown). A colony assay after transduction with Ad vectors revealed that the number of total colonies and mixed colonies in the cells transduced with Ad-DN-Lnk was slightly increased in comparison with that in the cells transduced with Ad-LacZ (control vector) (Fig. 5a, c). Moreover, the number of hematopoietic cells increased in Ad-DN-Lnk-transduced cells after 7-day cultivation on OP9 stromal cells (Fig. 5b, d). Thus, our data indicate that the transient inhibition of Lnk also enhances the differentiation and proliferation of hematopoietic cells derived from pluripotent stem cells.

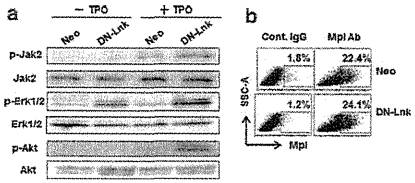

FIG. 4. Enhanced TPO-induced signaling pathway in DN-Lnk-expressing cells. After the EB cells, which were cultured for 7 days, had been plated and cultured on OP9 stromal cells for 14 days, and the hematopoietic cells were harvested as described in the Materials and Methods section. **(a)** Hematopoietic cells derived from *Neo*- or DN-Lnk-expressing cells were starved for 4–6 h in the absence of TPO, and the cells were then stimulated with 20 ng/mL of TPO. Total cell lysates were subjected to western blot analysis using the indicated antibodies. **(b)** After hematopoietic cells were collected, the rate of Mpl/TPOR-expressing cells was examined by flow cytometry. Representative results from 1 of 2 independent experiments performed are shown. TPO, thrombopoietin.

Discussion

In this report, we successfully generated and expanded hematopoietic cells, including immature hematopoietic cells, with colony-forming potential, from mouse ES and iPS cells by the suppression of an adaptor protein Lnk (Fig. 3). We also demonstrated that the expression levels of hematopoietic transcription factors such as *Scl* and *Runx1* in DN-Lnk-expressing total EB cells were significantly increased in comparison with those in *Neo*-expressing total EB cells (Fig. 2c, d), and that cytokine response was augmented in DN-Lnk-expressing cells (Fig. 4). Therefore, the data obtained in this study suggest that Lnk inhibition by enforced expression of a *DN-Lnk* gene in ES and iPS cells would lead both to a promotion of mesodermal differentiation during EB formation and to an increase in the expansion potential of ES and iPS cell-derived hematopoietic cells on an OP9 coculture system, and thus Lnk inhibition could enhance the hematopoietic cell production.

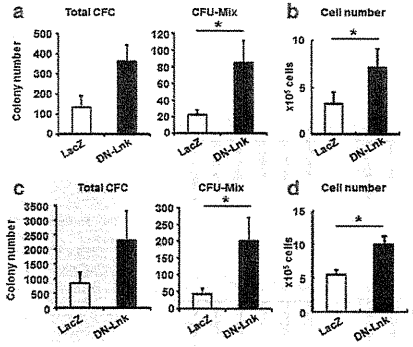

FIG. 5. Expansion of ES cell- and iPS cell-derived hematopoietic cells by the transient expression of DN-Lnk in EB cells. After ES cell- **(a, b)** or iPS cell- **(c, d)** derived EB cells, which were cultured for 7 days, had been transduced with Ad-LacZ or Ad-DN-Lnk at 3,000 VP/cell for 1.5 h, the cells were cultured on OP9 cells with cytokines for 7 days. Hematopoietic cells were collected, and then a colony assay was performed **(a, c)**. The colony number was normalized to the total number of cells. We also counted the number of hematopoietic cells derived from Ad-LacZ- or Ad-DN-Lnk-transduced EB cells **(b, d)**. The data were expressed as mean±SD ($n=3$); $^{*}p<0.05$ as compared with Ad-LacZ. Ad, adenovirus.

In developing mouse embryos, Lnk is shown to be expressed in the aorta-gonad-mesonephros (AGM) region, the site of hematopoiesis [38]. It has also been reported that the production of $CD45^{+}$ hematopoietic cells was severely impaired by the enforced expression of Lnk in AGM-derived cells, suggesting that Lnk suppresses hematopoietic commitment [38]. However, the function of Lnk in hematopoiesis is not fully understood. In the current study, we found that Lnk was highly expressed in $Flk\text{-}1^{+}$ cells (Fig. 1b), which are known to be hemoangiogenic progenitor cells during ES cell differentiation [29]. Furthermore, it was of note that levels of expression of *Scl/Tal-1*, which is essential for hematopoietic commitment of hemoangiogenic progenitor cells derived from ES cells [34], were slightly upregulated in $Flk\text{-}1^{+}$ cells by the inhibition of Lnk function (Fig. 2e). Thus, it is possible that Lnk might negatively regulate the hematopoietic commitment in $Flk\text{-}1^{+}$ cells by modulating the expression of *Scl/Tal-1*. We also showed that the percentage of $Flk\text{-}1^{+}$ cells was increased in DN-Lnk-expressing EB cells (Fig. 2b), and this could result in the elevated expression of other key hematopoietic transcription factors, such as *Runx1* and *Gata-1*, in DN-Lnk-expressing total EB cells compared with that in *Neo*-expressing total EB cells (Fig. 2c, d). This indicates that the functional $Flk\text{-}1^{+}$ mesodermal cells would be efficiently generated from DN-Lnk-expressing ES and iPS cells. On the other hand, at earlier days of differentiation, the percentage of $CD41^{+}$ cells, an early hematopoietic progenitor cells generated from pluripotent stem cells [39], in DN-Lnk-expressing EB cells was mostly equal to that in *Neo*-expressing EB cells (Supplementary Fig. S4). Taken together, the findings suggest that Lnk inhibition in ES and iPS cells could be effective for the generation of mesodermal cells with the potential for hematopoietic differentiation, but would not enhance the emergence of hematopoietic progenitor cells at earlier days of EB differentiation.

We examined the cytokine responses of iPS cell-derived hematopoietic cells, and observed the augmented phosphorylation of Erk and Akt in DN-Lnk-expressing cells (Fig. 4). This result is consistent with that of a previous report in which TPO-treated megakaryocytes derived from Lnk-deficient mice enhanced the extent of the activation of Erk and Akt [40]. By contrast, it was reported that Lnk-deficient adult HSCs or bone marrow-derived macrophages showed an enhanced Akt, but not Erk, activation after cytokine stimulation [16,41]. This difference in the activation of downstream molecules is most likely due to differences in cell populations. Because ES cell- and iPS cell-derived hematopoietic cells are heterogeneous, both Akt and Erk phosphorylation levels after cytokine treatment would be augmented in DN-Lnk-expressing cells relative to

Neo-expressing cells. In general, Akt and Erk are known to be involved in cell survival and cell growth [42,43]. Hence, our data indicate that the suppression of Lnk by the ectopic expression of DN-Lnk in ES and iPS cells would lead to an increase in hematopoietic cell production through enhanced cytokine responses.

Recently, Dravid et al. reported the expression of Lnk in human ES cell-derived $CD34^+$ hematopoietic progenitor cells, and they showed that the number of human ES cell-derived $CD34^+$ cells was increased by Lnk knockdown using a lentivirus vector carrying the short-hairpin RNA against Lnk (shLnk) [44]. Their results are mostly consistent with our data, indicating the suppressive function of Lnk in hematopoietic cell generation in both mouse and human pluripotent stem cells. However, the generation of hematopoietic CFCs in shLnk-transduced cells and the molecular mechanisms associated with the generation of $CD34^+$ cells by Lnk knockdown have not been addressed in detail. In this report, we clearly demonstrated that hematopoietic CFCs, including immature multipotent hematopoietic cells, were efficiently generated from mouse ES and iPS cells by Lnk inhibition, and these cells show potential for expansion on OP9 stromal cells (Fig. 3). In addition, we showed that the enhanced generation of hematopoietic cells in DN-Lnk-expressing cells was mediated by the promotion of mesodermal differentiation in EBs and augmented the sensitivity to cytokines in DN-Lnk-expressing cells as described above.

Another important finding of this study was that the transient inhibition of Lnk by Ad vector-mediated transduction of a *DN-Lnk* gene could also be an effective strategy for expanding hematopoietic cells (Fig. 5). Recently, the loss of Lnk and the mutation of Lnk have been reported to be associated with myeloproliferative diseases [45,46], indicating that oncogenesis may result from constitutive Lnk suppression in ES cell- and iPS cell-derived hematopoietic cells via the overexpression of a *DN-Lnk* gene or a lentivirus vector-mediated knockdown system, and such suppression would not be a directly applicable approach for clinical medicine. In this regard, our approaches using Ad vector-mediated transient Lnk inhibition are thought to be quite useful for the safe expansion of the ES cell- and iPS cell-derived hematopoietic cells. However, the number of ES cell- and iPS cell-derived hematopoietic cells in Ad-DN-Lnk-transduced cells was lower than that in the case of stably DN-Lnk-expressing cells (data not shown), possibly due to the low transduction efficiency of Ad vectors in EB cells. Therefore, it will still be necessary to establish methods for transiently inhibiting Lnk functionality using various types of Ad vectors [47] and short interference RNA.

In summary, we successfully developed efficient methods for differentiating mouse ES and iPS cells into hematopoietic cells by the suppression of the adaptor protein Lnk. Lnk functions downstream of multiple hematopoietic cytokine-signaling events, including those involving TPO, SCF, macrophage-colony stimulating factor, and erythropoietin [13,16,40,41,48,49], and Lnk-deficient mice show accumulation of pro-B cells in the bone marrow [48]. Therefore, various types of hematopoietic cells may be efficiently differentiated and expanded from ES and iPS cells by the inhibition of the Lnk function, when an appropriate cytokine is included in the culture; such work is currently ongoing in our laboratory.

Acknowledgments

We thank Misae Nishijima (National Institute of Biomedical Innovation) for her help. We thank Dr. Kazufumi Katayama (Osaka University, Osaka, Japan) for helpful discussion. We also thank Dr. S. Yamanaka and Dr. J. Miyazaki for kindly providing the mouse iPS cell line 38C2 and the CA promoter, respectively. This work was supported by a Grant-in-Aid for Young Scientists (B) (K. Tashiro) of the Ministry of Education, Culture, Sports, Science, and Technology (MEXT) of Japan and the Ministry of Health, Labour, and Welfare of Japan.

Author Disclosure Statement

The authors have no financial conflicts of interest.

References

1. Evans MJ and MH Kaufman. (1981). Establishment in culture of pluripotential cells from mouse embryos. Nature 292:154–156.
2. Thomson JA, J Itskovitz-Eldor, SS Shapiro, MA Waknitz, JJ Swiergiel, VS Marshall and JM Jones. (1998). Embryonic stem cell lines derived from human blastocysts. Science 282:1145–1147.
3. Takahashi K and S Yamanaka. (2006). Induction of pluripotent stem cells from mouse embryonic and adult fibroblast cultures by defined factors. Cell 126:663–676.
4. Takahashi K, K Tanabe, M Ohnuki, M Narita, T Ichisaka, K Tomoda and S Yamanaka. (2007). Induction of pluripotent stem cells from adult human fibroblasts by defined factors. Cell 131:861–872.
5. Nakano T, H Kodama and T Honjo. (1994). Generation of lymphohematopoietic cells from embryonic stem cells in culture. Science 265:1098–1101.
6. Chadwick K, L Wang, L Li, P Menendez, B Murdoch, A Rouleau and M Bhatia. (2003). Cytokines and BMP-4 promote hematopoietic differentiation of human embryonic stem cells. Blood 102:906–915.
7. Schmitt TM, RF de Pooter, MA Gronski, SK Cho, PS Ohashi and JC Zuniga-Pflucker. (2004). Induction of T cell development and establishment of T cell competence from embryonic stem cells differentiated *in vitro*. Nat Immunol 5: 410–417.
8. Hiroyama T, K Miharada, K Sudo, I Danjo, N Aoki and Y Nakamura. (2008). Establishment of mouse embryonic stem cell-derived erythroid progenitor cell lines able to produce functional red blood cells. PLoS One 3:e1544.
9. Choi KD, J Yu, K Smuga-Otto, G Salvagiotto, W Rehrauer, M Vodyanik, J Thomson and I Slukvin. (2009). Hematopoietic and endothelial differentiation of human induced pluripotent stem cells. Stem Cells 27:559–567.
10. Lei F, R Haque, L Weiler, KE Vrana and J Song. (2009). T lineage differentiation from induced pluripotent stem cells. Cell Immunol 260:1–5.
11. Benezra R, RL Davis, D Lockshon, DL Turner and H Weintraub. (1990). The protein Id: a negative regulator of helix-loop-helix DNA binding proteins. Cell 61:49–59.
12. Hong SH, JH Lee, JB Lee, J Ji and M Bhatia. (2011). ID1 and ID3 represent conserved negative regulators of human embryonic and induced pluripotent stem cell hematopoiesis. J Cell Sci 124:1445–1452.
13. Takaki S, H Morita, Y Tezuka and K Takatsu. (2002). Enhanced hematopoiesis by hematopoietic progenitor cells lacking intracellular adaptor protein, Lnk. J Exp Med 195: 151–160.
14. Velazquez L, AM Cheng, HE Fleming, C Furlonger, S Vesely, A Bernstein, CJ Paige and T Pawson. (2002). Cytokine signaling and hematopoietic homeostasis are disrupted in Lnk-deficient mice. J Exp Med 195:1599–1611.
15. Ema H, K Sudo, J Seita, A Matsubara, Y Morita, M Osawa, K Takatsu, S Takaki and H Nakauchi. (2005). Quantification of self-renewal capacity in single hematopoietic stem cells from normal and Lnk-deficient mice. Dev Cell 8:907–914.
16. Seita J, H Ema, J Ooehara, S Yamazaki, Y Tadokoro, A Yamasaki, K Eto, S Takaki, K Takatsu and H Nakauchi. (2007). Lnk negatively regulates self-renewal of hematopoietic stem cells by modifying thrombopoietin-mediated signal transduction. Proc Natl Acad Sci U S A 104:2349–2354.
17. Kwon SM, T Suzuki, A Kawamoto, M Ii, M Eguchi, H Akimaru, M Wada, T Matsumoto, H Masuda, et al. (2009). Pivotal role of lnk adaptor protein in endothelial progenitor cell biology for vascular regeneration. Circ Res 104:969–977.
18. Yokota Y. (2001). Id and development. Oncogene 20:8290–8298.
19. Takizawa H, C Kubo-Akashi, I Nobuhisa, SM Kwon, M Iseki, T Taga, K Takatsu and S Takaki. (2006). Enhanced engraftment of hematopoietic stem/progenitor cells by the transient inhibition of an adaptor protein, Lnk. Blood 107: 2968–2975.
20. Mizuguchi H and MA Kay. (1998). Efficient construction of a recombinant adenovirus vector by an improved *in vitro* ligation method. Hum Gene Ther 9:2577–2583.
21. Mizuguchi H and MA Kay. (1999). A simple method for constructing E1- and E1/E4-deleted recombinant adenoviral vectors. Hum Gene Ther 10:2013–2017.
22. Kawabata K, F Sakurai, T Yamaguchi, T Hayakawa and H Mizuguchi. (2005). Efficient gene transfer into mouse embryonic stem cells with adenovirus vectors. Mol Ther 12: 547–554.
23. Niwa H, K Yamamura and J Miyazaki. (1991). Efficient selection for high-expression transfectants with a novel eukaryotic vector. Gene 108:193–199.
24. Tashiro K, K Kawabata, H Sakurai, S Kurachi, F Sakurai, K Yamanishi and H Mizuguchi. (2008). Efficient adenovirus vector-mediated PPAR gamma gene transfer into mouse embryoid bodies promotes adipocyte differentiation. J Gene Med 10:498–507.
25. Tashiro K, K Kawabata, M Omori, T Yamaguchi, F Sakurai, K Katayama, T Hayakawa and H Mizuguchi. (2012). Promotion of hematopoietic differentiation from mouse induced pluripotent stem cells by transient HoxB4 transduction. Stem Cell Res 8:300–311.
26. Maizel JV, Jr., DO White and MD Scharff. (1968). The polypeptides of adenovirus. I. Evidence for multiple protein components in the virion and a comparison of types 2, 7A, and 12. Virology 36:115–125.
27. Okita K, T Ichisaka and S Yamanaka. (2007). Generation of germline-competent induced pluripotent stem cells. Nature 448:313–317.
28. Tashiro K, M Inamura, K Kawabata, F Sakurai, K Yamanishi, T Hayakawa and H Mizuguchi. (2009). Efficient adipocyte and osteoblast differentiation from mouse induced pluripotent stem cells by adenoviral transduction. Stem Cells 27:1802–1811.
29. Nishikawa SI, S Nishikawa, M Hirashima, N Matsuyoshi and H Kodama. (1998). Progressive lineage analysis by cell sorting and culture identifies FLK1+VE-cadherin+ cells at a diverging point of endothelial and hemopoietic lineages. Development 125:1747–1757.
30. Yamashita J, H Itoh, M Hirashima, M Ogawa, S Nishikawa, T Yurugi, M Naito and K Nakao. (2000). Flk1-positive cells derived from embryonic stem cells serve as vascular progenitors. Nature 408:92–96.
31. Huber TL, V Kouskoff, HJ Fehling, J Palis and G Keller. (2004). Haemangioblast commitment is initiated in the primitive streak of the mouse embryo. Nature 432:625–630.
32. Wilson NK, SD Foster, X Wang, K Knezevic, J Schutte, P Kaimakis, PM Chilarska, S Kinston, WH Ouwehand et al. (2010). Combinatorial transcriptional control in blood stem/progenitor cells: genome-wide analysis of ten major transcriptional regulators. Cell Stem Cell 7:532–544.
33. Robb L, NJ Elwood, AG Elefanty, F Kontgen, R Li, LD Barnett and CG Begley. (1996). The scl gene product is required for the generation of all hematopoietic lineages in the adult mouse. EMBO J 15:4123–4129.
34. D'Souza SL, AG Elefanty and G Keller. (2005). SCL/Tal-1 is essential for hematopoietic commitment of the hemangioblast but not for its development. Blood 105:3862–3870.
35. Inamura M, K Kawabata, K Takayama, K Tashiro, F Sakurai, K Katayama, M Toyoda, H Akutsu, Y Miyagawa, et al. (2011). Efficient generation of hepatoblasts from human ES cells and iPS cells by transient overexpression of homeobox gene HEX. Mol Ther 19:400–407.
36. Takayama K, M Inamura, K Kawabata, K Tashiro, K Katayama, F Sakurai, T Hayakawa, Furue MK, H Mizuguchi. (2011). Efficient and directive generation of two distinct endoderm lineages from human ESCs and iPSCs by differentiation stage-specific SOX17 transduction. PLoS One 6: e21780.
37. Takayama K, M Inamura, K Kawabata, K Katayama, M Higuchi, K Tashiro, A Nonaka, F Sakurai, T Hayakawa, F Kusudaurue M and H Mizuguchi. (2012). Efficient generation of functional hepatocytes from human embryonic stem cells and induced pluripotent stem cells by HNF4alpha transduction. Mol Ther 20:127–137.
38. Nobuhisa I, M Takizawa, S Takaki, H Inoue, K Okita, M Ueno, K Takatsu and T Taga. (2003). Regulation of hematopoietic development in the aorta-gonad-mesonephros region mediated by Lnk adaptor protein. Mol Cell Biol 23: 8486–8494.
39. Matsumoto K, T Isagawa, T Nishimura, T Ogaeri, K Eto, S Miyazaki, J Miyazaki, H Aburatani, H Nakauchi and H Ema. (2009). Stepwise development of hematopoietic stem cells from embryonic stem cells. PLoS One 4:e4820.
40. Tong W and HF Lodish. (2004). Lnk inhibits Tpo-mpl signaling and Tpo-mediated megakaryocytopoiesis. J Exp Med 200:569–580.
41. Gueller S, HS Goodridge, B Niebuhr, H Xing, M Koren Michowitz, H Serve, DM Underhill, CH Brandts and HP Koeffler. (2010). Adaptor protein Lnk inhibits c-Fms-mediated macrophage function. J Leukoc Biol 88:699–706.
42. Geest CR and PJ Coffer. (2009). MAPK signaling pathways in the regulation of hematopoiesis. J Leukoc Biol 86:237–250.
43. Martelli AM, C Evangelisti, F Chiarini, C Grimaldi, A Cappellini, A Ognibene and JA McCubrey. (2010). The emerging role of the phosphatidylinositol 3-kinase/Akt/mammalian target of rapamycin signaling network in normal myelopoiesis and leukemogenesis. Biochim Biophys Acta 1803: 991–1002.
44. Dravid G, Y Zhu, J Scholes, D Evseenko and GM Crooks. (2011). Dysregulated gene expression during hematopoietic

differentiation from human embryonic stem cells. Mol Ther 19:768–781.
45. Bersenev A, C Wu, J Balcerek, J Jing, M Kundu, GA Blobel, KR Chikwava and W Tong. (2010). Lnk constrains myeloproliferative diseases in mice. J Clin Invest 120:2058–2069.
46. Oh ST, EF Simonds, C Jones, MB Hale, Y Goltsev, KD Gibbs, Jr., JD Merker, JL Zehnder, GP Nolan and J Gotlib. (2010). Novel mutations in the inhibitory adaptor protein LNK drive JAK-STAT signaling in patients with myeloproliferative neoplasms. Blood 116:988–992.
47. Kawabata K, F Sakurai, N Koizumi, T Hayakawa and H Mizuguchi. (2006). Adenovirus vector-mediated gene transfer into stem cells. Mol Pharm 3:95–103.
48. Takaki S, K Sauer, BM Iritani, S Chien, Y Ebihara, K Tsuji, K Takatsu and RM Perlmutter. (2000). Control of B cell production by the adaptor protein lnk. Definition Of a conserved family of signal-modulating proteins. Immunity 13:599–609.
49. Tong W, J Zhang and HF Lodish. (2005). Lnk inhibits erythropoiesis and Epo-dependent JAK2 activation and downstream signaling pathways. Blood 105:4604–4612.

Address correspondence to:
Dr. Hiroyuki Mizuguchi
Laboratory of Biochemistry and Molecular Biology
Graduate School of Pharmaceutical Sciences
Osaka University
1-6 Yamadaoka, Suita
Osaka 565-0871
Japan

E-mail: mizuguch@phs.osaka-u.ac.jp

Received for publication February 27, 2012
Accepted after revision June 27, 2012
Prepublished on Leibert Instant Online June 28, 2012

SCD-2013-0469-ver9-Tashiro_1P
Type: research-article

STEM CELLS AND DEVELOPMENT
Volume 00, Number 00, 2014

DOI: 10.1089/scd.2013.0469

ORIGINAL RESEARCH REPORT

Plasma Elevation of Vascular Endothelial Growth Factor Leads to the Reduction of Mouse Hematopoietic and Mesenchymal Stem/Progenitor Cells in the Bone Marrow

Katsuhisa Tashiro,[1,*] Aki Nonaka,[1,2,*] Nobue Hirata,[1] Tomoko Yamaguchi,[1] Hiroyuki Mizuguchi,[3–6] and Kenji Kawabata[1,2]

Vascular endothelial growth factor (VEGF) is reported to exhibit potent hematopoietic stem/progenitor cell (HSPC) mobilization activity. However, the detailed mechanisms of HSPC mobilization by VEGF have not been examined. In this study, we investigated the effect of VEGF on bone marrow (BM) cell and the BM environment by intravenous injection of VEGF-expressing adenovirus vector (Ad-VEGF) into mice. A colony assay using peripheral blood cells revealed that plasma elevation of VEGF leads to the mobilization of HSPCs into the circulation. Granulocyte colony-stimulating factor (G-CSF) is known to mobilize HSPCs by decreasing CXC chemokine ligand 12 (CXCL12) levels in the BM. However, we found almost no changes in the CXCL12 levels in the BM after Ad-VEGF injection, suggesting that VEGF can alter the BM microenvironment by different mechanisms from G-CSF. Furthermore, flow cytometric analysis and colony forming unit-fibroblast assay showed a reduction in the number of mesenchymal progenitor cells (MPCs), which have been reported to serve as niche cells to support HSPCs, in the BM of Ad-VEGF-injected mice. Adhesion of donor cells to the recipient BM after transplantation was also impaired in mice injected with Ad-VEGF, suggesting a decrease in the niche cell number. We also observed a dose-dependent chemoattractive effect of VEGF on primary BM stromal cells in vitro. These data suggest that VEGF alters the distribution of MPCs in the BM and can also mobilize MPCs to peripheral tissues. Taken together, our results imply that VEGF-elicited egress of HSPCs would be mediated, in part, by changing the number of MPCs in the BM.

Introduction

HEMATOPOIETIC STEM CELLS (HSCs) sustain blood production throughout life. In a steady state, HSCs exist within the bone marrow (BM) and remain largely quiescent and self-renew at a low rate to avoid their exhaustion. By contrast, HSCs can actively proliferate, differentiate into progenitor cells, or egress from the BM into the circulation in some situations, such as tissue damage-induced cell death and increased plasma levels of hematopoietic cytokines, including the granulocyte colony-stimulating factor (G-CSF). These dynamic behaviors of HSCs are controlled by a local specific microenvironment called niches [1–8]. The non-hematopoietic cells, such as endosteal osteoblasts and perivascular mesenchymal progenitor cells (MPCs), are reported to function as niche cells by supplying several HSC maintenance factors, including the CXC chemokine ligand 12 (CXCL12). Indeed, previous studies have shown that decreased levels of CXCL12 in the BM caused hematopoietic stem/progenitor cell (HSPC) mobilization, indicating the pivotal role of CXCL12 signaling in HSPC egress [9,10].

Not only is the vascular endothelial growth factor (VEGF) a well-known factor in angiogenesis, but it also plays an important role in the growth and differentiation of hematopoietic cells. Homozygous or heterozygous deletion of VEGF in mice leads to early embryonic lethality because of impaired vascular angiogenesis and hematopoiesis [11,12]. By conditional deletion of VEGF in hematopoietic cells, but not in stromal cells, Ferrara and colleagues clearly showed that VEGF is required for survival and repopulation

[1]Laboratory of Stem Cell Regulation, National Institute of Biomedical Innovation, Ibaraki, Japan.
Laboratory of [2]Biomedical Innovation and [3]Biochemistry and Molecular Biology, Graduate School of Pharmaceutical Sciences, Osaka University, Ibaraki, Japan.
[4]iPS Cell-based Research Project on Hepatic Toxicity and Metabolism, Graduate School of Pharmaceutical Sciences, Osaka University, Ibaraki, Japan.
[5]Laboratory of Hepatocyte Regulation, National Institute of Biomedical Innovation, Ibaraki, Japan.
[6]The Center for Advanced Medical Engineering and Informatics, Osaka University, Ibaraki, Japan.
*These two authors contributed equally to this work.

of adult HSCs [13]. Furthermore, VEGF has been shown to be an essential factor for HSC niche formation through endochondral ossification [14]. These observations clearly demonstrate that VEGF exerts physiological actions on hematopoietic systems through both cell-autonomous and -nonautonomous mechanisms.

In addition to the functions described above, VEGF also has a potent HSPC mobilization capacity [15], although the mechanisms of VEGF-induced HSPC mobilization have not been addressed in detail. In the current study, we investigated the effect of VEGF on the BM cell mobilization and BM environment after the intravenous injection of VEGF-expressing adenovirus (Ad) vector (Ad-VEGF) into mice. The results showed that VEGF overexpression in mice could lead to a reduction of not only the HPSC number, but also the MPC number in the BM. We also observed an enhanced chemoattractive activity of BM stromal cells by VEGF. Our data suggest that the plasma elevation of VEGF in mice alters the distribution of MPCs in the BM, and this might cause HSPC egress from the BM.

Materials and Methods

Ad vectors

Ad vectors were constructed by an improved in vitro ligation method [16,17]. The mouse $VEGF_{165}$ cDNA and human G-CSF cDNA were obtained from pBLAST49-mVEGF and pORF9-hGCSFb, respectively (Invivogen). Each cDNA was cloned into a multicloning site of pHMCMV10 [18,19], which contains the cytomegalovirus (CMV) promoter/enhancer and intron A sequence flanked by the I-*Ceu*I and PI-*Sce*I sites, thereby resulting in pHMCMV10-VEGF and pHMCMV10-G-CSF. pHMCMV10-VEGF and pHMCMV10-G-CSF were digested with I-*Ceu*I/PI-*Sce*I and ligated into I-*Ceu*I/PI-*Sce*I-digested pAdHM41-K7 (C) [20], resulting in pAd-VEGF and pAd-G-CSF, respectively. To generate the virus, Ad vector plasmids were digested with *Pac*I and purified by phenol–chloroform extraction and ethanol precipitation. Linearized DNAs were transfected into 293 cells with SuperFect (Qiagen) according to the manufacturer's instructions. The viruses were amplified in 293 cells. Before virus purification, the cell lysates were centrifuged to remove cell debris and were digested for 30 min at 37°C with 200 μg/mL DNase I and 200 μg/mL RNase A in the presence of 10 mM $MgCl_2$. Viruses were purified by $CsCl_2$ step gradient ultracentrifugation followed by $CsCl_2$ linear gradient ultracentrifugation. The purified viruses were dialyzed against a solution containing 10 mM Tris-HCl (pH 7.5), 1 mM $MgCl_2$, and 10% glycerol and were stored at −80°C. The control vector, Ad-Null, is similar in design, except that it contains no transgene in the expression cassette. The biological titers [infectious unit (ifu)] of Ad-VEGF, Ad-G-CSF, and Ad-Null were determined by using an Adeno-X Rapid Titer kit (Clontech).

Administration of Ad vectors in mice

C57BL/6j female mice aged 7–9 weeks were obtained from Nippon SLC, and all animals were maintained under specific pathogen-free conditions. Each Ad vector was intravenously injected into C57BL/6j mice at 1×10^9 ifu through the tail vein. All experiments were conducted according to the institutional ethics guidelines for animal experimentation of the National Institute of Biomedical Innovation.

Cell preparation

Blood and BM were harvested from mice using standard methods on day 5 after injection of Ad vector into mice, and the number of nucleated cells in these tissues was then counted using a Nucleocounter (Chemometec). To collect the nonhematopoietic cells from the femur and tibia, the bone fragments were minced with scissors, and were then incubated at 37°C with a type I collagenase (3 mg/mL; Worthington) in the Dulbecco's modified Eagle's medium (DMEM) with 10% fetal bovine serum (FBS) for 90 min [21]. The cells were filtered with a cell strainer to remove debris and bone fragments, and suspended in a staining buffer [phosphate buffer saline (PBS)/2% FBS]. These cell suspensions were kept on ice for further analysis.

Flow cytometry

The following antibodies (Abs), conjugated with fluorescein isothiocyanate (FITC), phycoerythrin (PE), allophycocyanin (APC), or PECy7, were used for flow cytometric analysis and cell sorting: biotinylated lineage cocktail [CD3 (145-2C11), B220 (RA3-6B2), Gr-1 (RB6-8C5), CD11b (M1/70), Ter119 (Ter-119)], c-Kit-APC (2B8), Sca-1-PECy7 (D7), Ter119-FITC (Ter-119), CD45-FITC (30-F11), CD11b-FITC (M1/70), Gr-1-PE (RB6-8C5), CD31-FITC (390), CD31-APC (390), CD51-PE (RMV-7), PDGFRa-APC (APA-5), Flt-1-PE (141522), Flk1-PE (Avas12a1), and Alcam-PE. For detection of biotinylated Abs, PerCP-Cy5.5- or FITC-conjugated streptavidin was used. Abs were purchased from e-Bioscience, BD Bioscience, Biolegend, and R&D Systems. Cells were incubated with primary Abs at 4°C for 30 min and washed twice with PBS/2% FBS. After staining, cells were analyzed and isolated by flow cytometry on an LSR II and FACSAria flow cytometer, respectively, using FACSDiva software (BD Bioscience).

Enzyme linked immunosorbent assay

Blood samples were collected through the inferior vena cava on day 5 after Ad vector injection, and transferred to polypropylene tubes containing heparin. Plasma was harvested by centrifugation. The BM supernatant was obtained by flushing a femur with 500 μL of PBS, followed by centrifugation at 500*g* for 5 min. The levels of VEGF and CXCL12 in the plasma and BM supernatant were measured using a commercial ELISA kit (R&D Systems) following the manufacturer's instructions.

RT-polymerase chain reaction analysis

CD45-negative($^-$) $Ter119^-$ nonhematopoietic cells in the BM were sorted from mice injected with Ad-VEGF or Ad-Null, and total RNA was then extracted using ISOGEN (Nippon Gene). cDNA was synthesized from DNase I-treated total RNA with a Superscript VILO cDNA synthesis kit (Invitrogen), and quantitative real-time RT-polymerase chain reaction was performed using the Fast SYBR Green Master Mix with an ABI StepOne Plus system (Applied Biosystems). Relative quantification was performed against a standard curve and the values were normalized against the input determined for the housekeeping gene, glyceraldehyde 3-phosphate dehydrogenase. The sequences of the primers used in this study are listed in Table 1.

Colony assay

BM cells (2×10^4 cells) and peripheral blood cells (2×10^5 cells) were plated in the Methocult M3434 medium (StemCell Technologies, Inc.). Cultures were plated in duplicate and placed in a humidified chamber with 5% CO_2 at 37°C for 10 days. The number of individual colonies was counted by microscopy. The colony number was normalized to the total number of the nucleated cells.

Colony forming unit-fibroblast assay

BM-derived $CD45^-Ter119^-$ cells were added to the MesenCult MSC Basal Medium, including supplements (Stem Cell Technologies, Inc.), and then plated on a six-well plate at 1×10^5 cells per well. Cells were cultured for 14 days and stromal cell colonies (fibroblast-like colonies: >50 cells) derived from colony forming unit-fibroblasts (CFU-Fs) were stained with the Giemsa solution (Wako) after fixation with methanol. The colony number was counted by microscopy.

Cell migration assay

BM-derived stromal cells, including MPCs, were tested for migration toward VEGF using 8-μm pore-sized cell culture inserts (BD Falcon). Stromal cells (1×10^5 cells) resuspended in 200 μL of DMEM/2% FBS were added to the upper chamber, and 750 μL of DMEM/2% FBS containing recombinant mouse VEGF (10 or 100 ng/mL; Peprotech) was added to the bottom chamber. After 6 h of incubation at 37°C, the upper side of the filters was carefully washed with PBS, and cells remaining on the upper face of the filters were removed with a cotton wool swab. The filters were fixed with 100% methanol and stained with the Giemsa solution. Cells migrating into the lower compartment were counted manually in three random microscopic fields (×200).

Homing assay

Mice were administrated with Ad-Null or Ad-VEGF at 1×10^9 ifu. Five days later, BM cells (1×10^7 cells) derived from green fluorescent protein (GFP)-expressing transgenic mice [22] were intravenously transplanted into Ad-Null- or Ad-VEGF-injected mice. At 16 h after BM transplantation, the percentage of GFP-expressing donor cells in the BM was determined by flow cytometry.

Results

Effect of systemic VEGF overexpression on the distribution of myeloid cells and HSPCs in mice

To evaluate the effect of VEGF on the mobilization of hematopoietic cells, we generated a VEGF-expressing Ad vector, Ad-VEGF, because plasma VEGF levels were rapidly decreased with a $t_{1/2}$ of ~25 min after intravenous injection of recombinant VEGF [23]. Single intravenous injection of Ad-VEGF (1×10^9 ifu) into mice led to a significant elevation of VEGF levels in plasma on day 5 compared with Ad-Null-injected mice (control mice) (Fig. 1a). On the other hand, unexpectedly, BM VEGF levels in the Ad-VEGF-injected mice were almost equivalent to those in the Ad-Null-injected mice (Fig. 1b). There were no signs of toxicity in mice treated with Ad-VEGF and Ad-Null at this dose (1×10^9 ifu). To investigate whether the hematopoietic cells could be mobilized from the BM into the circulation after injection of Ad-VEGF, we examined the number of total nucleated cells, myeloid cells ($Gr\text{-}1^+CD11b^+$ cells), and HSPCs [$c\text{-}Kit^+Sca\text{-}1^+Lineage^-$ (KSL) cells or CFU-GEMM/CFU-Mix] in the peripheral blood. Compared with Ad-Null-injected mice, Ad-VEGF-injected mice showed an increased number of total nucleated cells and myeloid cells in the peripheral blood (Fig. 1c, d). We found that the number of multipotent hematopoietic progenitor cells, CFU-GEMM/CFU-Mix, in the blood of Ad-VEGF-injected mice was four times as great as that of Ad-Null-injected mice (Fig. 1e). Importantly, in Ad-VEGF-injected mice, the number of KSL cells in the blood was also increased (Fig. 1f). These results indicate that hematopoietic cells, including immature hematopoietic cells with colony-forming potentials, would be mobilized from the BM following systemic Ad-VEGF administration.

An increased number of mobilized cells in VEGF-treated mice were reported previously [15], but little is known about the effect of VEGF on BM cells during the mobilization period. Thus, we next investigated the number of total BM cells, myeloid cells, and HSPCs. In contrast to the peripheral blood, the number of total hematopoietic cells, myeloid cells, and CFU-Mix was significantly decreased (Fig. 2a–c). It is of note that the VEGF overexpression in mice resulted in the reduction in both the frequency and the absolute

TABLE 1.

Gene name	*(5′) Sense primers (3′)*	*(5′) Antisense primers (3′)*
Gapdh	TTCACCACCATGGAGAAGAAGGC	GGCATGGACTGTGGTCATGA
Cdh2	CAAGAGCTTGTCAGAATCAGG	CATTTGGATCATCCGCATC
Vcam-1	GACCTGTTCCAGCGAGGGTCTA	CTTCCATCCTCATAGCAATTAAGGTG
Angpt1	CTCGTCAGACATTCATCATCCAG	CACCTTCTTTTAGTGCAAAGGCT
Thpo	GGCCATGCTTCTTGCAGTG	AGTCGGCTGTGAAGGAGGT

Gapdh, glyceraldehyde 3-phosphate dehydrogenase; *cdh2*, N-cadherin; *Vcam-1*, vascular cell adhesion molecule-1; *Angpt1*, angiopoietin-1; *Thpo*, thrombopoietin.

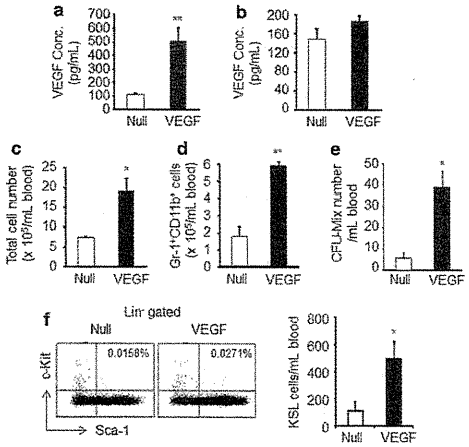

FIG. 1. Effect of vascular endothelial growth factor (VEGF) on the number of myeloid cells and hematopoietic stem/progenitor cells (HSPCs) in peripheral blood. (**a**, **b**) Mice were intravenously injected with adenovirus (Ad)-Null (Null) or Ad-VEGF (VEGF). Five days later, the concentration of plasma (**a**) and bone marrow (BM) (**b**) VEGF levels was determined by enzyme linked immunosorbent assay (ELISA). Data are expressed as mean ± standard deviation (SD) ($n=4$). (**c**) The number of total PBMCs was counted on day 5 after administration of each Ad vector. (**d**) The percentage of Gr-1$^+$CD11b$^+$ myeloid cells was determined by flow cytometric analysis, and the absolute number was then normalized to the total PBMC number. Data are expressed as mean ± SD ($n=4$). (**e**) The number of colony forming unit (CFU)-Mix/CFU-GEMM, a multipotent hematopoietic progenitor cells, in PBMCs was determined by a standard colony assay. The colony number was normalized to the total PBMC number. (**f**) A representative analysis of the c-Kit$^+$Sca-1$^+$Lineage$^-$(KSL) subset in the blood is shown (*left*). The proportion of cKit$^+$Sca-1$^+$ cells in the lineage-negative (Lin$^-$) population is indicated in the dot blot. The number of KSL cells in the blood was normalized to the total cell number (*right*). Data are expressed as mean ± SD ($n=4$). $^*P<0.05$, $^{**}P<0.01$ as compared with Null.

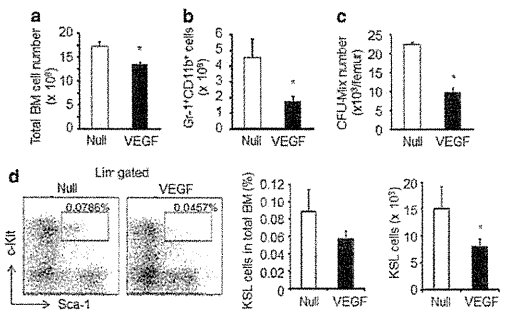

FIG. 2. Plasma elevation of VEGF leads to a decrease in the myeloid cells and HSPCs in the BM. (**a**) The number of total BM cells was counted on day 5 after Ad-Null or Ad-VEGF injection. (**b**) The number of Gr-1$^+$CD11b$^+$ cells in the BM was determined by flow cytometric analysis. (**c**) The number of CFU-Mix/CFU-GEMM in the BM was determined by a colony assay. The colony number was normalized to the total BM cell number. (**d**) A representative analysis of the KSL subset in the BM after administration of Ad-Null or Ad-VEGF is shown (*left*). The proportion of KSL cells in the total BM is indicated in the dot blot. Frequencies (*middle*) and absolute numbers (*right*) of KSL cells in the BM were calculated. Data are expressed as mean ± SD ($n=5$). $^*P<0.05$ as compared with Null.

number of KSL cells in BM (Fig. 2d). Thus, these data suggest that VEGF exerts a physiological effect on the various types of cells within the BM.

Unchanged level of CXCL12 after VEGF overexpression

To examine the mechanisms of BM cell mobilization by VEGF treatment, we analyzed the expression levels of genes associated with HSC maintenance in the BM [*N-cadherin* (*cdh2*), *vascular cell adhesion molecule-1* (*Vcam-1*), *angiopoietin-1* (*Angpt1*), and *thrombopoietin* (*Thpo*)]. The expression levels of these genes in BM nonhematopoietic cells were modestly downregulated after Ad-VEGF injection (Fig. 3a). We next measured the CXCL12 levels in Ad-VEGF-injected mice. Chemokine CXCL12 is an indispensable factor for the maintenance and retention of HSPCs in the BM [5,24]. Previous studies showed that the BM CXCL12 levels were reduced by the injection of mobilization-inducing factors, such as G-CSF and stem cell factor (SCF) [10,25]. We also found that the CXCL12 levels were markedly reduced in the BM, but not the plasma, of Ad-G-CSF-injected mice (Fig. 3b). However, there was almost no difference in the BM CXCL12 levels between Ad-VEGF-injected mice and Ad-Null-injected mice (Fig. 3b). Therefore, these data indicate that VEGF would alter the BM microenvironment, probably by a different mechanism from other mobilization factors.

Reduction of MPCs in the BM after Ad-VEGF injection

Recent studies have demonstrated that MPCs play a pivotal role in HSPC maintenance in the BM [4,6–8]. Therefore, we examined the disposition of MPCs in the BM after Ad-VEGF administration. Flow cytometric analysis of the enzymatically dissociated BM cells revealed that Ad-VEGF overexpression led to a significant reduction of CD45$^-$Ter119$^-$CD31$^-$Alcam$^-$Sca-1$^+$ cells, which are reported to be MPCs [21,26] (Fig. 4a). In addition, the percentage of other MPC populations, such as CD45$^-$Ter119$^-$PDGFRα$^+$Sca-1$^+$ cells [27] and CD45$^-$Lineage$^-$CD31$^-$CD51$^+$Sca-1$^+$ cells [28], in the BM of Ad-VEGF-injected mice was also lower than those of Ad-Null-injected mice (Fig. 4b, c). These data clearly showed the decreased number of phenotypically identified MPCs in the BM after injection of Ad-VEGF.

Next, to investigate whether functional MPCs in the BM were reduced in Ad-VEGF-injected mice, we performed a CFU-F assay and homing assay. Consistent with the above data, we observed decreased CFU-F numbers in the BM in Ad-VEGF-injected mice (Fig. 4d). For homing studies, Ad-Null- or Ad-VEGF-injected mice were used as the recipient mice. Donor BM cells derived from GFP transgenic mice were intravenously injected into nonirradiated recipient mice, and the frequency of GFP-expressing cells in the recipient BM was then estimated by flow cytometry. The results showed that the homing activity of GFP-expressing cells was partially inhibited in Ad-VEGF-treated recipient mice (Fig. 4e). Thus, the decreased homing efficiency of donor HSPCs in Ad-VEGF-injected mice suggests the decreased number of niche cells in the BM. Taken together, our findings indicate that overexpression of VEGF in mice leads to a reduction of phenotypic and functional MPCs in the BM.

VEGF stimulates the migration of MPCs

We next examined the mechanisms of the reduction of MPCs in the BM after VEGF overexpression. In vitro-expanded primary mouse BM stromal cells (mBMSCs), including MPCs, showed slight expression of Flt-1 (VEGFR1), but not Flk-1 (VEGFR2), on the cellular surface (Fig. 5a). We speculated that MPCs might egress from the BM in response to the plasma level of VEGF, because there was almost no change in the BM VEGF levels in Ad-VEGF-injected mice (Fig. 1b). We performed an in vitro migration assay and found a dose-dependent chemoattractive effect of VEGF on mBMSCs (Fig. 5b), suggesting the possibility that a decreased number of BM MPCs in Ad-VEGF-injected mice would result from the mobilization of MPCs to the peripheral tissue in response to an elevation of plasma VEGF.

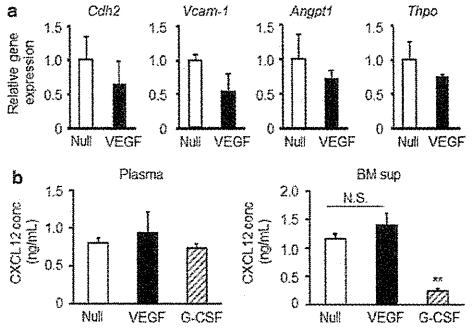

FIG. 3. Expression of HSPC maintenance factor genes after Ad-VEGF administration. (**a**) Expression levels of cadherin2 (Cdh2), vascular cell adhesion molecule-1 (Vcam-1), angiopoietin-1 (Angpt1), and thrombopoietin (Thpo) in nonhematopoietic cells (CD45$^-$Ter119$^-$ cells) were measured by quantitative polymerase chain reaction analysis. Data are expressed as mean ± SD ($n=3$). (**b**) The plasma and BM supernatants of mice injected with Ad-Null, Ad-VEGF, or Ad-GCSF were collected. The levels of CXC chemokine ligand 12 (CXCL12) in the plasma (*left*) and the BM supernatant (*right*) were measured by ELISA. $^{**}P<0.01$ as compared with Null. N.S. stands for not significant.

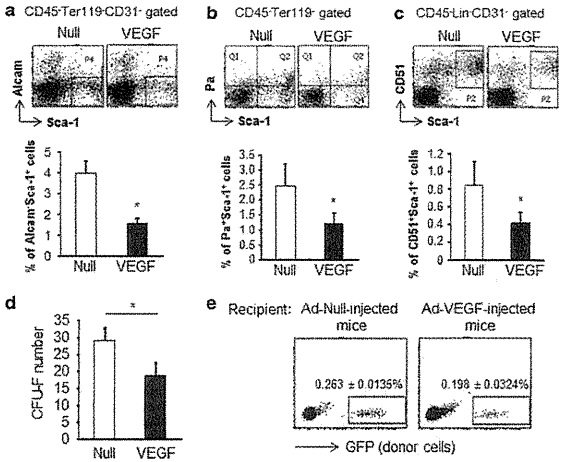

FIG. 4. The number of mesenchymal progenitor cells (MPCs) in the BM is decreased following Ad-VEGF injection. (**a–c**) After BM stromal cells were collected from bone by treatment with collagenase, the proportion of MPC populations [$CD45^-Ter119^-CD31^-Alcam^-Sca\text{-}1^+$ MPCs (**a**), $CD45^-Ter119^-$ $PDGFRa^+$ (Pa^+) $Sca\text{-}1^+$ MPCs (**b**), or $Lin^-CD45^-CD31^-CD51^+Sca\text{-}1^+$ MPCs (**c**)] in the BM was determined by flow cytometry. Data are expressed as mean ± SD ($n=5$). (**d**) A colony-forming unit-fibroblast (CFU-F) assay was performed using $CD45^-Ter119^-$ BM cells. The number of CFU-Fs was counted using a microscope after staining with the Giemsa solution. Data are expressed as mean ± SD ($n=3$). (**e**) Homing assay. After injection of Ad-Null or Ad-VEGF into mice, green fluorescent protein (GFP) transgenic mice-derived BM cells (donor cells) were transplanted into Ad vector-administrated mice. The percentage of donor cells (GFP-expressing cells) in the BM of Ad-Null- or Ad-VEGF-injected mice was analyzed by flow cytometry at 16 h after BM transplantation. The percentage of donor cells in the BM is indicated in the dot blot. Data are expressed as mean ± SD ($n=5$). $^*P<0.05$ as compared with Null.

Discussion

Recent studies have clearly reported that the HSPC numbers in the BM are significantly decreased by conditional deletion of MPCs, including nestin-expressing stromal cells [4] and CXCL12-abundant reticular cells [5]. It is of note that deletion of MPCs led to the increased number of HSPCs in the spleen, demonstrating the mobilization of HSPCs from BM to peripheral tissues [4]. Therefore, maintenance and retention of HSPCs in the BM would considerably be dependent on the number of MPCs [4,5]. In the present study, we examined the effect of VEGF on the disposition of BM HSPCs and MPCs in mice. Our main finding was that VEGF overexpression in mice resulted in a reduction of not only HSPCs but also MPCs in the BM. We also found that VEGF could promote the migration of mBMSCs in vitro. The data described here suggest that, as in the case of HSPCs, MPCs would also be mobilized to the peripheral tissues in response to an elevation of plasma VEGF levels, and a reduced number of BM MPCs by VEGF would lead to HSPC egress from the BM, because MPCs would function as niche cells in the BM.

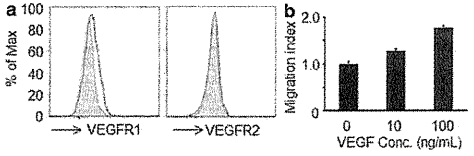

FIG. 5. VEGF enhances the migration capacity of MPCs. BM-derived stromal cells were collected and propagated in a tissue culture dish. (**a**) Expression levels of VEGF receptors, VEGFR1 (*left*) and VEGFR2 (*right*), in the cells was determined by flow cytometry. Staining profiles of specific mAb (dotted lines) and an isotype-matched control mAb (gray area) are shown. (**b**) BM stromal cells were exposed to various doses of recombinant VEGF. Cells that had migrated toward the VEGF (lower chamber) by passing through a membrane filter were counted by microscopy after staining with the Giemsa solution. Data are expressed as mean ± SD ($n=3$).

It is well known that BM CXCL12 levels are downregulated following G-CSF administration and thereby induce an egress of HSPCs [25,29]. Christopher et al. previously showed the reduced BM CXCL12 levels after administration of other mobilization factors, such as SCF and Flt3-ligand [10]. In addition to their mobilization-inducing effects, these factors also impact the number of stem and progenitor cells in the BM. For instance, it has been reported that the number of HSPCs and MPCs in the BM was significantly increased after G-CSF administration [30,31]. Unlike in the case of G-CSF and other mobilization factors, however, VEGF had almost no effect on BM CXCL12 levels (Fig. 3b). Furthermore, systemic VEGF expression resulted in a significant reduction in the number of HSPCs (KSL cells and CFU-Mix) in the BM (Fig. 2). The number of MPCs in the BM was also reduced in Ad-VEGF-injected mice (Fig. 4). Therefore, these data strongly indicate that VEGF would induce HSPC mobilization by altering the BM environment through different mechanisms from G-CSF. Notably, a recent study showed that HSPCs could be mobilized from the BM into the circulation by administration of a prostagrandin E_2 (PGE_2) inhibitor, and this effect was independent of CXCL12-CXCR4 signaling [32]. A nucleotide sugar, uridine diphosphate (UDP)-glucose, has also been shown to mobilize subsets of HSPCs functionally distinct from those mobilized by G-CSF, suggesting that UDP-glucose-induced HSPC mobilization would be mediated, at least in part, by different mechanisms from G-CSF [33]. Thus, it would be of interest to examine whether VEGF could influence the levels of BM PGE_2 and/or plasma UDP glucose.

The expression levels of HSC maintenance genes (*Cdh2*, *Vcam-1*, *Angpt1*, and *Thpo*) in BM nonhematopoietic cells were decreased in Ad-VEGF-injected mice (Fig. 3a). This would be due to the reduction in the number of MPCs in the BM after Ad-VEGF injection (Fig. 4). However, we have no idea why BM CXCL12 levels were not changed in Ad-VEGF-injected mice, because MPCs abundantly produce CXCL12 [7,8]. A detailed investigation would be required to clarify the regulation of CXCL12 expression in niche cells, including MPCs, endosteal osteoblasts, and endothelial cells.

We observed enhanced in vitro migration activities of mBMSCs by VEGF, suggesting the possibility that MPCs in the BM would be mobilized to the peripheral tissue in response to the plasma VEGF concentration. However, at present, we did not detect the CFU-F in the blood in Ad-VEGF-injected mice (data not shown). MPCs are known to be rare cells even in the BM, representing ~1 in 10,000–100,000 total nucleated cells [34], and it is therefore possible that the frequency of MPCs in the blood was too low to detect under our experimental conditions. Alternatively, it is also possible that VEGF overexpression in mice might lead to the homing of MPCs to organs, such as the liver, because transgene expression in the liver was extremely high following systemic Ad vector injection [35]. Therefore, it might be necessary to investigate whether or not the frequency and the number of MPCs are changed in tissues or organs other than the peripheral blood.

Recently, Liu et al. showed that MPCs could be mobilized to the peripheral tissue when rats were exposed to hypoxic conditions, and this hypoxia-induced MPC mobilization was caused by the elevation of plasma CXCL12 levels and BM VEGF levels [36]. Under our conditions, however, plasma CXCL12 levels and the BM VEGF levels in Ad-VEGF-injected mice were almost equal to those in Ad-Null-injected mice (Figs. 1b and 3b), suggesting that the mechanisms of decreased number of BM MPCs in Ad-VEGF-injected mice would be different from those of hypoxia-induced MPC mobilization.

Consistent with previous reports [15], we confirmed the HSPC mobilization from BM into the circulation by VEGF overexpression using an Ad vector system (Fig. 1). On the other hand, a previous report was that administration of a recombinant VEGF protein into mice failed to induce the HSPC mobilization [37]. In our Ad vector systems, plasma VEGF levels were maintained at 400–600 ng/mL on day 3–5 after single intravenous injection. Although we do not know the VEGF levels in the plasma under their experimental protocols, plasma VEGF levels might not be sufficient for HSPC egress from the BM, because exogenous VEGF levels in the plasma were rapidly decreased after administration of a recombinant VEGF protein [23]. Therefore, this difference would be partly due to the difference in the plasma VEGF levels, and we concluded that an Ad vector system would be an appropriate one to estimate the in vivo physiological action of VEGF.

In summary, our results showed that plasma VEGF levels could regulate the distribution of BM HSPCs and MPCs, probably by a mechanism distinct from that of other mobilization factors, and we suggest that a reduction in the number of MPCs in the BM would be one of the mechanisms involved in VEGF-induced HSPC mobilization. Although further investigation of the BM environment will be needed to uncover the VEGF-mediated HSPC mobilization, our findings obtained in this study provide a novel insight into the mechanisms of HSPC mobilization and would be helpful in the development of new clinical mobilizing agents.

Acknowledgments

This work was supported by grants from the Ministry of Health, Labour, and Welfare of Japan, and by the Sasakawa Scientific Research Grant from The Japan Science Society.

Author Disclosure Statement

The authors have no financial conflict of interests.

References

1. Calvi LM, GB Adams, KW Weibrecht, JM Weber, DP Olson, MC Knight, RP Martin, E Schipani, P Divieti, et al.